SELECTED PROBLEMS OF CHATTER

SELECTED PROBLEMS OF MACHINE TOOL CHATTER

By

LEONARD HAROLD BAXTER, B. Eng.

A Thesis

Submitted to the School of Graduate Studies

in Partial Fulfilment of the Requirements

for the Degree

Master of Engineering

McMaster University

April 1974

MASTER OF ENGINEERING (1974) McMASTER UNIVERSITY
Hamilton, Ontario

TITLE: Selected Problems of Machine Tool Chatter

AUTHOR: Leonard Baxter, B.Eng. (G.M.I., Flint, Michigan)

SUPERVISOR: Dr. J. Tlusty

NUMBER OF PAGES: xii, 150

ABSTRACT

This work applies previous research in the field of chatter in metal cutting to some practical problems of chatter during metal removal.

Investigations into the stability of a machine tool structure were performed in order to make an analysis of the present stability during machining and how the level of stability can be increased.

Computation of the dynamic response of a grinding spindle was carried out as an example of a typical procedure usually used in checking a design change with respect to requirements resulting from stability analysis.

A practical case of chatter in milling slots in an automobile component was examined. A simplified experimental analysis was used and two possible solutions investigated; one of eliminating regeneration of vibration and the other of using a damper.

The last part deals with an attempt to solve the problem of pseudostatic instability in reaming tapered holes.

ACKNOWLEDGEMENTS

I would like to express my thanks and appreciation to Dr. J. Tlusty for his patience and guidance throughout my research, and to Mr. W.H. El Maraghy for his help with the computer programs that were used.

Also, I express my thanks to McMaster University and General Motors Institute for their mutual co-operation that made this thesis possible.

TABLE OF CONTENTS

LIST OF FIGURES

LIST OF SYMBOLS

B_{lim}	Limit width of cut
c	Damping coefficent
f	Frequency
f_I	Frequency of chatter
F	Force
G	Weight
in	Inches
J	Mass moment of inertia
K	Spring constant
lb	Pounds
M	Mass
R	Radius of rotation
t	Irregularity of tooth pitch
V	Cutting velocity
X	Displacement
W	Circular frequency
ξ	Damping ratio
θ or ψ	Rotation

INTRODUCTION

CHAPTER I

INTRODUCTION

1.1 General Introduction

The theory of chatter has been investigated by a number of distinguished persons such as Tlusty [1] Tobias [2], Slavicek [3].* These men have presented numerous reasons for chatter and have pursued the investigation of chatter in a thorough, academic manner.

The primary intent of this thesis and my work at McMaster was not to further the research in the nature of chatter but to learn the basic principles of chatter and to apply the current techniques to some practical Engineering problems.

The work divided itself into four basic units. First, learning the basic techniques and instrumentation for determining the stability of machine tools through the Mazak Lathe investigation as outlined in Chapter II and reference [4]. Secondly, the Grinding Spindle Investigation (Chapter III) gave some exposure to computational methods of determining the stability of machine tools as well as reinforcing the first phase. Finally, two real problems

---

* Numbers in square brackets indicate references given in biblipgraphy.

from the General Motors Plant in St. Catharines forced application of the techniques learned and exposed more of the complex nature of chatter. These two problems were Chatter During Slot Milling (Chapter IV) and Lobing During Taper Reaming (Chapter V).

Before describing these investigations in the chapters to follow, the basics of regenerative chatter, as presented in reference [1], will first be described since it is mainly regenerative chatter that is dealt with later in the text. A very complete and detailed presentation of the theory of chatter and stability analysis can be found in reference [1], Chapters I and II.

1.2 The Basics of Regenerative Chatter

The regenerative chatter principle is usually explained using a simple single degree-of-freedom system as shown in Fig. 1.1. In the real world a tool always cuts a surface which it has already cut during the previous revolution (in turning), during the previous stroke (in planing), or which has been cut by the preceding tooth (in milling). Therefore, if there was a vibration between the tool and the workpiece during the ith cut and the produced surface has become undulated, the chip of the $(i + 1)^{th}$ cut is removed from that undulated surface. If the amplitude of vibration in the direction of the normal to the cut surface in the ith cut was Y_o and in the $(i + 1)^{th}$ cut is Y, then

the amplitude of chip thickness variation is $(Y-Y_o)$. Because of the undulation Y_o, the cutting force contains a variable component which excites vibration X of the vibratory system with the "normal" component Y. Vibration Y creates again an undulated surface on the workpiece and the regeneration of the undulation proceeds in subsequent cuts.

The frequency of the vibrations and the phase shift between the undulation in subsequent cuts will adjust themselves so that maximum energy is delivered to the vibration of the system. If the energy is sufficient to cover the losses of energy caused by the damping in the vibratory system the vibrations in subsequent cuts do not diminish but increase and regenerative chatter occurs. In practical cases, regenerative chatter always occurs when the chip width is sufficiently large.

CHAPTER II

MAZAK LATHE STABILITY ANALYSIS

2.1 Introduction to the Analysis

A large portion of my time at McMaster was spent learning the instrumentation, techniques and theory needed for a practical understanding of the dynamic analysis of machine tools.

To this end I participated in the investigation of the Mazak-24 lathe in the Production Engineering laboratory. The lathe was being studied so that its dynamic characteristics would be available in the future. One such case was later in my research since the information gathered in this investigation was needed in order to properly design the cutting tests with two tools described in Chapter IV.

In the investigation the receptances and mode shapes for various configurations of the workpiece and different orientations of the tool are determined using the shock excitation technique as described in reference [5]. Cutting tests were also performed to find the limit width of cut b_{lim} at each workpiece configuration and tool orientation. B_{lim} is also computed from the receptance curves and a comparison of computed values and values obtained in cutting tests is presented. A very detailed report on this investigation is available in reference [4].

2.2 Receptance Measurements

The receptances for the three configurations of the workpiece and for the seven orientations of the tool (see Fig. 2.1) were measured as relative receptances between the tool and the workpiece. The shock force was measured by a piezo-electric crystal transducer fixed to the hammer. The change in charge during impact was converted to a proportional change in voltage by a Kistler Charge Amplifier.

The relative vibration between the tool and workpiece was measured by a capacitive probe fixed to the annular plate in the particular orientation being investigated. A Wayne Kerr capacitive bridge converted the capacitive variation into a proportional change in voltage. Both the force and vibration signals were fed into the Fourier Analyser which digitized the signals and processed them by the program in reference [5] , page 148 to obtain the transfer function. The real part of the transfer function was plotted on a H.P. x-y Plotter for future evaluation.

The horizontal, vertical and cross receptances are shown in Figs. 2.2 (a), 2.2 (b) and 2.2 (c) respectively for the A, B, and C configurations of the workpiece.

From these curves the cross receptances for each orientation of the tool and thus the limit width of cut can be computed by two methods both of which are outlined in detail in reference [4]. The resulting cross-receptance

curves for each orientation and the comparison between the cutting tests and the computed value for B_{lim} are shown in Figs. 2.3 (a-f), 2.4 (a), (b)&(c). These curves were used in the slot milling investigation in Chapter IV when the Mazak-24 lathe was used in the simulation of milling without regeneration.

2.3 Mode Shape Measurement

Mode shape determination by means of shock excitation was found to be a very powerful technique once the correct way of interpreting the data was found.

The Phillips velocity pickup was used to measure the vibration at the point of interest (the point of cutting) as the lathe was hit in all the desired points corresponding to the orientation of the Phillips pickup. The hammer was instrumented with an impact transducer so that for each shock excitation of the structure, two simultaneous signals, force and vibration, were fed to the Hewlett-Packard Fourier Analyser. The Fourier Analyser was programed so that once it was triggered by the force signal it would perform the Fourier transforms on both signals, divide to obtain the transfer function, change to polar form, print out the magnitude and phase at the frequency of interest and then reset to accept the next input set. In this way measurements are taken on many points of the machine and all the results recorded automatically. The only things that must be done

by hand were the identification of the data as to the location of the pickup and the position of shock excitation. The correct way of interpreting the data is to record the phase of the reference point by hitting parallel and close to the Phillips pickup and then compare the phase of all other hits to that of the reference point. All points with a phase angle close to that the reference phase angle may be considered in phase and those with a phase angle different by 180° or close to it are taken as out of phase.

In practice it turns out that the phase angles of the points to be considered in phase, when plotted on a vector diagram, are usually scattered about close to the vector of the reference point and those out of phase are scattered about a vector on the other side of the circle.

The mode shapes of the Mazak, including some indication of the phase relationships obtained, for each of the cutting positions are shown in Figs. 2.5 (a) - (b). Fig. 2.6 is a polar plot of phase angles for "B" configuration (vertical, spindle).

In this case it can be said that each of the receptances contains two dominant modes in each of the configurations. One of them is close to horizontal, the other close to vertical.

For configuration A the "horizontal" mode is inclined by 15° and has natural frequency 190 HZ. The vertical mode

is inclined by 7.5° and has natural frequency 220 Hz. In configuration B practically the same modes were found which means that the location of the saddle does not really influence these mode shapes. Indeed, it is seen that the amplitudes measured on the guideway on the bed are small and, with exception of Fig. 2.5 (c) they are uniform all along the bed. In both the vertical and the horizontal modes the main vibrating mass is the workpiece and the main "springs" are: the tailstock spindle and the live centre, in the first instance; the clamping in the chuck comes second as an obvious flexibility. The spindle itself with its bearings on one side and the tailstock body including its connection with the bed on the other side are next in order of flexibility.

For configuration C the main mass of both the modes is again the workpiece and the main flexibility is in the chuck and, further, in the spindle.

In all the three configurations the difference between the vertical and the horizontal modes is caused by the flexibilities of the bodies of the headstock and of the tailstock, different in the two directions, with respect to the bed. These flexibilities are greater horizontally than vertically which accounts for higher vertical than horizontal natural frequencies.

2.4 Cutting Tests

Cutting tests were performed to obtain the actual b_{lim} values. A feed of 0.004"/rev. and a cutting speed of 300 ft/min. were used in all cases. A carbide tool with positive rake angle and 45° side cutting edge angle tool was clamped on to the annular plate and vibration of the tool during cutting was sensed by a Phillips velocity pick-up and recorded by an oscilloscope. The workpieces were round cylinders of exactly same dimensions as those used for excitation tests. They were of 1045 steel. The depth of cut was increased till chatter occurred. The results of cutting tests consisted of maximum widths of cut b_{lim} and chatter frequencies f_{lim}. The values f_{lim} and b_{lim} were tabulated and plotted in Figs. 2.4 (a), (b), & (c) along with the computed values.

2.5 Analysis of Stability

From Figs. 2.4 (a), (b), & (c)it may be seen that for all the three configurations a rather good agreement was obtained between cutting test results and limits of stability evaluated from excitation tests. For this comparison, in all cases the value of r = 310,000 lb/in^2 was used which gives the best overall fit.

First of all, with the same value of r applied for all the three configurations, it may be stated that the excitation tests revealed the correct comparative level of

stability of the three configurations. Such a comparison is then practically best expressed by stating that for the usual horizontal position (0°) of the tool the limit widths of cut were 0.400 in., 0.110 in. and 0.310 in. for configurations A, B, C respectively. Thus, turning in the middle of the long workpiece supported by the tailstock gives maximum stability. The case of overhang turning came second and turning at the tailstock end of the long workpiece was worse with about a quarter of stability of the case A.

It is further found that best stability is obtained in all the three cases just for this 0° position and, it is the same for 180°. In all the three cases two minime of stability with respect to tool orientation are found: one at 60° which is less important and one at 150° which is very pronounced: limit of stability in this orientation is about <u>three</u> times lower than for the 0° orientation.

This variation of stability with the change in the orientation of the tool is understood when we look at the graphs in Fig. 2.3 . Let us first consider the configuration A for which we remember that the main horizontal mode has 190 Hz natural frequency and the main vertical one has 213 Hz frequency. In the various orientations each of the two modes has a different significance depending on its corresponding directional factor. The resulting receptance is the sum of the receptances corresponding to the individual modes. The

minimum of the resulting receptance which determines the limit of stability is obtained here mainly by the interaction of the two principal modes as it is seen, e.g. in the cases A 120° and A 150° where around the minimum both curves are negative and their effects are added together. In this way the rather low stability of the A 150° case is obtained. The low stability of the A 60° case is due to the rather high directional factor of the vertical mode. The high stability of the A 0° case is obtained because of the low directional factor for the horizontal mode and practically zero directional factor for the vertical mode. Thus, in this most significant and the only practical orientation no adverse interaction of the modes is found, mainly thanks to the very small deviation of the "vertical" mode of the purely vertical direction. Any further improvement of stability could be obtained mainly by stiffening the horizontal mode. For the configuration B, the situation is exactly analogous to that of the configuration A with the only difference that all modes are more flexible. Again, in the case B 0° it is practically the horizontal mode only which matters.

In the configuration C the situation is analogous again to the two preceding ones although in some instances: C 30°, C 60°, C 90° a third, higher mode with 360 Hz natural frequency is almost the decisive one. Because, however, these cases are insignificant practically we do not even

try to identify this mode. For the practically most significant orientation C 0° it is the horizontal mode which determines the limit of stability.

2.6 Conclusion

For configurations A and C rather high degrees of stability were found for the usual and only practical orientation of 0° (tool horizontal). With the very typical machining conditions of our cutting tests and the rather high lead angle of 45° the corresponding limit widths of cut were 0.4 in. and 0.32 in. respectively. For lead angles of 30° or even 0° the limits will be still higher.

The limit depth of cut of 0.11 is found in the B 0° case is rather low. It is true that this applied to turning at the end of a rather heavy workpiece and to 45° lead angle. However, in most of our tool life testing this is just the size of workpiece used. According to the preceding analysis an improvement should be expected by eliminating some of the flexibility of the tailstock spindle and of the live centre. However, the centre used is one of the sturdiest on the market. A centre hole 1.25 in. diameter was used. Thus, if there is any chatter interfering with tool life testing, extension of the tailstock spindle must be decreased to an absolute minimum. If this does not help improvements in the stiffness of the live centre will have to be sought.

For any special experiments in which other orientations of tools than the 0° one will be used, as in Chapter IV, the analyses given in Fig. 2.3 will serve as basis. The same applies to experiments in which additional vibratory systems will be used, e.g. boring bars.

CHAPTER III

GRINDING SPINDLE REDESIGN

3.1 An Introduction To The Problem

As an exercise in another aspect of dynamic analysis the spindle of the Thompson grinder in the Production Engineering Laboratory was analysed experimentally and through computational methods. The aim was two-fold. First to gain experience in the computational methods of dynamic analysis and secondly to gain experience in the experimental technique of shock excitation. A redesign of the spindle to have two bearings instead of three is also described.

The approach taken for this problem was to remove the headstock from the grinder and mount it on rubber on the bed plate in the lab. Then, using the shock excitation technique, as described in reference [5], to determine the receptance curves and mode shapes for the three possible bearing configurations. Three bearing configurations (see Fig. 3.1) were used in order to be able to solve for the stiffness and damping of the bearings which, unlike the spindle itself, cannot be computed. Then the receptance curves and mode shapes for the spindle were determined by using a computational method described in reference [6]. Once the mathematical model was perfected it was used to

determine the natural frequencies, mode shapes and receptance curves of the new designs considered.

3.2 Shock Excitation Experiments

The theory of using shock excitation and the use of the Hewlet Packard Fourier Analyser for the purpose of Dynamic analysis is well documented in reference [5]. This section will only deal with the details of using the shock excitation technique as they pertain to this particular problem.

As previously mentioned, the headstock was removed from the machine and mounted on the bed plate (see Fig. 3.2). The spindle was then removed and suspended on long ropes for determining the receptance and mode shapes for the free-free case. The use of the free-free case allowed a check on the computational model without the unknowns of being stiffness and damping in the bearings entering in. The vibration, for this case, was picked up using an accelermeter rigidly attached to the spindle at position number one (see Fig. 3.1). The signal was fed into the B channel of the Fourier Analyser. The force signal was picked up by the impact transducer attached to the hammer. It was then fed through the Kistler charge amplifier to channel A of the Fourier Analyser. These two simultaneous signals were digitized and processed by the program outlined in reference [5], page 148 for receptance measurement and reference [5], page

150 for mode shape measurement. For the tests with various configurations of bearings (Front and middle; Rear and middle, All bearings) the spindle was mounted in the headstock, the accelerometer was replaced by a capacitive probe rigidly held to the headstock at position one (see Fig. 3.3) thus obtaining the relative vibration between the headstock and the spindle.

For direct receptance measurement the spindle was hit at position one and vibration measured at position one. For mode shape measurement the spindle was hit at all 16 points and vibrations were measured at position one. This is the same as hitting at position one and picking up the vibrations at all 16 points on the spindle except that it is easier to leave the capacitive probe at one point once it is set up.

The results of the receptance measurements are shown in Fig. 3.4, and the mode shapes in Fig. 3.5. As can be seen from the receptance curves the compliance of the three bearing case is only slightly less than that of the Front and Middle bearings only, but over twenty-five times less than the case of the Rear and Middle bearings only. Damping was determined from the real receptance curves by use of the following equation for determining the damping ratio

$$\xi = \frac{W_{min} - W_{max}}{W_{max} + W_{min}}$$

where W_{min} is the frequency of the positive peak and W_{max} is the frequency of the negative peak. Background on the theory of damped forced vibration may be obtained from references [1] and [7].

It should be noted at this time that a problem was encountered with the holding of the probe rigid enough so that the probe holder has a resonant frequency higher than that of the spindle. Also, the clamping of the headstock to the bed plate tended to introduce errors into the results and this is why it was set on rubber. Fig. 3.6 is the receptance curve for all bearings with a magnetic dial indicator stand holding the probe and the headstock clamped to the base plate. As can be seen this figure is much different than the correct version shown in Fig. 3.4 and this difference is due to the flexibility of the probe holder and the clamping of the headstock to the bed plate. Once a probe holder was fabricated that was extremely stiff (see Fig. 3.7) and the headstock isolated from the base structure by the rubber, very repeatable results were obtained for the relative receptance and mode shapes.

3.3 Computer Modelling of the Spindle

Once the experimental results were obtained the next step toward being able to predict the dynamic characteristic

of a new spindle design was to create a mathematical model of the existing spindle that could reproduce on the computer results that were gained by experiment.

The technique used was to make use of the natural frequency and mode shape programs in Appendix A to first match the results for the free-free condition by using extremely soft bearings (100#/in.) and then to vary the bearing stiffness to obtain a combination of bearing stiffnesses, front and middle being the same and the rear bearing being not as stiff, that give the closest answer to the experimental results. Then the forced vibration program listed in Appendix B was used, with the bearing stiffnesses previously obtained, to match the receptance curves by adjusting the damping. The computed receptance curves are shown in Fig. 3.8 and the computed mode shapes in Fig. 3.9. The comparison between the experimental and the computed results is shown in Table 3.1. The comparison was quite close except for the case with the rear and middle bearings only, where there is a larger percent difference between the measured and computed results. This could be due to an inaccuracy in the geometrical description of the spindle but more likely by the poor fit of the middle bearing to the housing bore which was felt to be slightly oversize.

The receptance curves for each bearing configuration and free-free were obtained by a forced vibrations program

Table 3.1 Comparison of Experimental and Computed Data

Bearing Configuration	Dominant Resonant Frequency	Static Stiffness lb/in	Dynamic Stiffness lb/in
Free-Free			
Experimental	220 HZ 585 HZ	N/A	N/A
Computed	234 HZ 584 HZ		
Front & Middle			
Experimental	695 HZ	5.55×10^5	1.33×10^4
Computed	703 HZ	6.66×10^5	1.25×10^4
Middle & Rear			
Experimental	119 HZ	2.0×10^4	7.69×10^2
Computed	97 HZ	2.2×10^4	6.45×10^2
Front, Middle & Rear			
Experimental	527 HZ	7.14×10^5	1.33×10^4
Computed	480 HZ	10.0×10^5	1.22×10^4

(see Appendix B) that uses the Complex Algebra technique proposed in reference [6], page 45. Basically the technique of using complex algebra for obtaining the response of a multi-degree of freedom system involves the writing of the basic differential equations of motion in matrix form

$$[M]\{\ddot{X}\} + [C]\{\dot{X}\} + [K]\{X\} = \{F\}$$

now by substitution of the trial solution $\{X\} = \{\bar{X}\} e^{iwt}$ and $\{F\} = \{F_0\} e^{iwt}$ the equation below is obtained

$$[(K - w^2 M) + iwC]\{\bar{X}\} = \{F_0\}$$

If the quantity in the brackets is represented by the square matrix $[Z]$ then the solution of the system is

$$\{\bar{X}\} = [Z^{-1}]\{F_0\}$$

As noted in reference [6] this method is ideal for a system having a large number of degrees of freedom when a digital computer that is capable of observing the rules for manipulating complex numbers.

In order to eliminate the need for formulating the reduced mass matrix and the corresponding reduced stiffness matrix as noted in reference [8] the mass moments of inertia were calculated for all nodes and experimentally determined for the grinding wheel and fan. The experimental method used to determine these values for J is outlined in Appendix C.

Since this method of computing a receptance curve requires that the whole range of frequency under consideration be swept by incrementing W in a do-loop and reformulating

the problem for each value of W, a large amount of computer time is used for each run. The program in the Appendix required approximately 260 octal seconds for a 19 x 19 matrix size.

The natural frequencies and mode shapes were obtained for each bearing configuration by two methods. One with damping and one without. The method with damping is outlined in reference [6], page 63. The nondamped method was taken from reference [8], page 14. Both of these methods solve the eigenvalue problem to obtain the natural frequencies (eigenvalues) and mode shapes (eigenvectors) however, it was found that the program without damping was a lot faster as the number of elements in its matrix were one quarter of that contained in the damped program. A listing of both programs used is in Appendix A.

One stumbling block was encountered during the computational part of this problem and that was the order in which the stiffness matrix was formulated. As noted in reference [9] each node of the beam has two degrees of freedom, displacement (X) and rotation (θ) and these are usually ordered by one of two methods

$$\begin{Bmatrix} X_1 \\ X_2 \\ \vdots \\ \theta_1 \\ \theta_2 \end{Bmatrix} \quad \text{OR} \quad \begin{Bmatrix} X_1 \\ \theta_1 \\ X_2 \\ \theta_2 \\ \vdots \end{Bmatrix}$$

However, when the first ordering method was used the answers obtained were all incorrect. By using the second order everything worked as expected. The error probably occurred in the inversion routine as this was the only routine in common to both the forced vibration and the natural frequency program. However, this was beyond the scope of the investigation and when the second order was used the correct answers were found.

3.4 Design of a Two-Bearing Spindle

Having determined a satisfactory mathematical model of the spindle, the prediction of the dynamic stiffness of a new spindle configuration that eliminates the centre bearing is a relatively simple task. Fig. 3.10 shows the two configurations chosen to compare to the original spindle. One case has a 3.5 inch diameter section from node 4 to node 12 inclusive, which requires no changes in the headstock casting. The second case has a 4.5 inch diameter section from node 4 to node 12 and requires a new headstock casting.

Both configurations were used with the bearing stiffnesses and dampings previously determined. The direct receptance curves of these two cases are shown in Fig. 3.11 and mode shapes in Fig. 3.12. Since there was some question as to whether the rotor would be able to move too much, a series of receptance curves were run with the spindle being forced in the centre of the rotor to obtain the dynamic and

static compliance at node #13 (see Fig. 3.10) of the original spindle and the two new cases. These receptance curves are shown in Fig. 3.13. Finally, the effect of increasing bearing stiffnesses for the three cases previously mentioned was tried. A comparison of all the configurations tried is shown in Table 3.2.

As can be seen from this table of comparison, the new design with only front and rear bearings and the 4.5 inch diameter section is the closest to the present three bearing spindle being almost the same in static compliance and only twice the dynamic compliance.

In trying to understand why the 4.5 inch diameter spindle has essentially the same static stiffness when measured at the wheel but only one-half the dynamic stiffness let us refer to a simple case of the single degree of freedom system as shown below.

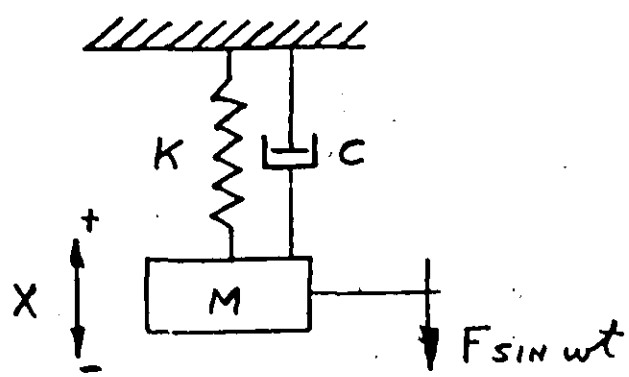

Table 3.2 Comparison of New (Two Bearing) Spindle Designs to the Original Three Bearing Design

Bearing Configuration	Dominant Resonant Frequency	Static Stiffness lb/in	Dynamic Stiffness lb/in
Forced at Wheel			
Original Spindle (3 bearings)	480 HZ	10×10^5	1.22×10^4
3.5 in. dia. Spindle (2 bearings)	210 HZ	10×10^5	4.76×10^3
4.5 in. dia. Spindle (2 bearings)	212 HZ	10×10^5	6.66×10^3
Forced in Rotor Centre			
Original Spindle (3 bearings)	480 HZ	50×10^5	3.0×10^4
3.5 in. dia. Spindle (2 bearings)	210 HZ	5.26×10^5	1.31×10^3
4.5 in. dia. Spindle (2 bearings)	212 HZ	10×10^5	1.66×10^3

movement of the mass m, which is assumed possible only in one direction denoted (X), is resisted by a force composed of two components, one proportional to the velocity of the mass and the other proportional to the displacement. Now for a constant damping coefficient c, a decrease in the natural frequency of the system, which is a decrease in the velocity for a constant amplitude, results in less energy being dissipated by the damping. This is why the dynamic compliance peak will be higher for the two bearing case than the three.

The reason for the static on low frequency compliance being the same for both cases is because of the negligible effect of damping at low frequencies and the compliance measured is mainly the compliance of the front bearing which is the same for both the original three bearing spindle and the proposed two bearing spindle.

CHAPTER IV

CHATTER DURING SLOT MILLING

4.1 An Introduction to the Problem

The operation that this chapter is concerned with is the milling of the mounting slot for the disk brake caliper on the cast knuckle for the front end of General Motors' large and intermediate sized automobiles (see Fig. 4.1). The parts are mounted on pallets and passed through a fully automatic transfer line for machining (see Figs. 4.2, 4.3).

The problem is that the milling of this slot which is done at one station of the transfer line is such a severe operation to be completed in the machine cycle time that there is chatter. The chatter is of such a magnitude that it creates a problem with tool life and the noise is above current acceptable industrial levels.

The cutting conditions are listed in Table 4.1. It should also be noted that the milling conditions are further complicated by the fact that there are two milling cutters on the same head and each cutter cuts two sections simultaneously as shown by Fig. 4.4. A drawing of the milling cutter used on this operation is shown in Fig. 4.5.

4.2 Measurements at the G.M. Plant

In order to evaluate the problem some basic vibration measurements had to be gathered and for this purpose a trip to the G.M. plant in St. Catharines was arranged.

Items measured were the frequency of the vibrations while cutting, natural frequency of the part while clamped in the pallet and the natural frequency of the cutter mounted on the spindle. The data obtained is listed in Table 4.1. The measurements were taken using the Phillips velocity pickup as a vibration transducer and the U-V chart recorder. Fig. 4.6 shows the Phillips pickup being held in the vertical orientation during cutting.

Analysis of the data revealed that the chatter was due to the spindle which has a natural frequency in the area of 790 to 850 HZ which coincides with the vibration measured during cutting of 770 HZ as well as the frequency determined by the chatter marks of 762 HZ.

Now that the part responsible for the chatter has been located there are three methods that we chose to investigate in an effort to decrease or eliminate the chatter. They are:

1. Irregular tooth pitch;
2. Alternate helix angles of the cutter teeth to eliminate regenerative chatter;
3. Damping the vibration by means of a vibration absorber.

Table 4.1 Slot Milling Cutting Conditions And Recorded Vibration Data

CUTTING CONDITIONS	
Revolutions per minute	190
Diameter	7.66 inches
Surface feet per minute	381
Feed	16.8 inches per minute
Teeth	28 per side
Feed per tooth	.0047 inches

VIBRATION DATA	
Natural Frequency of Part Clamped in Fixture	
Horizontal	390 HZ
Vertical	545 HZ
Natural Frequency of Cutter in Spindle	
Horizontal	790 HZ
Vertical	850 HZ
Frequency of Vibration on Fixture	
Horizontal & Tangent	90 HZ
Horizontal & Frontal	500 HZ
Vertical	1100 HZ
Frequency of Vibration on Headstock	
Vertical	770 HZ
Frequency of Vibration as Calculated From The Chatter Marks	760 HZ

4.3 Eliminating Chatter by Means of Irregular Tooth Spacing

An investigation into the possibility of designing an irregular pitched cutter was undertaken to see if this would be a feasible solution.

The basic idea behind using an irregular pitched milling cutter is to disturb regeneration (See reference [10] and [1] for the theory of regenerative chatter).

According to reference [3] the correct phase relationship to eliminate chatter at a specific frequency f_1 is given by the equation below (equation 20 in reference [3]):

$$f_1 = n \cdot \frac{v}{4t} \qquad n = 1, 3, 5$$

where v is the velocity of the cutter and t is the irregularity of the tooth pitches

$$t = \frac{l_1 - l_2}{2}$$

where l_i is the spacing between the i and i + 1 teeth

When rewritten for t, the equation is

$$t = n \frac{v}{4f_1}$$

which when the values for v and f from Table 4.1 are inserted (n = 1) a value for t of .024 in. is obtained.

This means that an optimum effect of the irregular pitch would be obtained for an alternation of pitches of 1.00 and 1.048 in. It is now obvious that very small frequency changes may compensate for such a small change in

the distance of two subsequent cuts in order to set a phase shift between them which would be favourable for regeneration of chatter. In other words with the given unusually high frequency of the system causing waviness on the cut surface with wavelengths of the order of 0.1 in. and the given tooth pitch the effect of irregular tooth pitch on stability would be rather small.

4.4 Alternate Helix Angles of the Cutter Teeth to Eliminate Regenerative Chatter

As another method of eliminating regenerative chatter the possibility of inclining alternate teeth at opposite helix angles was investigated. Fig. 4.7 is of a milling cutter using this principle.

The reason for the use of alternate helix angles is to have each tooth span at least 2 waves thus its average cutting force would not vary but remain relatively constant and eliminating the feedback loop (see Fig. 4.8) for the regenerative chatter.

Two experiments to prove this point were performed in our laboratory. One on the Mazak lathe and the other on the Tos milling machine.

I shall first deal with the experiment performed on the lathe.

In order to simulate the sequence of the milling cutter teeth on the lathe a special rig was designed and

constructed to rigidly hold two Kennametal #KSDN-856C tool holders which would be cutting simultaneously. The rig also allowed for the rotation of both tools about a point in the centre of the cutting edge. See Figs. 4.9, 4.10, 4.11, 4.12. At maximum inclinations of both tools it was possible to span approximately two full waves.

In the selection of the cutting conditions, workpiece length, support and tool orientation the previous investigation of the Mazak lathe as explained in Chapter II (see also reference [4]) allowed the selection to be made with some guidance rather than just hit or miss.

The intention was to cut with two tools not inclined and obtain chatter and thus b_{lim} and then to incline the tools and to obtain b_{lim} (inclined). Since b_{lim} (inclined) was expected to be at least twice that of b_{lim} and we were limited in the maximum width of carbide available we had to choose a workpiece length and cutter orientation that would give a low value of b_{lim} and still have a relatively high frequency of chatter since it was desirable to have the wavelength as small as possible so that the tool could span as many waves as possible. For these reasons workpiece configuration A and orientation 150° were chosen for the test (see Figs. 2.1, 2.3 (b) and 2.4 (a)).

The actual mechanics of the testing were rather

straightforward. The b_{lim} value for each of the tools cutting separately were found and then the b_{lim} for the two tools cutting simultaneously but not in the same groove was found. It should be noted that the sum of the b_{lim} values for the two tools should add up to the b_{lim} for one tool. This was found to be so. Then the two tools were put in the same groove to determine the b_{lim} value for the non-inclined state (see Figs. 4.13 and 4.14). It should be noted that in this part of the test the speed of the workpiece had to be varied slightly so that a number of waves that gives a phase-shift most favourable for regenerative chatter could be obtained between the two tools thus satisfying the geometric condition for chatter as described in reference [1]. Once again the sum of the b_{lim} values of the two tools added to equal that of one tool.

The two tools were now inclined and the procedure repeated to determine the sum of the b_{lim} (inclined).

One should note the procedure for obtaining equal feed for each tool. For this purpose a square shoulder, not helical, must be obtained on the workpiece with one tool and then set each tool exactly against this shoulder. Each tool then sees exactly one half the set feed.

The results of the tests (see Table 4.2) showed that the limit for two tools not inclined was .350 and with the tools inclined the maximum width of cut possible with the

Table 4.2 Details and Results of the Cutting Test with Two Tools to Eliminate Regenerative Chatter (Mazak Lathe)

Test Conditions

Carbide Tooling - 45° approach angle

Material - 1045 steel

Workpiece diameter - 4.960 inches

Cutting speed - 195 feet per minute

Nominal cutting plane of the tools inclined $\pm$ 30° from the normal horizontal position

Inclination of tools from nominal cutting plane
- front tool 14°
- rear tool 7°

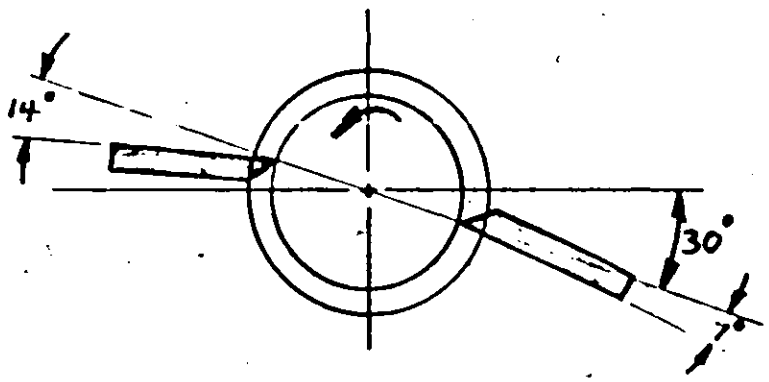

View From Tailstock in the Inclined Position

Tool(s) Used	Limit Width of Cut	Frequency of Chatter
Front only	.350 (in)	184 HZ
Rear only	.325	191 HZ
Front & Rear Cutting Simultaneously in Different Grooves	.180 (Front) .170 (Rear)	190 HZ
Front & Rear Cutting Simultaneously in the Same Groove	.225	189 HZ
Front & Rear Cutting Simultaneously in the Same Groove But Tools Inclined	.475 (Test Limited by Tool Width)	No Chatter

carbide insert available, .950 in., was taken with no chatter. This is an improvement of at least 300%.

The milling machine experiment was much simpler than that of the lathe. Two cutters were obtained with each having a 6" dia. and 24 teeth. They both had a 15° helix angle except that on one cutter the helix angle was in the same direction for each tooth as shown in Fig. 4.15 and for the other cutter the helix angle was staggered, left hand, right hand, left hand, etc. as shown in Fig. 4.7.

The milling test was performed with a two-inch wide piece of cold rolled steel having a set of precut steps on it so that the cutter was just plunged into the workpiece until chatter (see Fig. 4.16) developed and the thickness of the material at the point of chatter was the indicator of the relative stability of that cutter.

The details of the tests and the results are shown in Table 4.3. As can be seen from the results, the staggered tooth cutter had at least 100% more stability than the non-staggered tooth cutter.

4.5 The Elimination of Chatter by use of a Vibration Absorber

Another alternative considered to increase the stability of the slot milling at G.M. was the use of a vibration absorber or damper. The design of a vibration absorber is very straightforward and can be found in almost any vibration text (see reference [7]).

Table 4.3 Details and Results of Milling Tests with an Alternate Helix Angle Cutter and a Vibration Absorber to Eliminate Chatter

Test Conditions

Cutter Diameter	6	inches
Teeth	24	
Feed Per Tooth	.003	inches
Revolutions Per Minute	45	
Workpiece Material	1020	steel

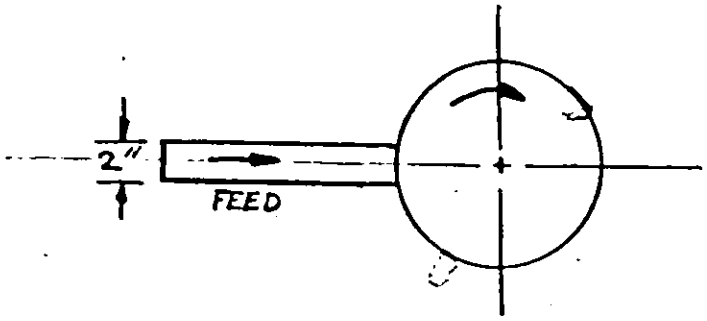

View From Top

Milling Cutter	Limit Depth of Cut	Frequency of Chatter
With each Tooth Helix Angle the same	.380 inches	70 HZ
With alternate Helix Angles	.625 (Test Limited by Width of Cutter)	No Chatter
With the same Helix Angles & Vibration Absorber tuned to 70 HZ	.550 inches	67 HZ.

The basic principle is to add a spring and a mass to an existing system such that the natural frequency of this new spring-mass system is exactly that of the original system. The vibration of the original mass will become zero at this frequency since the force exerted on the original mass by the added spring-mass system is equal and opposite to the impressed force due to the cutting process. The size of the absorber mass m_2 will depend on the magnitude of the disturbing force since the absorber must exert a force equal and opposite to the disturbing force which will depend on the allowable deformation of the absorber spring.

In the case of milling, the damper was designed using four rubber cylinders as the spring and a circular steel disk as a mass. This system was tuned to the frequency of chatter previously experienced, 70 HZ. The mass was made as large as possible since it would be working against the large mass of the cutter and spindle.

This damper was attached to the cutter without staggered teeth as shown in Figs. 4.17 and 4.18. The test was run as in the previous section. The results were not as good as hoped since the damper only increased the limit depth of cut from .330 to .550 an increase in stability of 66%. Originally a 100% increase of stability was hoped for.

4.6 Conclusions and Recommendations for Slot Milling at G.M.

Both methods tried for the stabilizing of the cutting process, alternate angled teeth and the vibration absorber, were successful. However, the alternate angled teeth method stabilized the cutting by a factor of at least 100% in the milling experiment and at least 300% on the lathe experiment. This is to be compared to only a 66% increase in stability for the damper. Fig. 4.19 shows the cutter design recommended to G.M., St. Catharines. It incorporates the alternate angle feature as well as the use of indexable throwaway carbide inserts with eight cutting edges per insert.

CHAPTER V

LOBING DURING TAPER REAMING

5.1 An Introduction to the Problem

The ball joint and tie rod end mounting holes on the front end of any modern automobile are tapered and are usually produced by reaming. A typical front end knuckle and the method of machining it are shown in Figs. 5.1, 5.2, 5.3, 5.4.

However, at General Motors of Canada, St. Catharines, a problem developed in the process of producing these holes such that the holes were not round but lobed. An exaggerated profile of the lobing is shown by the Talyround graph in Fig. 5.5. The lobing always made a pattern such that the number of lobes was N + 1, where N is the number of flutes on the reamer. Figs. 5.6 and 5.7 show a typical reamer used on this operation. The size of the lobing was between .00005 and .002 in.

5.2 The Investigation into the Nature of the Lobing

A trip to the G.M. plant was taken in order to collect the necessary data to attempt to understand the lobing phenomena. Vibration records using the Phillips velocity pickup and the U-V chart recorder were taken during the actual cutting operations (see Fig. 5.8). The cutting

tools and necessary holders were obtained for tests in our laboratory. Table 5.1 shows the cutting and vibration data obtained for the taper reaming at G.M.

Analysis of the data obtained on the field trip did not show any low frequency vibration in the order of 10 - 20 HZ which was needed in order to produce the lobes. This was probably due to the fact that the Phillips velocity pickup accents the higher frequencies and any low frequency vibration would have been hidden in the larger amplitude high frequency record.

5.3 Cutting Tests with the Taper Reamer

Cutting tests with the tools obtained from G.M. were performed in our laboratory on the Tos vertical milling machine (see Fig. 5.9). The intent of the tests was to reproduce the lobing so that it could be studied. We were able to produce lobes but in order to avoid having to go to G.M. or Mohawk College to make use of a Talyround to discover if we had, in any one test, produced lobes and if so the number and size a "Talyround" of our own had to be constructed (see Fig. 5.10). The lobe detector consisted of a lever on which a small ball was fixed to the end to follow the given contour and the Bendix inductive pickup which was moved by the lever as the ball followed the given contour. The output of the inductive pickup was fed to a Simpson chart recorder which recorded the signal for one revolution

Table 5.1 Taper Reaming Cutting Conditions And Recorded Vibration Data

CUTTING CONDITIONS	Rough Ream R.H. Spiral - R.H. Cut	Finish Ream L.H. Spiral - R.H.Cut
Nominal Diameter	.5559 inches	.5859 inches
Surface Feet/Minute	42	44
Revolutions/Minute	290	290
Feed/Revolution	.0266 inches	.0266 inches
Flutes	3	5
Feed/Tooth	.0089 inches	.0054 inches
VIBRATION DATA		
Frequency of Chatter	190 HZ	
Natural Frequency of Knuckle in Fixture	580 HZ	
Natural Frequency of Reamer in Spindle	680 HZ	

of the lobe detector in a hole. Fig. 5.11 shows the "Taly-round", chart recorder and Bendix inductive probe and amplifier as set up to record the profile of a taper reamed hole. Then by simply counting the number of peaks on the record the number of lobes was found. A sample record is shown in Fig. 5.12. This device was found to be very accurate and was capable of measuring to less than 1/10,000 of an inch.

During the cutting tests the tool holder was covered by an aluminum collar which was used as a reference circle for two capacitive probes set to measure the relative displacements between the tool and the workpiece at 90° to each other. The aluminum collar was trued by a high speed steel lathe tool mounted on the table of the machine in order to eliminate the runout of approximately .004 inch which would hide any vibration signal due to the tool vibrating during cutting. A photo of the capacitive probes set up on the aluminum collar is shown in Fig. 5.13 and a typical vibration record obtained in Fig. 5.14.

The results of the cutting tests are summarized on the Table 5.2.

The magnitude of the lobes produced were from .0001 in. to .015 in. and it was found that the phenomena would work at all the speeds tested from 125 RPM to 500 RPM.

Table 5.2 Details and Results of Taper Reaming Tests

Test Conditions

Cutter used	3 Flute
Revolutions/Minute (one set of tests at each RPM)	125 180 250 350 500
Workpiece material	1020 Steel
Feed	Hand Feed (Slow & Fast)

Cutter Flutes	Probe #1 *	Probe #2 **	Lobes Produced
3	6 cycles/cutter rev.(lagging)	6 cycles/cutter rev.(leading)	7
3	9 cycles/cutter rev.(lagging)	9 cycles/cutter rev.(leading)	10
3	12 cycles/cutter rev.(lagging)	12 cycles/cutter rev.(leading)	13
3	15 cycles/cutter rev.(lagging)	15 cycles/cutter rev.(leading)	16

* First Encountered as Spindle Rotates

** Second Encountered as Spindle Rotates

5.4 Kinematics of Lobing

As a result of the cutting tests a model of the kinematics of the lobing was constructed. The model, in words, is as follows; the tapered reamer rotates about the axis of the spindle with a frequency F and a direction clockwise. However, the axis of the spindle is rotating with some eccentricity about its centre at a frequency INF in the counter-clockwise direction. (N is the number of flutes on the reamer and I = 1, 2, 3 - - -). This kinematic arrangement produces INF + 1 lobes. Fig. 5.15 shows a graphical development of this model. A program was written in Fortran to verify this model and as can be seen from Figs. 5.16 and 5.17, a three fluted reamer and a four fluted reamer for various values of I, the model behaves exactly as previously stated. A listing of the program is in Appendix D.

5.5 Dynamic Characteristics of Lobing

In the previous section it was explained what the tool was doing in the kinematic sense in the production of lobes. Now the task is to discover what in the cutting process forces the tool to follow the path previously described and to increase the lobing with increasing time.

To this end we were unable to arrive at a completely satisfactory answer, however, a feasible solution is proposed.

But, before describing this solution, let us look at the case of drilling with a large diameter drill into relatively thin metal which produces a chatter with similar features to the case under study. Fig. 5.18 is a photograph of the chatter pattern produced by drilling. This type of chatter pattern can be explained by assuming that one of the two cutting edges has become "stuck" and that the cutter is forced by the driving torque to rotate about this point until the other cutting edge drives itself deeper into the metal than the currently "stuck" edge and becomes "stuck" causing the driving torque to force the previously "stuck" edge to rotate about this new rotation point and the cycle is repeated. This model is shown graphically in Fig. 5.19 where the pattern is developed from a circle by making the assumption that for some reason, perhaps cutter runout, the first cutting edge became "stuck".

Now, if this model is applied to the case of the tapered reamer which has three flutes, the correct pattern is formed as shown in Fig. 5.20 but the proportions are incorrect. The only proportion that will work is as shown where the lobing, peak to peak, is in the order of one half of the hole diameter.

However, modifying the model so that instead of a cutting edge becoming stuck, it is allowed to move but the increased cutting forces plus the driving torque deflect the

centre of the spindle such that it is forced to follow a circular path with a direction opposite to that of the cutter rotation. This has the effect of slowing down the blade that is taking the deeper cut and speeding up the blades taking the lighter cuts. A listing of the computer program that was written to digitally simulate this process is in Appendix E.

It was hoped that the computer simulation of the reaming process using cutting forces (based on the sum of the depths of cuts for each tooth) to deflect the spindle would develop a lobing pattern similar to that observed in the experimentation. However, the lobing pattern was not developed since the model went unstable after a number of cutter revolutions which indicates chatter. The instability was caused by the positive feedback loop as shown in Fig. 4.8 which was duplicated in the computer program. Since there was no damping and the variation of cutting forces caused a change in the depth of cut which in turn caused a variation in cutting forces, the cycle repeated itself until the deflections became large enough to cause a Mode 2 error and halt execution of the program.

In spite of the fact the program would not generate the desired lobing pattern it did shed some light on the problem. First, it did chatter as a result of cutting force variations, which indicates that the theory that the cutting

forces are causing the deflections has merit. Secondly, it was noted that increasing the ratio of spindle stiffness to cutting stiffness increased the cutting time (i.e. the number of revolutions) before the chatter increased without bound causing the program to halt. This indicates that increasing the machine stiffness will decrease the amount of lobing.

5.6 Summary of the Taper Reaming Investigation

We have determined that the vibration causing the lobing is of a very low frequency and that any damping in the system or added to the system will have negligible effect. Also, the actual motion the cutter makes relative to the workpiece has been determined in section 5.2 and proven in section 5.3. A cause for this motion (the cutting process itself) has been proposed in section 5.4, however the program to generate the lobing was not successful even though it indicated that an increase in the stiffness of the machine base, spindle, clamping fixtures and workpiece portion of the chatter feedback loop would by brute force decrease the lobing to an acceptable level.

Two looks at the problem have been made but the volume of the work required to totally define a solution is too great. Therefore, the problem remains unsolved in the present thesis.

APPENDIX A

COMPUTER PROGRAMS FOR THE DETERMINING OF THE NATURAL FREQUENCIES & MODE SHAPES OF A SPINDLE

As stated in the text, one of the computer programs written for the computation of natural frequencies and corresponding mode shapes of a multi-degree of freedom system used the method of complex algebra as outlined in reference [6]. The other program, which did not consider damping, was written by Cedric Park and is listed in reference [8].

The listing of the program that includes damping follows this brief description of how to use it. For a description of the theory of the complex algebra method, refer to reference [6], pages 63 - 65.

This program is very easy to use since the user need only input the physical characteristics of the spindle and the program will generate all needed matrices. The first data card inputs the density, modulus of elasticity and damping coefficient for the damping in the bearings.

On the next N-1 data cards (N Nodes, N-1 sections) is punched, in the appropriate format, the diameter to be used for stiffness calculations, the diameter to be used for mass calculations, the section length, additional NODAL stiffnesses (bearings), additional sectional rotary inertias and additional sectional masses. Subroutine Data uses this data to generate the stiffness, mass and damping matrices.

In the main program only N, the number of nodes, must be declared before the call to subroutine Data. The program then forms the G matrix (as described in reference [6]) and then performs the eigenvalue search. The eigenvalues are then outputed along with the eigenvectors, both real and imaginary, and the natural frequencies both damped and undamped.

```
C     NATURAL FREQ AND MODE SHAPES
C
C
C     A(I,J) MASS MATRIX
C
C     B(I,J) STIFFNESS MATRIX
C     C(I,J) DAMPING MATRIX
C
C
   10 N=19
      N1=N-1
      NM=N*2
      CALL DATA(A,B,C,SSD,SMD,SL,AS,AJ,AM,SS,SJ,SI,SM,N,NM,N1,B1,B2,B3)
      N=N*2
      NM=NM*2
      DO 20 I=1,N
      WRITE (6,15) A(I,I)
   15 FORMAT (F20.6)
   20 CONTINUE
      DO 30 I=1,N
      WRITE(6,25) B(I+3,I),B(I+2,I),B(I+1,I),B(I,I),B(I,I+1),
     1B(I,I+2),B(I,I+3)
   25 FORMAT(7E19.4)
   30 CONTINUE
C
C     INVERTING AND NEG OF THE MASS MATRIX
C
      CALL INVMAT(A,N,N,1.0E-7,IEER,M)
      WRITE(6,35) IEER
   35 FORMAT(///,I10,///)
      DO 40 I=1,N
      DO 40 J=1,N
   40 A(I,J)=-A(I,J)
C
C     MULTIPLY -A*B AND -A*C
C
      CALL MULT (A,B,N,AB)
      CALL MULT (A,C,N,AC)
C
C     FORM THE G MATRIX
C
      N1=N+1
```

```
      DO 50 I=1,NM
      DO 50 J=1,NM
   50 G(I,J)=0.0
      DO 60 I=1,N
   60 G(I,I+N)=1.0
      DO 70 I=N1,NM
      DO 70 J=1,N
   70 G(I,J)=AB(I-N,J)
      DO 80 I=N1,NM
      DO 80 J=N1,NM
   80 G(I,J)=AC(I-N,J-N)
C
C     PERFORM THE EIGENVALUE SEARCH
C
      T=48.0
      CALL EIGENP(NM,NM,G,T,EVR,EVI,VECR,VECI,INDIC)
C
C      OUTPUT
C
      WRITE(6,100)
  100 FORMAT(////,20X*  EIGENVALUES  *//)
      DO 110 I=1,NM
      WRITE(6,105) EVR(I),EVI(I)
  105 FORMAT(5X,2E20.4)
  110 CONTINUE
      WRITE(6,120)
  120 FORMAT(////,5X* EIGENVECTORS    REAL    IMAGINARY  *//)
      DO 135 I=1,NM,2
      WRITE(6,125)I
  125 FORMAT(//,5X*EIGENVECTORS FOR THE *I10* EIGENVALUE *//)
      DO 135 J=39,NM,2
      WRITE(6,130) VECR(J,I),VECI(J,I)
  130 FORMAT(5X,E20.5,20X,E20.5)
  135 CONTINUE
      WRITE(6,150) (INDIC(I),I=1,NM)
  150 FORMAT(5X,I5)
C     CALCULATING THE NATURAL FREQUENCES
C
      DO 180 I=1,NM
      IF(EVI(I) .EQ. 0.0) GO TO 175
      FND(I)=ABS(EVI(I))/6.2856
      IF(EVR(I) .EQ. 0.0) GO TO 176
      FN(I)=SQRT((EVR(I)*EVR(I))+(EVI(I)*EVI(I)))/6.2856
      GO TO 179
  175 FND(I)=0.0
      FN(I)=0.0
      GO TO 179
```

```
176 FN(I)=FND(I)
179 CONTINUE
180 CONTINUE
    WRITE(6,190)
190 FORMAT(////,10X*  NATURAL FREQUENCES        DAMPED NATURAL FREQS*//)
    DO 210 I=1,NM
    WRITE(6,200) FN(I),FND(I)
200 FORMAT(5X,2F20.5)
210 CONTINUE
    STOP
    END
```

```
    SUBROUTINE DATA(A,B,C,SSD,SMD,SL,AS,AJ,AM,SS,SJ,SI,SM,N,NM,N1,B1,
   1B2,B3)
    DIMENSION A(NM,NM),B(NM,NM),C(NM,NM)
    DIMENSION SSD(N1),SMD(N1),SL(N1),AS(N) ,AJ(N1),AM(N1),SS(N1)
    DIMENSION SJ(N1),SI(N1),SM(N1),B1(N1),B2(N1),B3(N1)

    DATA GENERATING FOR A SPINDLE MOUNTED IN TWO OR MORE BEARINGS

    UNITS/LBS/INCHES/SECONDS

    IDENTIFICATION OF VARABLES

    N              NUMBER OF NODES
    NM             SIZE OF MATRICES
    A              MASS MATRIX
    B              STIFFNESS MATRIX
    C              DAMPING MATRIX

    INPUT SEQUENCE  (N-1 SECTIONS)

    DENS           DENSITY
    EMOD           MODULUS OF ELASTISITY
    SSD(I)         STIFFNESS DIAMETER OF SECTIONS
    SMD(I)         MASS DIAMETER OF SECTIONS
    SL(I)          SECTION LENGTH
    AS(I)          ADDITIONAL SECTIONAL STIFFNESSES (BEARINGS)
    AJ(I)          ADDITIONAL ROTATIONAL INERTIAS
    AM(I)          ADDITIONAL SECTIONAL MASSES
```

```
      NN=NM-1
      READ(5,10) DENS,EMOD,DAMP
   10 FORMAT(F10.4,F20.3,F10.4)
      DO 20 I=1,N1
      READ(5,15) SS(I),SM(I),SL(I),AS(I),AJ(I),AM(I)
   15 FORMAT(3F10.4,F10.1,2F10.4)
   20 CONTINUE
      READ(5,25) AS(N)
   25 FORMAT(F10.1)
      WRITE(6,30)
   30 FORMAT(//,25X*  INPUT DATA*//)
      WRITE(6,40)
   40 FORMAT(//,5X*      N            DENS            EMOD            SS
     1   SM          SL          AS          AJ          AM          DAMP*)
      WRITE(6,45) N,DENS,EMOD,DAMP
   45 FORMAT(//,2X,I10,2X,F10.4,5X,F10.1,70X,F10.4,//)
      DO 48 I=1,N1
      WRITE(6,47) SS(I),SM(I),SL(I),AS(I),AJ(I),AM(I)
   47 FORMAT(45X,3F10.4,F10.1,2F10.4)
   48 CONTINUE
      DO 49 I=1,N1
      SSD(I)=SS(I)
   49 SMD(I)=SM(I)
C
C     CALCULATE MASS ROTATING INERTIA,AREA INERTIA OF EACH SECTION
C
      DO 50 I=1,N1
      SM(I)=(((SMD(I)/2.0)*(SMD(I)/2.0)*3.14*SL(I)*DENS)/386.0)+AM(I)
      SJ(I)=SM(I)*((((SL(I)/2.0)*(SL(I)/2.0))/3.0)+(((SMD(I)/2.0)*(SMD(
     1)/2.0))/4.0))+AJ(I)
   50 SI(I)=.049*SSD(I)*SSD(I)*SSD(I)*SSD(I)
C
C     FORMING THE MASS MATRIX
C
      DO 60 I=1,NM
      DO 60 J=1,NM
   60 A(I,J)=0.0
      A(1,1)=SM(1)/2.0
      A(NN,NN)=SM(N1)/2.0
      A(2,2)=SJ(1)/2.0
      A(NM,NM)=SJ(N1)/2.0
      DO 70 I=2,N1
      K=(2*I)-1
      A(K,K)=(SM(I-1)/2.0)+(SM(I)/2.0)
      A(2*I,2*I)=(SJ(I-1)/2.0)+(SJ(I)/2.0)
   70 CONTINUE
```

```
C
C     FORMING THE DAMPING MATRIX
C
      DO 80 I=1,NM
      DO 80 J=1,NM
   80 C(I,J)=0.0
      C(1,1)=-.002
      C(1,3)=-.002
      DO 85 I=3,NN,2
      C(I,I-2)=-.002
      C(I,I)=-.004
   85 C(I,I+2)=-.002
      DO 86 I=1,NM
      DO 86 J=1,NM
   86 C(I,J)=-C(I,J)
C
C     FORMING THE STIFFNESS MATRIX
C
      DO 90 I=1,NM
      DO 90 J=1,NM
   90 B(I,J)=0.0
C
      DO 100 I=1,N1
      B1(I)=EMOD*(SI(I)/SL(I))
      B2(I)=B1(I)/SL(I)
  100 B3(I)=B2(I)/SL(I)
C
C     FILLING IN THE LEADING DIAGONAL
C
      B(1,1)=12.0*B3(1)
      B(2,2)=4.0*B1(1)
      B(NN,NN)=12.0*B3(N1)
      B(NM,NM)=4.0*B1(N1)
      DO 110 I=2,N1
      L=2*I-1
      B(L,L)=12.0*(B3(I)+B3(I-1))
      LL=2*I
  110 B(LL,LL)=4.0*(B1(I)+B1(I-1))
C     FILLING IN THE FIRST UPPER DIAGONAL
C
C
      B(1,2)=6.0*B2(1)
      B(NN,NM)=-6.0*B2(N1)
      DO 120 I=1,N1
      L=2*I
  120 B(L,L+1)=-6.0*B2(I)
      DO 130 I=2,N1
      L=2*I
  130 B(L-1,L)=6.0*(B2(I)-B2(I-1))
```

```
C
C     FILLING IN THE SECOND UPPER DIAGONAL
C
      DO 140 I=1,N1
      L=2*I
      B(L-1,L+1)=-12.0*B3(I)
  140 B(L,L+2)=2.0*B1(I)
C
C     FILLING IN THE THIRD UPPER DIAGONAL
C
      DO 150 I=1,N1
      L=2*I
  150 B(L-1,L+2)=6.0*B2(I)
C
C     FILLING IN THE LOWER DIAGONALS
C
      DO 160 I=2,NM
      L=I-1
      DO 160 J=1,L
  160 B(I,J)=B(J,I)
C
C     ADDING ADDITIONAL STIFFNESS (BEARINGS)
C
      DO 170 I=1,NN,2
      K=(I+1)/2
      IF(AS(K) .EQ. 0.0) GO TO 170
      C(I,I)=DAMP
  170 B(I,I)=B(I,I)+AS(K)
      RETURN
      END
```

APPENDIX B

COMPUTER PROGRAM FOR THE COMPUTATION OF THE RECEPTANCE CURVE OF A SPINDLE

This program uses a method outlined in reference [6], pages 45 - 49. It also uses the same data generating subroutine (Subroutine Data) as the program listed in Appendix A. Therefore, the input sequence is the same as was previously described except that the forcing matrix must be declared at the beginning of the MAIN Program.

However, this program is different from the one previously described since it uses Complex variables. Also, it incorporates a loop to sweep through the desired frequency range in steps of WSAVE starting at W and continuing for as many loops as called for in the DO statement in line #55 (DO 50 K = 1,50). In this case there are 50 loops.

At every frequency considered, a Z matrix is formed (see reference [6]), inverted and multiplied by the forcing matrix to obtain the response of all the nodes at that frequency. The response is then outputed and the loop recycled. At the end of the frequency scan a plot of the real, imaginary and absolute receptance is generated and outputed. The program is listed on the next page.

It should be noted that the subroutines INVCOM and CMULT were developed by W.H. El Maraghy.

```
C
C         FORCED VIBRATION
C
C
C
C
C     (N,N)          SIZE OF MATRICES
C     A(I,J)         MASS MATRIX
C     B(I,J)         STIFFNESS MATRIX
C     C(I,J)         DAMPING MATRIX
C     B(I,J)         STIFFNESS MATRIX
C     C(I,J)         DAMPING MATRIX
C      F(I)          FORCING MATRIX
C
C
C
      K1=10
      K2=20
      K3=30
      N=19
      N1=N-1
      NM=N*2
      W=6.28*211.4
      WSAVE=6.28*.02
      WW=W-WSAVE
      M=1
      CALL DATA(A,B,C,SSD,SMD,SE,AS,AJ,AM,SS,SJ,SI,SM,N,NM,N1,B1,B2,B3)
      N=N*2
      NM=NM*2
      DO 5 I=1,N
    5 FR(I)=0.0
      FR(13)=100.0
      DO 12 I=1,N
      WRITE(6,11) A(I,I)
   11 FORMAT(F20.4)
   12 CONTINUE
      DO 14 I=1,N
      WRITE(6,13) B(I+3,I),B(I+2,I),B(I+1,I),B(I,I),B(I,I+1),
     1B(I,I+2),B(I,I+3)
   13 FORMAT(7E19.5)
   14 CONTINUE
      DO 19 I=1,N
      D=FR(I)
      E=0.0
   19 F(I,M)=CMPLX(D,E)
      WRITE(6,52)
   52 FORMAT(///,5X*  REAL PART                    IMAG PART */// )
      DO 50 K=1,50
```

```
      W2=W*W
C
C     FORMING THE Z MATRIX
C
      DO 20 I=1,N
      DO 20 J=1,N
      D=B(I,J)-(W2*A(I,J))
      E=W*C(I,J)
      Z(I,J)=CMPLX(D,E)
   20 CONTINUE
C
C      INVERSE OF THE Z MATRIX
C
      ZERO=1.0*E-08
      CALL INVCON(Z,N,N,ZERO,IERR,NI)
      WRITE(6,30) IERR
   30 FORMAT(I3)
C
C     MUL ZE-01 * F
C
      CALL CMULT(Z,F,X,N,M,N)
C
C     OUTPUT RECEPTANCE(W AND X)
C
      XXI(K)=AIMAG(X(13,1))
      XXR(K)=REAL(X(13,1))/FR(13)
      XXA(K)=CABS(X(13,1))
      HZ=W/6.28
      WRITE(6,55) HZ,XXR(K),XXI(K),XXA(K)
   55 FORMAT(/,5X,4F20.8)
      IF( K .EQ. K1) GO TO 51
      IF( K .EQ. K2) GO TO 51
      IF( K .EQ. K3) GO TO 51
      GO TO 49
   51 CALL SHAPE(N,X,M,HZ)
   49 CONTINUE
      PLT=XXR(K)
      CALL PLOTPT(HZ,PLT,4)
      W=W+WSAVE
   50 CONTINUE
      CALL OUTPLT
      HZ=WW/6.28
      DO 60 I=1,50
      PLT=XXI(I)
      HZ=HZ+(WSAVE/6.28)
      CALL PLOTPT(HZ,PLT,4)
   60 CONTINUE
      CALL OUTPLT
      HZ=WW/6.28
      DO 70 I=1,50
      PLT=XXA(I)
      HZ=HZ+(WSAVE/6.28)
      CALL PLOTPT(HZ,PLT,4)
   70 CONTINUE
      CALL OUTPLT
      STOP
      END
```

```
      SUBROUTINE INVCOM (A,N,NN,ZERO,IERR,NI)
C
C      THIS SUBROUTINE IS A MODIFICATION OF THE LIBRARY SUBROUTINE
C     INVMAT, THE CALL OF THE SUBROUTINE WOULD BE SIMILAR TO THE CALL
C     OF INVMAT(EXCEPT THAT THE MATRIX A IS COMPLEX)
C
      COMPLEX A,AA,TEM
      DIMENSION A(N,N), NI(NN)
      DO 1 I=1,NN
      NI(I)=0
1     CONTINUE
      DO 7 K=1,NN
      BB=0.0
      DO 2 J=1,NN
      IF (NI(J).NE.0) GO TO 2
      IF (CABS(A(K,J)).LT.BB) GO TO 2
      BB=CABS(A(K,J))
      JJ=J
2     CONTINUE
      IF (BB.GT.ZERO) GO TO 3
      IERR=K
      RETURN
3     NI(JJ)=K
      AA=A(K,JJ)
      A(K,JJ)=(1.0,0.0)
      DO 4 J=1,NN
      A(K,J)=A(K,J)/AA
4     CONTINUE
      DO 6 I=1,NN
      IF (I.EQ.K) GO TO 6
      AA=-A(I,JJ)
      A(I,JJ)=(0.0,0.0)
      DO 5 J=1,NN
      A(I,J)=A(I,J)+AA*A(K,J)
5     CONTINUE
6     CONTINUE
7     CONTINUE
      IERR=0
      DO 12 I=1,NN
      K=NI(I)
      IF (I.EQ.K) GO TO 12
      L=K
8     IF (I.EQ.NI(L)) GO TO 9
      L=NI(L)
```

```
      GO TO 8
9     DO 10 J=1,NN
      TEM=A(K,J)
      A(K,J)=A(I,J)
      A(I,J)=TEM
10    CONTINUE
      DO 11 J=1,NN
      TEM=A(J,L)
      A(J,L)=A(J,I)
      A(J,I)=TEM
11    CONTINUE
      NI(L)=K
12    CONTINUE
      RETURN
      END
C     C
      SUBROUTINE CMULT (A,B,C,N,M,L)
      COMPLEX A,B,C
      DIMENSION A(N,L), B(L,M), C(N,M)
      DO 2 I=1,N
      DO 2 J=1,M
      C(I,J)=0.0
      DO 1 K=1,L
      C(I,J)=C(I,J)+A(I,K)*B(K,J)
1     CONTINUE
      CONTINUE
      RETURN
      END
```

```
      SUBROUTINE DATA(A,B,C,SSD,SMD,SL,AS,AJ,AM,SS,SJ,SI,SM,N,NM,N1,B1,
     1B2,B3)
      DIMENSION A(NM,NM),B(NM,NM),C(NM,NM)
      DIMENSION SSD(N1),SMD(N1),SL(N1),AS(N) ,AJ(N1),AM(N1),SS(N1)
      DIMENSION SJ(N1),SI(N1),SM(N1),B1(N1),B2(N1),B3(N1)
C
C
C     DATA GENERATING FOR A SPINDLE MOUNTED IN TWO OR MORE BEARINGS
C
C     UNITS/LBS/INCHES/SECONDS
C
C     IDENTIFICATION OF VARABLES
C
C     N              NUMBER OF NODES
C     NM             SIZE OF MATRICES
C     A              MASS MATRIX
C     B              STIFFNESS MATRIX
C     C              DAMPING MATRIX
C
C
C     INPUT SEQUENCE  (N-1 SECTIONS)
C
C     DENS           DENSITY
C     EMOD           MODULUS OF ELASTISITY
C     SSD(I)         STIFFNESS DIAMETER OF SECTIONS
C     SMD(I)         MASS DIAMETER OF SECTIONS
C     SL(I)          SECTION LENGTH
C     AS(I)          ADDITIONAL SECTIONAL STIFFNESSES (BEARINGS)
C     AJ(I)          ADDITIONAL ROTATIONAL INERTIAS
C     AM(I)          ADDITIONAL SECTIONAL MASSES
C
C
```

```
      NN=NM-1
      READ(5,10) DENS,EMOD,DAMP
   10 FORMAT(F10.4,F20.3,F10.4)
      DO 20 I=1,N1
      READ(5,15) SS(I),SM(I),SL(I),AS(I),AJ(I),AM(I)
   15 FORMAT(3F10.4,F10.1,2F10.4)
   20 CONTINUE
      READ(5,25) AS(N)
   25 FORMAT(F10.1)
      WRITE(6,30)
   30 FORMAT(//,25X*  INPUT DATA*//)
      WRITE(6,40)
   40 FORMAT(//,5X*      N              DENS              EMOD              SS
     1   SM          SL          AS          AJ          AM          DAMP*)
      WRITE(6,45) N,DENS,EMOD,DAMP
   45 FORMAT(//,2X,I10,2X,F10.4,5X,F10.1,70X,F10.4,//)
      DO 48 I=1,N1
      WRITE(6,47) SS(I),SM(I),SL(I),AS(I),AJ(I),AM(I)
   47 FORMAT(45X,3F10.4,F10.1,2F10.4)
   48 CONTINUE
      DO 49 I=1,N1
      SSD(I)=SS(I)
   49 SMD(I)=SM(I)
C
C     CALCULATE MASS ROTATING INERTIA,AREA INERTIA OF EACH SECTION
C
      DO 50 I=1,N1
      SM(I)=(((SMD(I)/2.0)*(SMD(I)/2.0)*3.14*SL(I)*DENS)/386.0)+AM(I)
      SJ(I)=SM(I)*((((SL(I)/2.0)*(SL(I)/2.0))/3.0)+(((SMD(I)/2.0)*(SMD(I
     1)/2.0))/4.0))+AJ(I)
   50 SI(I)=.049*SSD(I)*SSD(I)*SSD(I)*SSD(I)
```

```
C
C     FORMING THE MASS MATRIX
C
      DO 60 I=1,NM
      DO 60 J=1,NM
   60 A(I,J)=0.0
      A(1,1)=SM(1)/2.0
      A(NN,NN)=SM(N1)/2.0
      A(2,2)=SJ(1)/2.0
      A(NM,NM)=SJ(N1)/2.0
      DO 70 I=2,N1
      K=(2*I)-1
      A(K,K)=(SM(I-1)/2.0)+(SM(I)/2.0)
      A(2*I,2*I)=(SJ(I-1)/2.0)+(SJ(I)/2.0)
   70 CONTINUE
C
C     FORMING THE DAMPING MATRIX
C
      DO 80 I=1,NM
      DO 80 J=1,NM
   80 C(I,J)=0.0
      C(1,1)=-.002
      C(1,3)=-.002
      DO 85 I=3,NN,2
      C(I,I-2)=-.002
      C(I,I)=-.004
   85 C(I,I+2)=-.002
      DO 86 I=1,NM
      DO 86 J=1,NM
   86 C(I,J)=-C(I,J)
C
C     FORMING THE STIFFNESS MATRIX
C
      DO 90 I=1,NM
      DO 90 J=1,NM
   90 B(I,J)=0.0
C
      DO 100 I=1,N1
      B1(I)=EMOD*(SI(I)/SL(I))
      B2(I)=B1(I)/SL(I)
  100 B3(I)=B2(I)/SL(I)
C
C     FILLING IN THE LEADING DIAGONAL
C
      B(1,1)=12.0*B3(1)
      B(2,2)=4.0*B1(1)
      B(NN,NN)=12.0*B3(N1)
      B(NM,NM)=4.0*B1(N1)
      DO 110 I=2,N1
      L=2*I-1
      B(L,L)=12.0*(B3(I)+B3(I-1))
      LL=2*I
  110 B(LL,LL)=4.0*(B1(I)+B1(I-1))
```

```
C
C     FILLING IN THE FIRST UPPER DIAGONAL
C
      B(1,2)=6.0*B2(1)
      B(NN,NM)=-6.0*B2(N1)
      DO 120 I=1,N1
      L=2*I
  120 B(L,L+1)=-6.0*B2(I)
      DO 130 I=2,N1
      L=2*I
  130 B(L-1,L)=6.0*(B2(I)-B2(I-1))
C
C     FILLING IN THE SECOND UPPER DIAGONAL
C
      DO 140 I=1,N1
      L=2*I
      B(L-1,L+1)=-12.0*B3(I)
  140 B(L,L+2)=2.0*B1(I)
C
C     FILLING IN THE THIRD UPPER DIAGONAL
C
      DO 150 I=1,N1
      L=2*I
  150 B(L-1,L+2)=6.0*B2(I)
C
C     FILLING IN THE LOWER DIAGONALS
C

      DO 160 I=2,NM
      L=I-1
      DO 160 J=1,L
  160 B(I,J)=B(J,I)
C
C     ADDING ADDITIONAL STIFFNESS (BEARINGS)
C
      DO 170 I=1,NN,2
      K=(I+1)/2
      IF(AS(K) .EQ. 0.0) GO TO 170
      C(I,I)=DAMP
  170 B(I,I)=B(I,I)+AS(K)
      RETURN
      END
```

```
      SUBROUTINE SHAPE(N,X,M,HZ)
      DIMENSION X(N,M)
      COMPLEX X
      WRITE(6,5) HZ
    5 FORMAT(//,5X*     MODE SHAPE FOR FREW = *F10.4*  HZ*//)
      DO 20 I=1,N,2
      AMX=REAL(X(I,1))
      WRITE(6,10) AMX
   10 FORMAT(/,5X,E20.5,/)
   20 CONTINUE
      RETURN
      END
C     C
```

APPENDIX C

EXPERIMENTAL DETERMINATION OF THE MASS MOMENT OF INERTIA

It is sometimes easier to determine a physical property of an object by experimentation rather than a computational method. Such was the case with the grinding wheel and cooling fan for the spindle of the Thompson grinder described in Chapter III.

The procedure for the determination of J for both the items involved their being suspended from the ceiling by a light cord as shown in Fig. B1. Then the wheel was rotated about its centroid by a small amount and released. The frequency of the oscillation can then be recorded and J solved for using the following equation:

$$F = \frac{1}{2\pi}\sqrt{\frac{RG}{J}}$$

where R is the radius of rotation, G is the weight and J is the mass moment of inertia as shown in Fig. B2.

The derivation of this equation is as follows.

Considering Fig. B2, if one sums the rotational forces on the wheel we get

$$R\Psi G = J\ddot{\Psi}$$

or

$$J\ddot{\Psi} + RG\Psi = 0$$

which is analogus to a simple linear spring mass system whose equation of motion is

$$m\ddot{x} + Kx = 0$$

therefore the solution for the frequency of oscillation is of the same form as the simple spring mass system

$$f = \frac{1}{2\pi}\sqrt{\frac{RG}{J}}$$

which when solved for J gives

$$J = \frac{RG}{(2\pi)^2 f^2} \qquad \text{OR} \qquad J = \frac{RGT^2}{2\pi^2}$$

where T is the period of oscillation.

The experimental results are presented in Table B1.

Table B1 Experimental Determination of Mass Moment of Inertia (J)

	Cycles	Time	Period	Weight	R
Grinding Wheel & Hub	24	7.0 (sec)	.291 (sec)	17.85 (lbs)	5.75 (in)
	14	4.2	.300		
	13	3.6	.276		
	20	6.2	.310		
	15	4.2	.280		
	18	5.0	.277		
	15	4.1	.273		
	14	4.0	.285		
	16	4.9	.306		
	13	4.0	.307		
	18	5.6	.311		
	Average Period		.292	$J_{calculated}$=.215 lb-in-sec	
Cooling Fan	41	15.0	.326	3.25	3.75
	30	9.4	.313		
	40	12.8	.320		
	30	9.0	.300		
	25	7.8	.315		
	25	7.8	.315		
	Average Period		.315	$J_{calculated}$=.0303 lb-in-sec	

APPENDIX D

COMPUTER PROGRAM TO GENERATE LOBING USING KINEMATICS

The program listed below was used to graphically prove the theory proposed in section 5.3 which explains the kinematics of lobing. The flow of the program is as follows;

1. Input parameters are declared to statement #5.
2. Calculate the rotational step sizes and direction for the cutting edges and the centre of the cutters rotation.
3. Move each cutting edge in turn through the desired amount of total rotation, saving the profile generated for plotting later.
4. Statement #10 uses the rotation and translation formulas to calculate the X and Y co-ordinates of the cutting edges taking in account the rotation (direction and speed) of the cutter and the rotation (direction and speed) of the centre of the cutter.
5. The resulting figure is then plotted and the program is repeated for a new value of RN.

```
C     TAPPER REAMER CHATTER INVESTIGATION
C
C
C     LIST OF INPUT VARIABLES
C
C
C     A            ANGULAR STEP SIZE OF CUTTER
C     IMAX         TOTAL NUMBER OF STEPS
C     DX           DIAMETER OF CUTTER
C     INX          NUMBER OF CUTTING EDGES
C     DE           DIAMETER OF ECCENTRICITY
C     RN           RATIO OF SPEEDS BETWEEN CUTTER AND
C     ECCENTRICITY   N=SE/SC
C     XDIR         DIRECTION OF ROTATION OF CUTTER (CCW IS +)
C     EDIR         DIRECTION OF ROTATION OF ECCENTRICITY (CCW IS +)
C
C
      DIMENSION XD(400),YD(400)
C
      CALL DATE(THE DATE)
      CALL LETTER(7.,24,90.,.5,1.0,6HDAXTER)
      CALL LETTER(10.,24,90.,1.0,1.0,THE DATE)
      CALL PLOT(10.0,0.0,-3)
C     INPUT DATA
C
      A=0.1
      IAMAX=63
      DX=5.0
      INX=3
      DE=1.0
    3 IKOUNT=0
      RN=2.0
      XDIR=-1.0
      EDIR=-1.0
    5 ICOUNT=1
      I=1
      THET=XDIR*A
      ALPA=EDIR*A*RN
      ATHET=0.0
      AALPA=0.0
   10 XD(I)=((DX/2.0)*COS(ATHET))+((DE/2.0)*COS(AALPA))
      YD(I)=((DX/2.0)*SIN(ATHET))+((DE/2.0)*SIN(AALPA))
      IF(I.LQ.IAMAX*ICOUNT) GO TO 50
      I=I+1
      ATHET=ATHET+THET
      AALPA=AALPA+ALPA
      GO TO 10
   50 CONTINUE
      RROT=(2.0*4.0*ATAN(1.0))/(FLOAT(INX))
      ATHET=RROT*FLOAT(ICOUNT)
      AALPA=0.0
      J=ICOUNT+2
      IF(ICOUNT.GE. INX+1 ) GO TO 100
      I=J+1
```

```
      GO TO 10
  100 NN=I
      XINCR=0.1
      YINCR=0.1
      CALL GRAPH (NN,XD,YD,XINCR,YINCR)
      CALL PLOT(15.0,0.0,-3)
      WRITE(6,101)
  101 FORMAT(5X* PLOT COMPLETE *)
      IKOUNT=IKOUNT+1
      GO TO (30,31,32,33,34,35,36,37,38,39,40,41,42,43,44,45) IKOUNT
   30 RN=3.0
      GO TO 5
   31 RN=4.0
      GO TO 5
   32 RN=5.0
      GO TO 5
   33 RN=6.0
      GO TO 5
   34 RN=7.0
      GO TO 5
   35 RN=8.0
      GO TO 5
   36 RN=9.0
      GO TO 5
   37 RN=10.0
      GO TO 5
   38 RN=11.0
      GO TO 5
   39 RN=12.0
      GO TO 5
   40 RN=13.0
      GO TO 5
   41 RN=14.0
      GO TO 5
   42 RN=15.0
      GO TO 5
   43 RN=16.0
      GO TO 5
   44 RN=17.0
      GO TO 5
   45 IF(INX .EQ. 6) GO TO 400
      INX=INX+1
      GO TO 3
  400 CONTINUE
      CALL PLOT(40.0,0.0,999)
      STOP
      END
```

APPENDIX E

COMPUTER PROGRAM TO GENERATE LOBING USING UNBALANCED CUTTING FORCES TO DEFLECT THE SPINDLE

The program listed below was used to graphically prove that the cutting forces themselves were sufficient to generate lobing. The flow of the program is as follows:

1. Initial positions of the cutting edges are established and then the centre of the cutter is deflected by a set of forces FR and FT to start the lobing.
2. The cutter is then rotated about this new (deflected) centre position and the radius of rotation is increased by an amount FEED to represent the feeding of the cutter into the material.
3. The position of the cutter is then compared to the previous profile to evaluate the depth of cut for each flute.
4. The unbalanced force is then calculated using the depth of cut of each of the teeth.
5. The new profile is then saved and the spindle deflected by the calculated unbalanced force and the sequence is repeated.
6. After every complete rotation of the cutter the profile is plotted by Subroutine Pltpro.

```
C     LIST OF VARABLES
C
C     R                 RADIUS OF CUTTER
C     F                 FEED/REV
C     N                 NUMBER OF CUTTING EDGES
C     CS                CUTTING STIFFNESS
C     SS                SPINDAL STIFFNESS
C     FR                RADIAL STARTING FORCE
C     FT                TANG   STARTING FORCE
C     PRO(JJ,I)=R       PROFILE IN THE JJ REVOLUTI/N
C     NROT              NO OF REV
C
C
      CALL DATE(THE DATE)
      CALL LETTER(7,.24,90.,.5,1.0,6HBAXTER)
      CALL LETTER(10,.24,90.,1.0,1.0,THE DATE)
      CALL PLOT(10.0,0.0,-3)
      IKOUNT=0
      IROT=0
      NROT=10
      JJ=1
      R=0.3
      F=0.005
      N=3
      CS=5000000.0
      SS=50000000.0
      FR=100.0
      FT=400.0
      CR=4.0
      DO 5 I=1,10
      DO 5 J=1,360
    5 PRO(I,J)=0.0
      DO 10 I=1,360
   10 PRO(JJ,I)=R
      THET=6.28/360.0
      FEED=F/360.0
C
C     ESTABLISH INITAL POSITIONS FOR CUTTING EDGES
C
      XCUT(1)=R
      YCUT(1)=0.0
      N1=N-1
      DO 30 I=1,N1
      XCUT(I+1)=R*COS(FLOAT(I)*6.28/FLOAT(N))
      YCUT(I+1)=R*SIN(FLOAT(I)*6.28/FLOAT(N))
   30 CONTINUE
      WRITE(6,25) XCUT(1),XCUT(2),XCUT(3),YCUT(1),YCUT(2),YCUT(3)
   25 FORMAT(6F10.5,//)
```

```
      XCEN=0.0
      YCEN=0.0
      SUMEX=-ER
      SUMEY=-ET
   35 XCEN=XCEN+(SUMEX/SS)
      YCEN=YCEN+(SUMEY/SS)
C     IROT=IROT+1
      XCENT(JJ,IROT)=XCEN
      YCENT(JJ,IROT)=YCEN
      IF(IROT .GE. 360) IROT=0
C
C     ROTATE CUTTER ABOUT THE NEW CENTER
C
      DO 40 I=1,N
      XSAVE=XCUT(I)
      YSAVE=YCUT(I)
      XCUT(I)=XSAVE*COS(THET)-YSAVE*SIN(THET)+XCEN
      YCUT(I)=XSAVE*SIN(THET)+YSAVE*COS(THET)+YCEN
   40 CONTINUE
      WRITE(6,25)  XCUT(1),XCUT(2),XCUT(3),YCUT(1),YCUT(2),YCUT(3)
C
C     FIND CUTTER
C
      DO 50 I=1,N
      AMAG=SQRT(((XCUT(I)-XCEN)*(XCUT(I)-XCEN))+((YCUT(I)-YCEN)*(YCUT(I
     1-YCEN)))
      ANG=ATAN((YCUT(I)-YCEN)/(XCUT(I)-XCEN))
      AMAGG=AMAG+CFED
      XCUT(I)=(AMAGG*((XCUT(I)-XCEN)/AMAG))+XCEN
   50 YCUT(I)=(AMAGG*((YCUT(I)-YCEN)/AMAG))+YCEN
      WRITE(6,25)  XCUT(1),XCUT(2),XCUT(3),YCUT(1),YCUT(2),YCUT(3)
C
C     COMPARE NEW POSITION TO OLD PROFILE
C
      SUMEX=0.0
      SUMEY=0.0
      DO 60 I=1,N
      AMAG=SQRT((XCUT(I)*XCUT(I))+(YCUT(I)*YCUT(I)))
      ANG=ATAN(ABS(YCUT(I))/ABS(XCUT(I)))
      ANGLE=INT(ANG*360.0/6.28)
      IF(XCUT(I) .LT. 0.0) GO TO 52
      IF(YCUT(I) .LT. 0.0) GO TO 54
      GO TO 56
   52 IF(YCUT(I) .GT. 0.0) GO TO 57
      ANGLE=ANGLE+180
      GO TO 59
   54 ANGLE=360-ANGLE
      GO TO 59
   57 ANGLE=180-ANGLE
      GO TO 59
```

```
 56 IF(ANGLE .EQ. 0.0) ANGLE=360
 59 CONTINUE
    CUT(I)=AMAG-PRO(JJ,ANGLE)
    IF(CUT(I) .LE. 0.0) CUT(I)=0.0
    SUMEX=SUMEX+(CUT(I)*CS*(YCUT(I)/AMAG))
    SUMEY=SUMEY-(CUT(I)*CS*(XCUT(I)/AMAG))
    SUMEX=SUMEX-((CUT(I)/CR)*CS*(XCUT(I)/AMAG))
    SUMEY=SUMEY-((CUT(I)/CR)*CS*(YCUT(I)/AMAG))
    WRITE(6,210) ANGLE,JJ,AMAG
210 FORMAT(//,50X,2I10,10X,F10.5)
 60 PRO(JJ+1,ANGLE)=AMAG
    IKOUNT=IKOUNT+1
    IF(IKOUNT .GE. 360) GO TO 70
    GO TO 35
 70 CALL PLTPRO(PRO,XCENT,YCENT,JJ)
    WRITE(6,110)
110 FORMAT(/,5X* PLOT *)
    JJ=JJ+1
    DO 75 I=1,360
    IF(PRO(JJ,I)  .EQ. 0.0) GO TO 76
    GO TO 77
 76 PRO(JJ,I)=PRO(JJ-1,I)
 77 CONTINUE
 75 CONTINUE
    IF(JJ .GE. NROT) GO TO 80
    IKOUNT=0
    GO TO 35
 80 CONTINUE
    STOP
    END
    SUBROUTINE PLTPRO(PRO,XCENT,YCENT,JJ)
    DIMENSION PRO(10,360),XD(360),YD(360),XCENT(10,360),YCENT(10,3
    DO 10 I=1,360
    ANG=FLOAT(I)
    XD(I)=PRO(JJ,I)*COS(ANG*6.28/360.0)
 10 YD(I)=PRO(JJ,I)*SIN(ANG*6.28/360.0)
    YINCR=0.1
    XINCR=0.1
    CALL GRAPH(NN,XD,YD,XINCR,YINCR)
    CALL PLOT(15.0,0.0,-3)
    DO 20 I=1,360
    XD(I)=XCENT(JJ,I)
 20 YD(I)=YCENT(JJ,I)
    CALL GRAPH(NN,XD,YD,XINCR,YINCR)
    CALL PLOT(15.0,0.0,-3)
    RETURN
    END
```

LIST OF REFERENCES

1 Tlusty, J. and F. Koenigsberger. "Machine Tool Structure", Vol. 1, Pergamon Press 1970.

2 Tobias, S.A. and J.D. Smith. "The Dynamic Cutting of Metals", Int. J. MTDR, Vol. 1, No. 4, 1961.

3 Slavicek, Jan. "The Effect of Irregular Tooth Pitch on Stability of Milling", Proceedings 6th MTDR Conference, Manchester 1965, Pergamon Press.

4 Tlusty, J., L.H. Baxter, K.C. Lau, K. Parthiban. "Stability Analysis of Mazak-24 Lathe", a Metalworking Research Group Report #39, McMaster University, 1974.

5 Parthiban, K. "Application of Shock Excitation Technique for Machine Tool Stability Analysis", a M.Eng. Thesis, McMaster University, 1973.

6 El Maraghy, W.H. "On the Dynamic Response of Railway Vehicles", a M.Eng. Thesis, McMaster University, 1972.

7 Thompson, W.T. "Vibration Theory and Applications", Prentice-Hall Inc.

8 Park, C. "Modelling of a Lathe Structure for the Computation of Dynamic Characteristics", a M.Eng. Thesis, McMaster University, 1973.

9 Prentis, Leckie. "Mechanical Vibrations: An Introduction to Matrix Methods." Longmans, 1963.

10 "Specifications and Tests of Metal Cutting Machine Tools." University of Manchester, 1970.

F I G U R E S

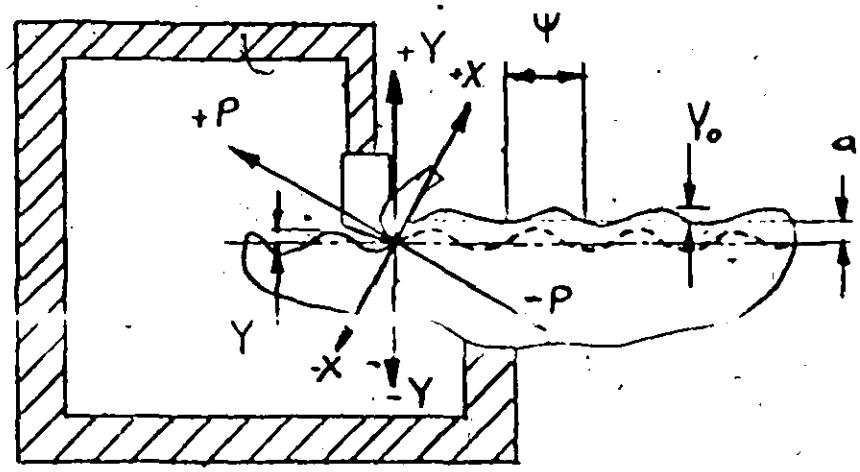

Fig. 1.1 Cutting an Undulated Surface

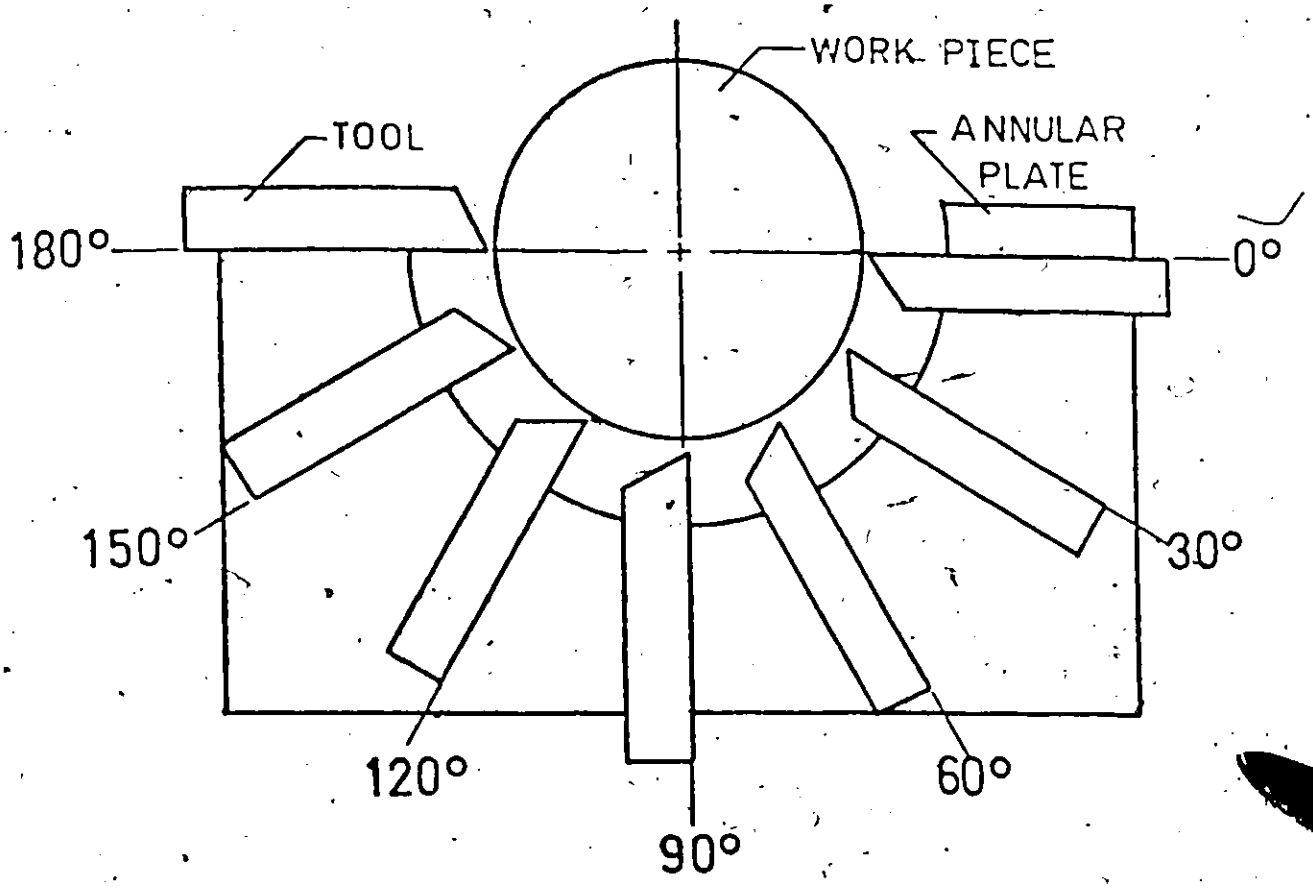

The seven positions of the tool

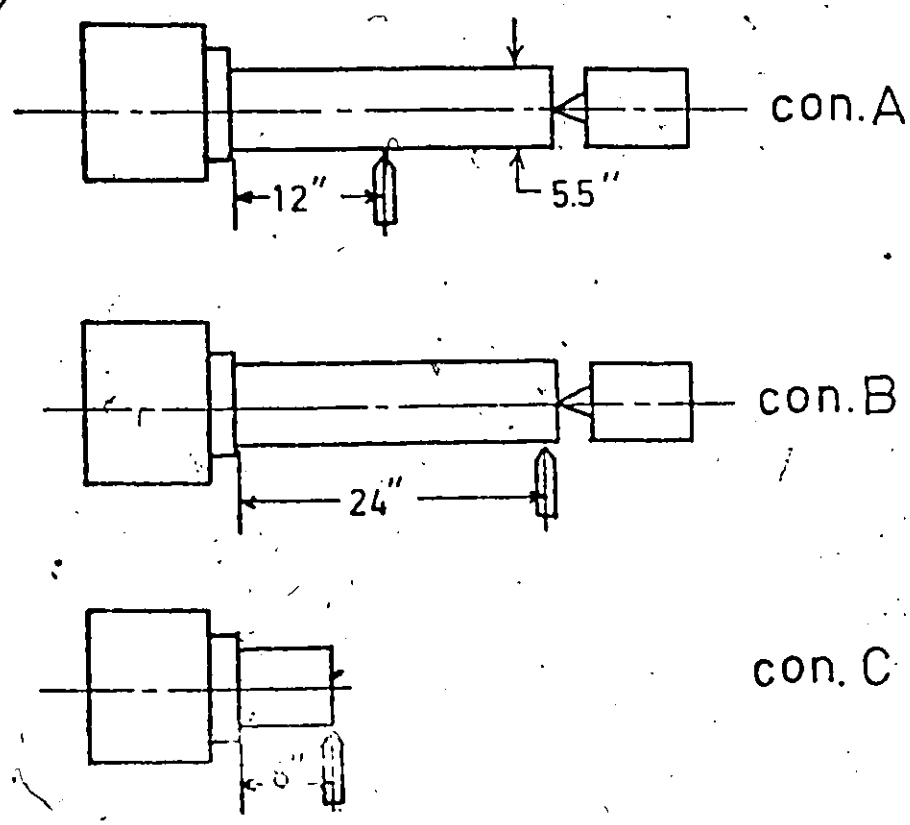

Fig. 2.1 The three Configurations of the tests

Fig. [illegible] (a) Horizontal, Vertical & Cross Receptances for Configuration A.

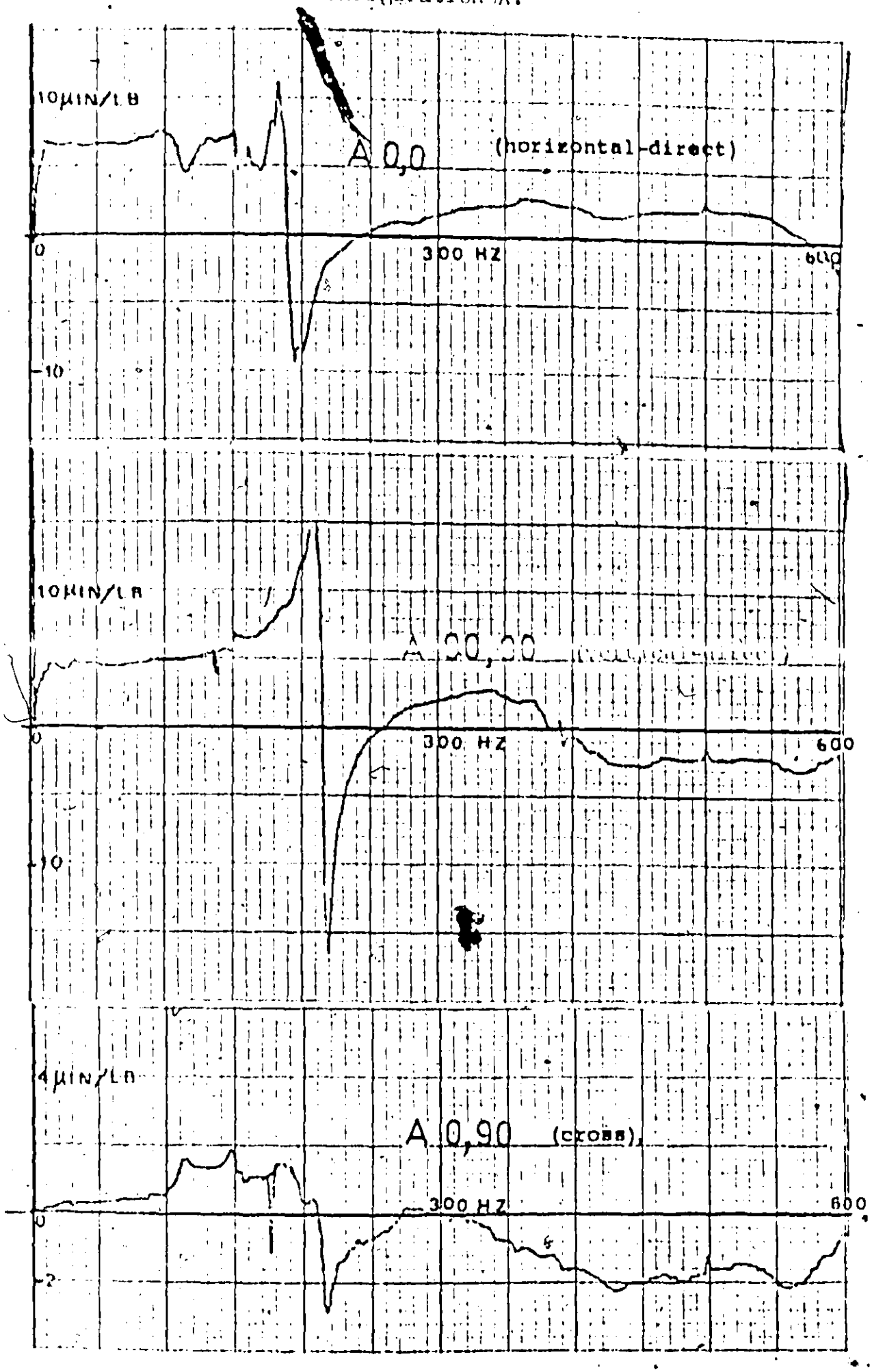

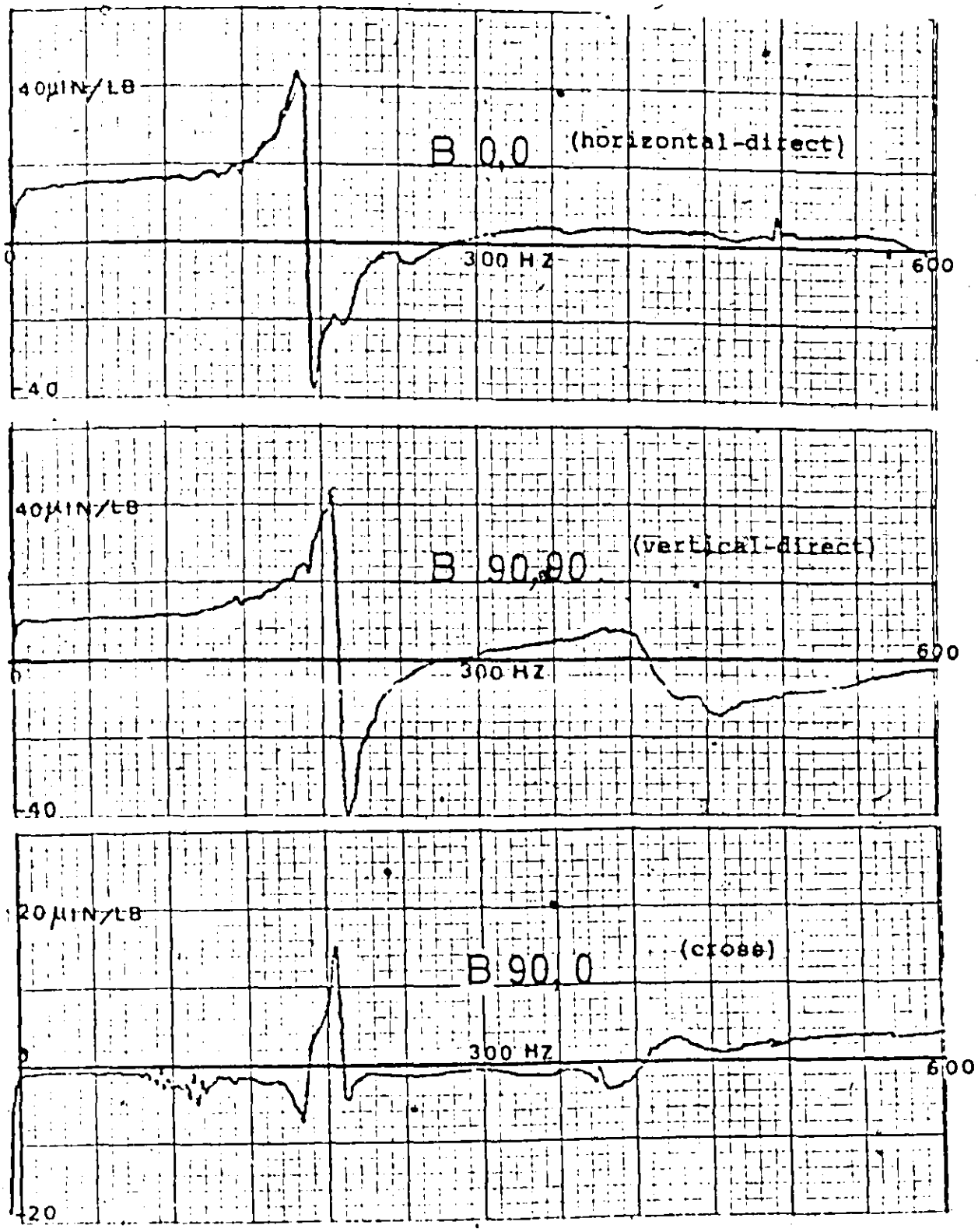

Fig. 2.2 (b) Horizontal, Vertical & Cross Receptances for Configuration B

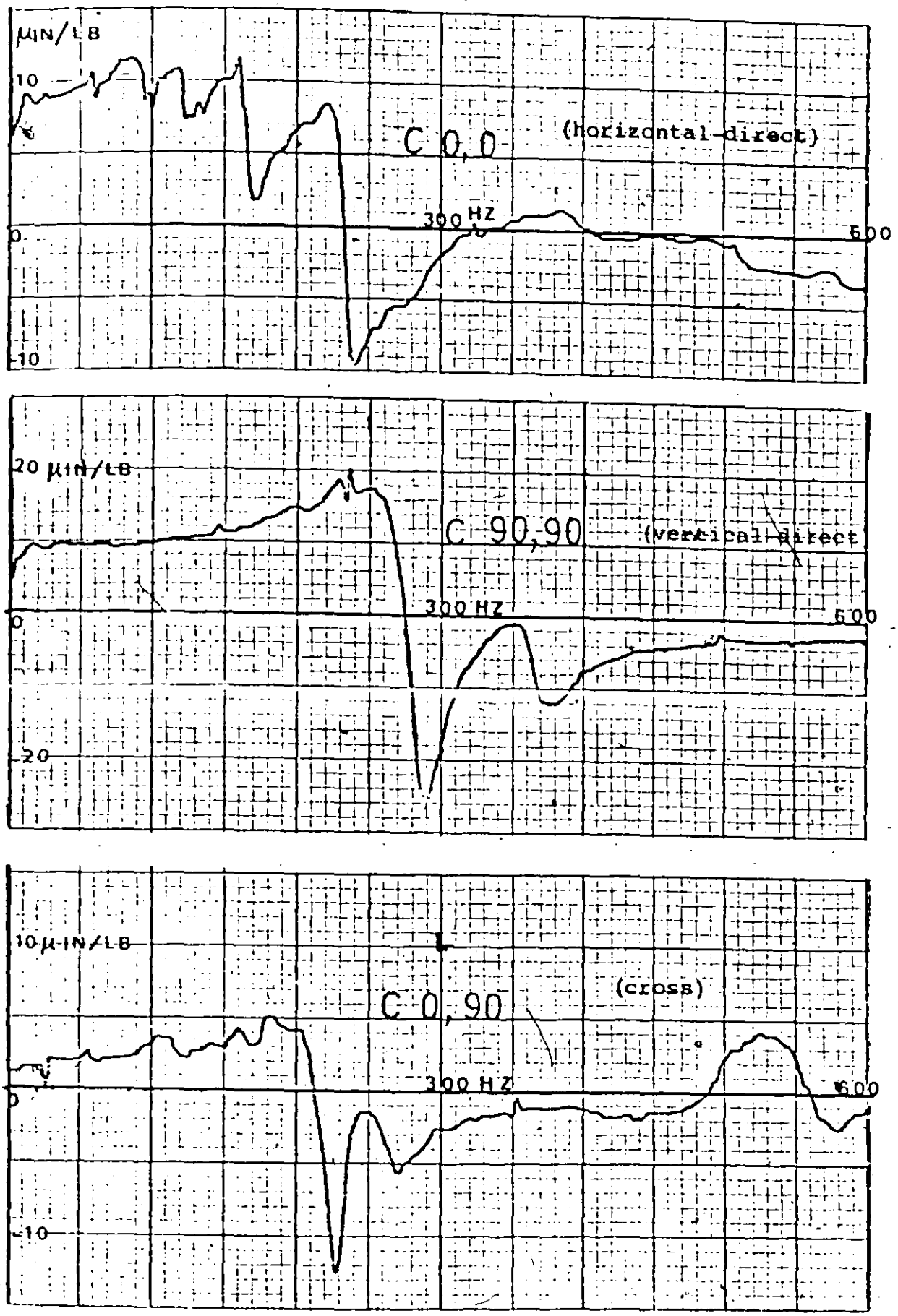

Fig. 2.2 (c) Horizontal, Vertical & Cross Receptances for Configuration C

Decomposed receptance curves for all tool orientations and workpiece configurations.

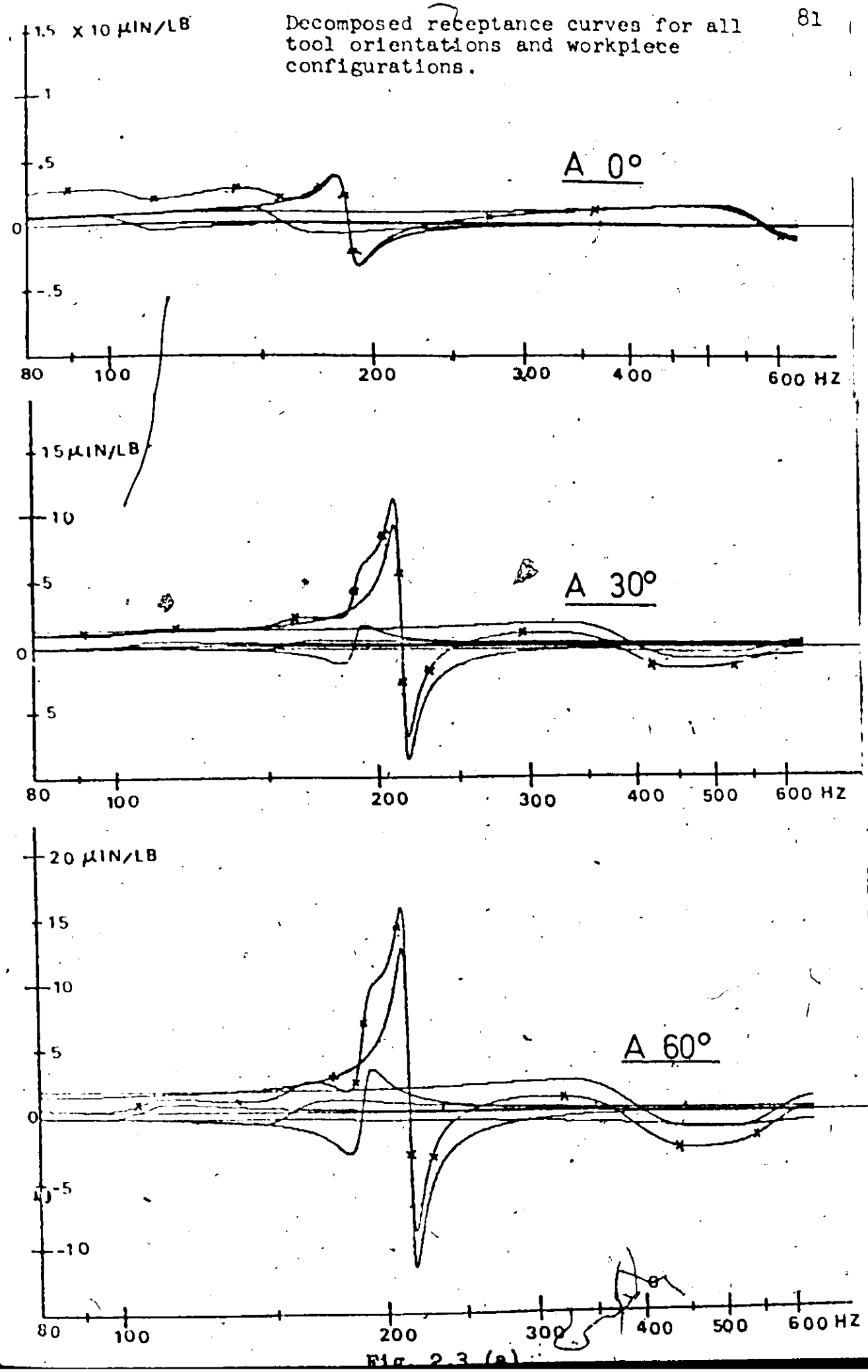

Fig. 2.3 (a)

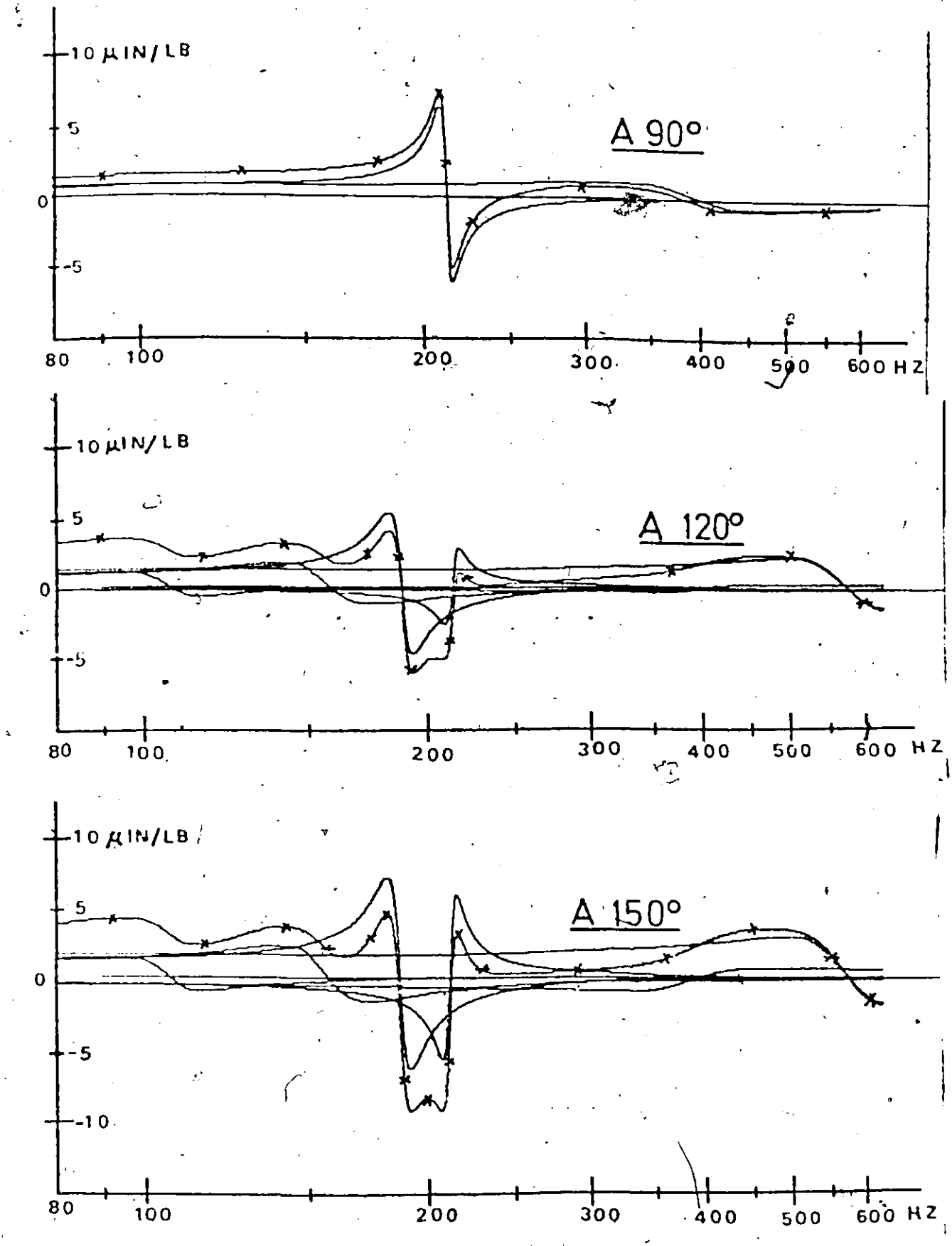
10 μIN/LB
5
0
-5
A 90°
80
100
200
300
400
500
600 HZ
10 μIN/LB
5
0
-5
A 120°
80
100
200
300
400
500
600 HZ
10 μIN/LB
5
0
-5
-10
A 150°
80
100
200
300
400
500
600 HZ

Fig. 2.3 (b)

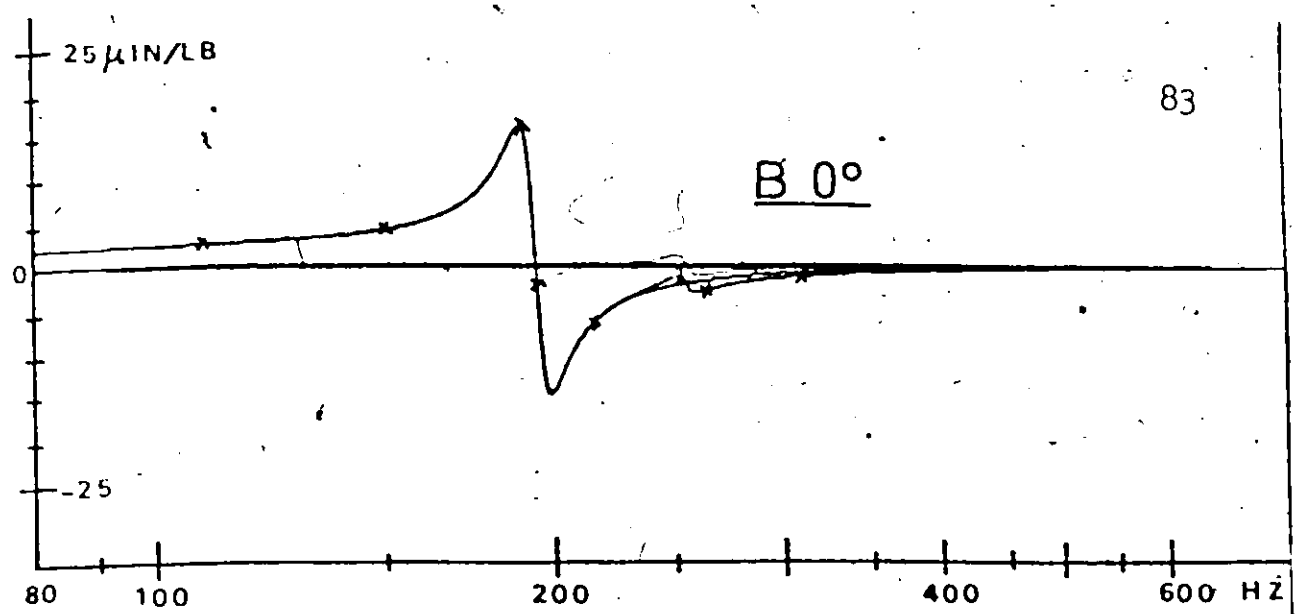
25μIN/LB
B 0°
0
-25
80
100
200
400
600 HZ

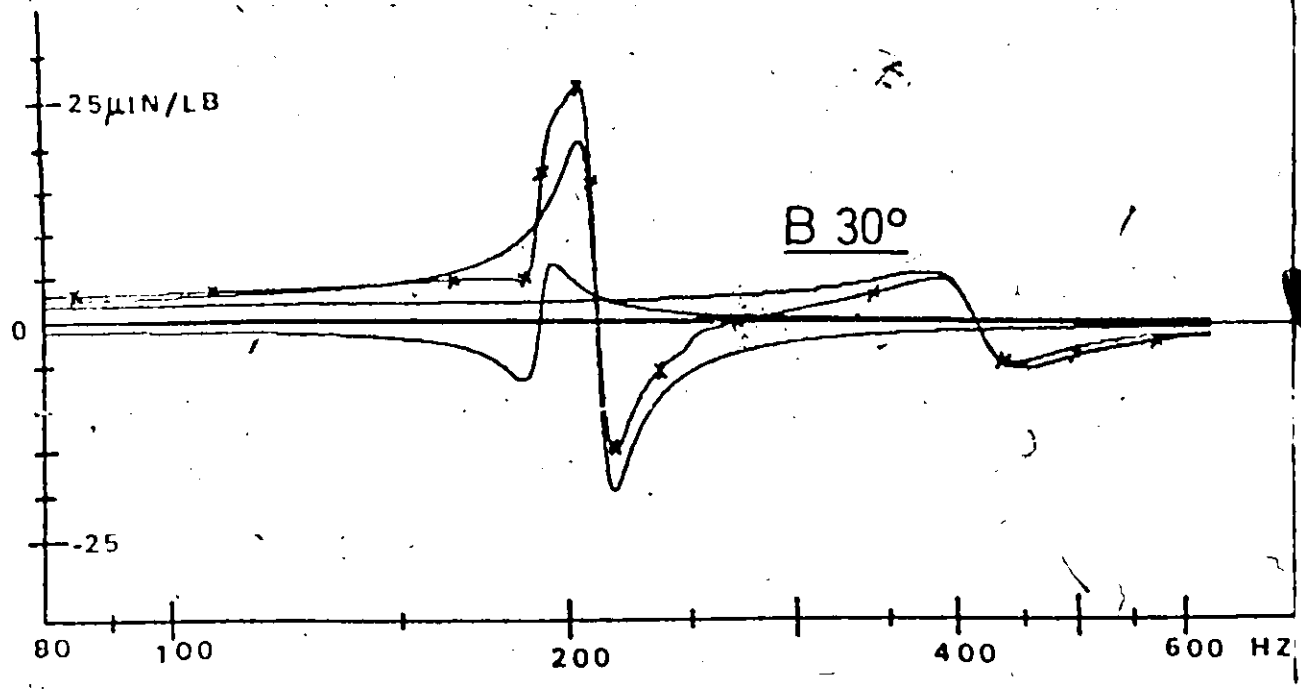
25μIN/LB
B 30°
0
-25
80
100
200
400
600 HZ

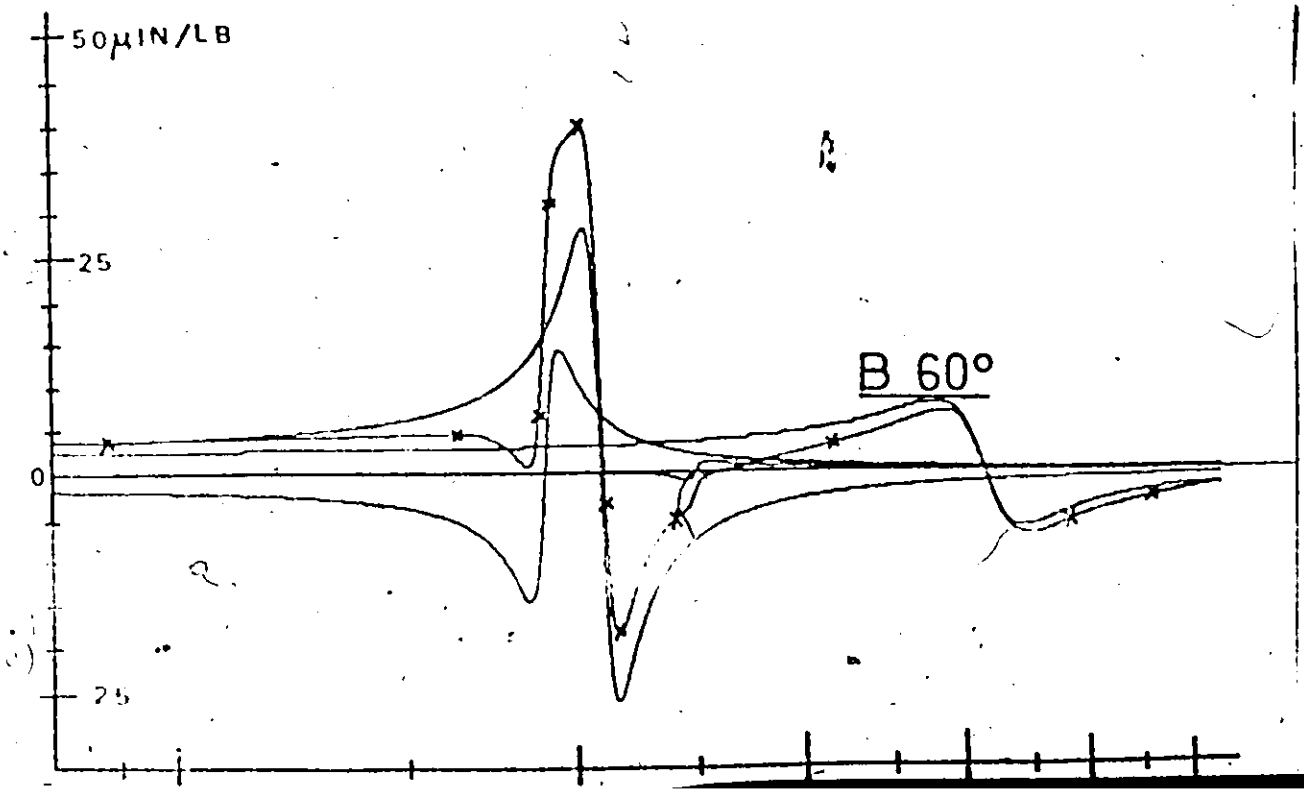
50μIN/LB
25
B 60°
0
-25

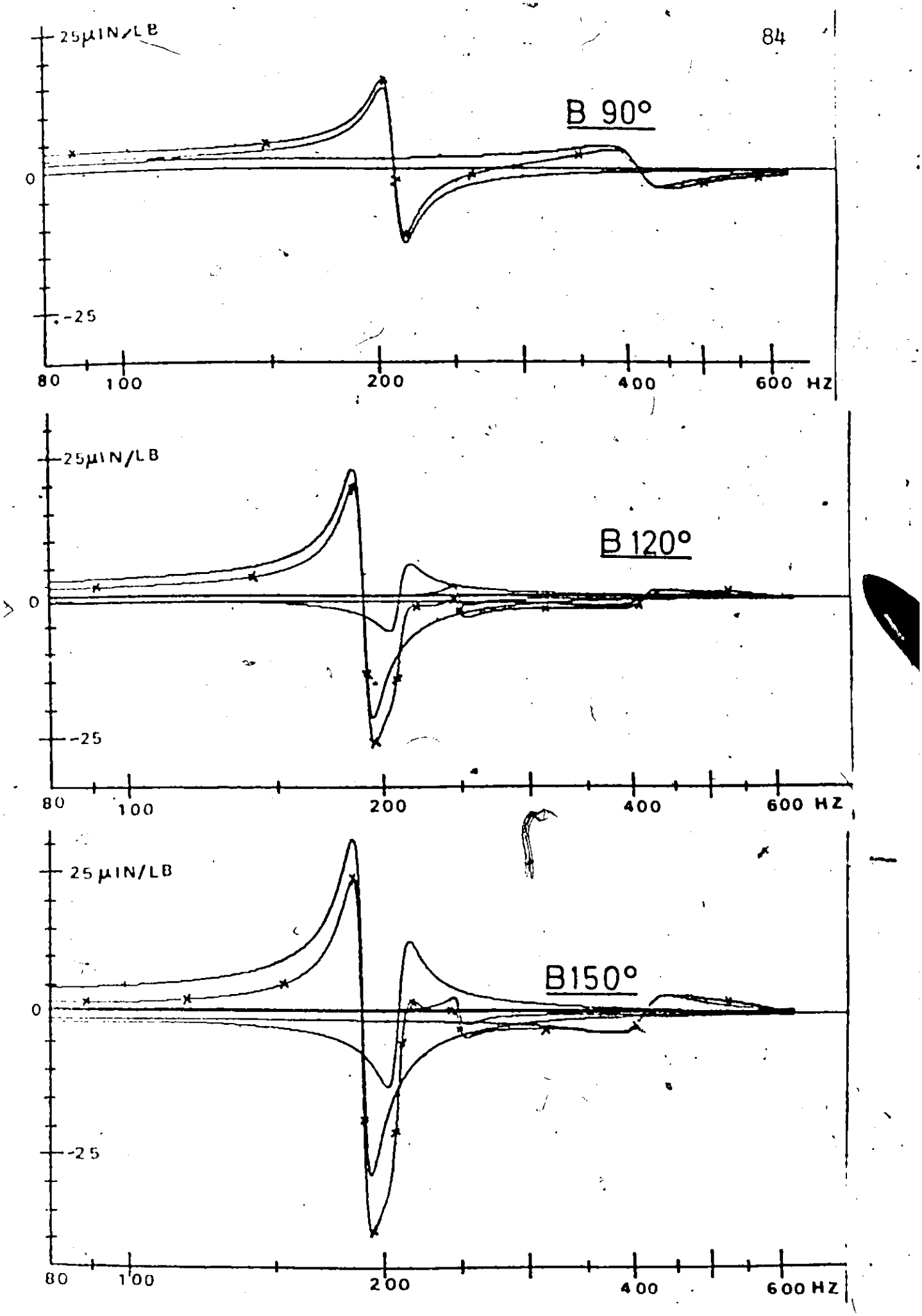
25μIN/LB
B 90°
0
-25
80
100
200
400
600 HZ
25μIN/LB
B 120°
0
-25
80
100
200
400
600 HZ
25 μIN/LB
B150°
0
-25
80
100
200
400
600 HZ

Fig. 2.3 (d)

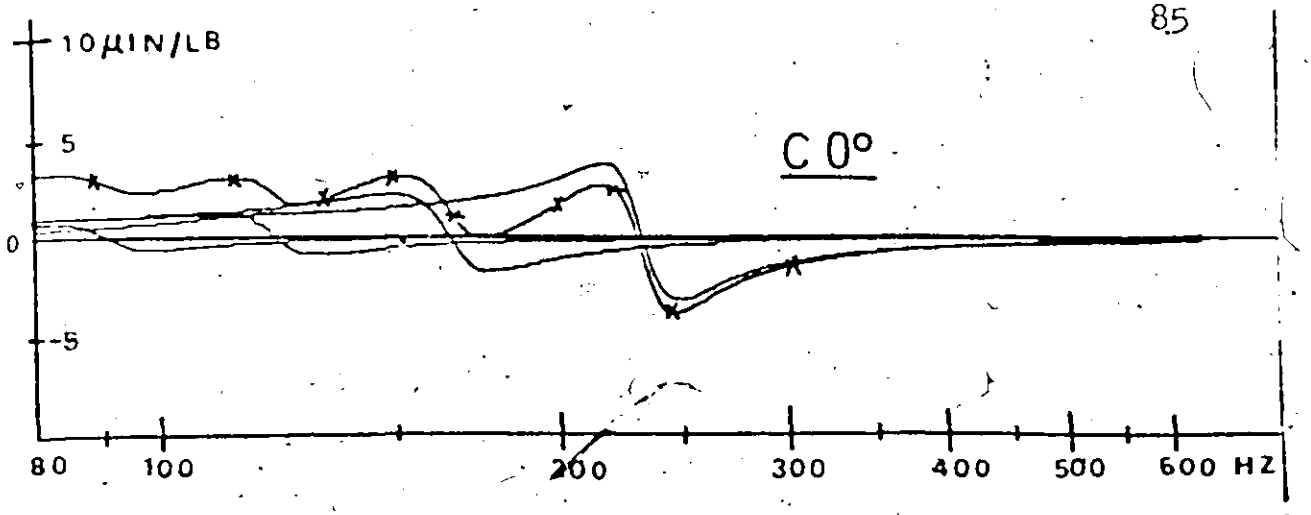
10μIN/LB
5
0
-5
C 0°
80
100
200
300
400
500
600 HZ

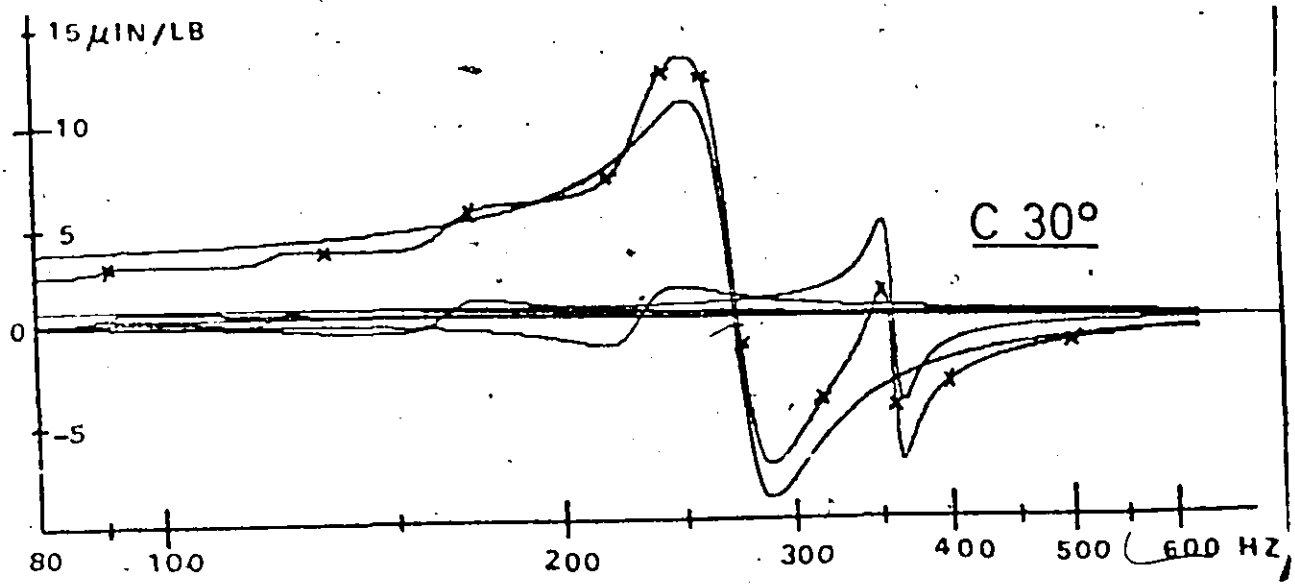
15μIN/LB
10
5
0
-5
C 30°
80
100
200
300
400
500
600 HZ

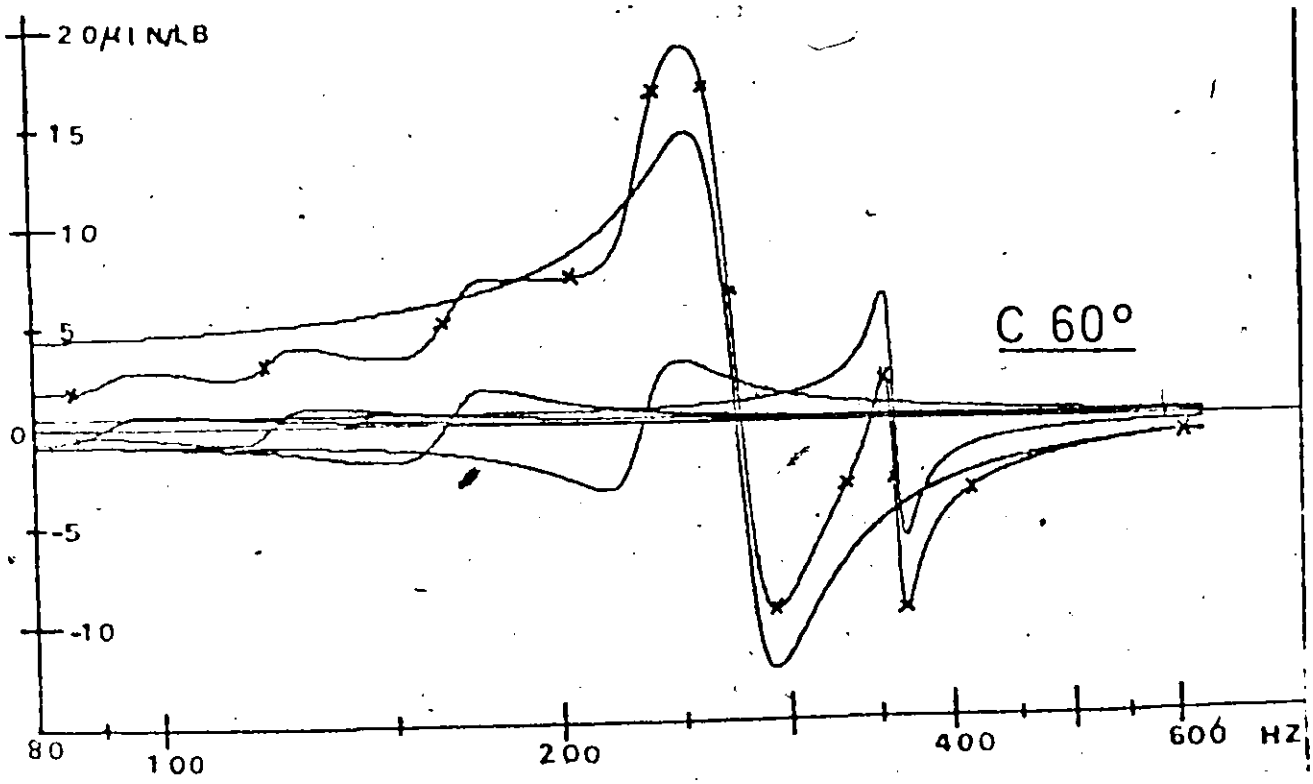
20μIN/LB
15
10
5
0
-5
-10
C 60°
80
100
200
400
600 HZ

Fig. 2.3 (e)

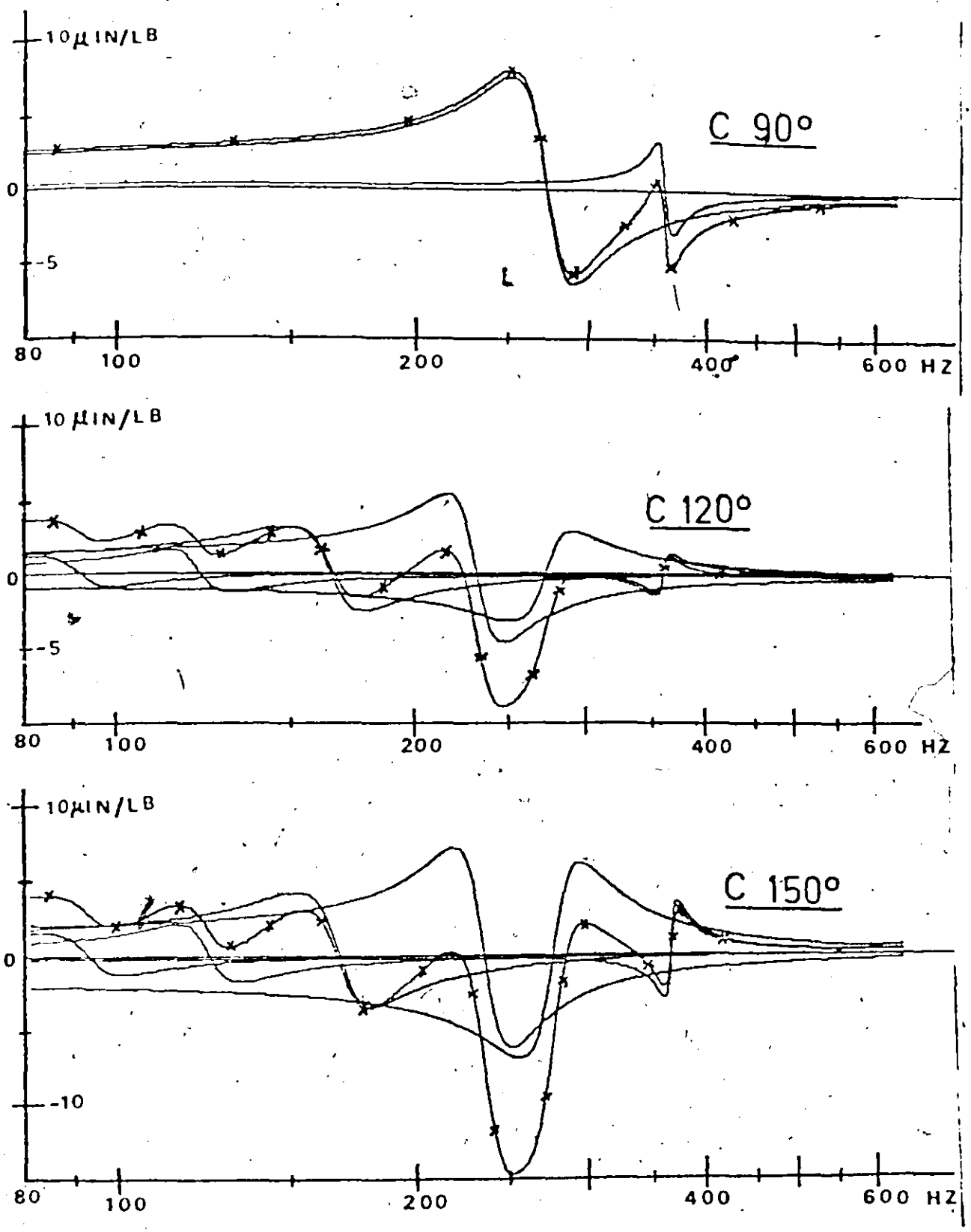
10μIN/LB
C 90°
0
-5
L
80
100
200
400
600 HZ
10 μIN/LB
C 120°
0
-5
80
100
200
400
600 HZ
10μIN/LB
C 150°
0
-10
80
100
200
400
600 HZ

Fig. 2.3 (f)

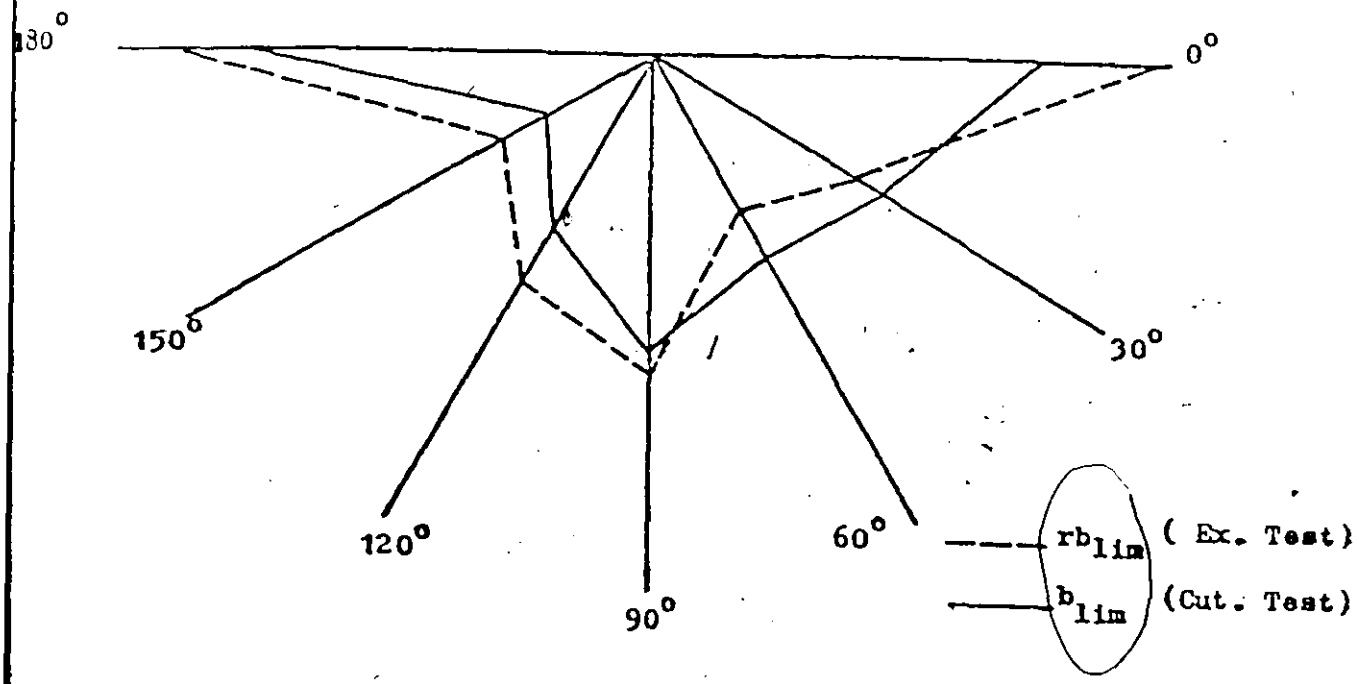

Tool loc.	Cutting test		Excitation Test		
	b_{lim} 10^{-3} in	f_{lim} Hz	$-G_{min}$ u in/lb	rb_{lim} 10^3 lb/in	f_{lim} Hz
0°	400.	170.	3.38	148.0	193.
30°	270.	208.	7.10	70.5	217.
60°	225.	205.	9.25	54.0	217.
90°	296.	220.	5.21	96.0	217.
120°	200.	186.	6.30	79.5	194.
150°	120.	184.	9.64	53.0	194.
180°	410.	175.	3.38	148.0	194.

Fig. 2.4 (a) Cutting Test Data as Compared to Computed Results - Configuration A

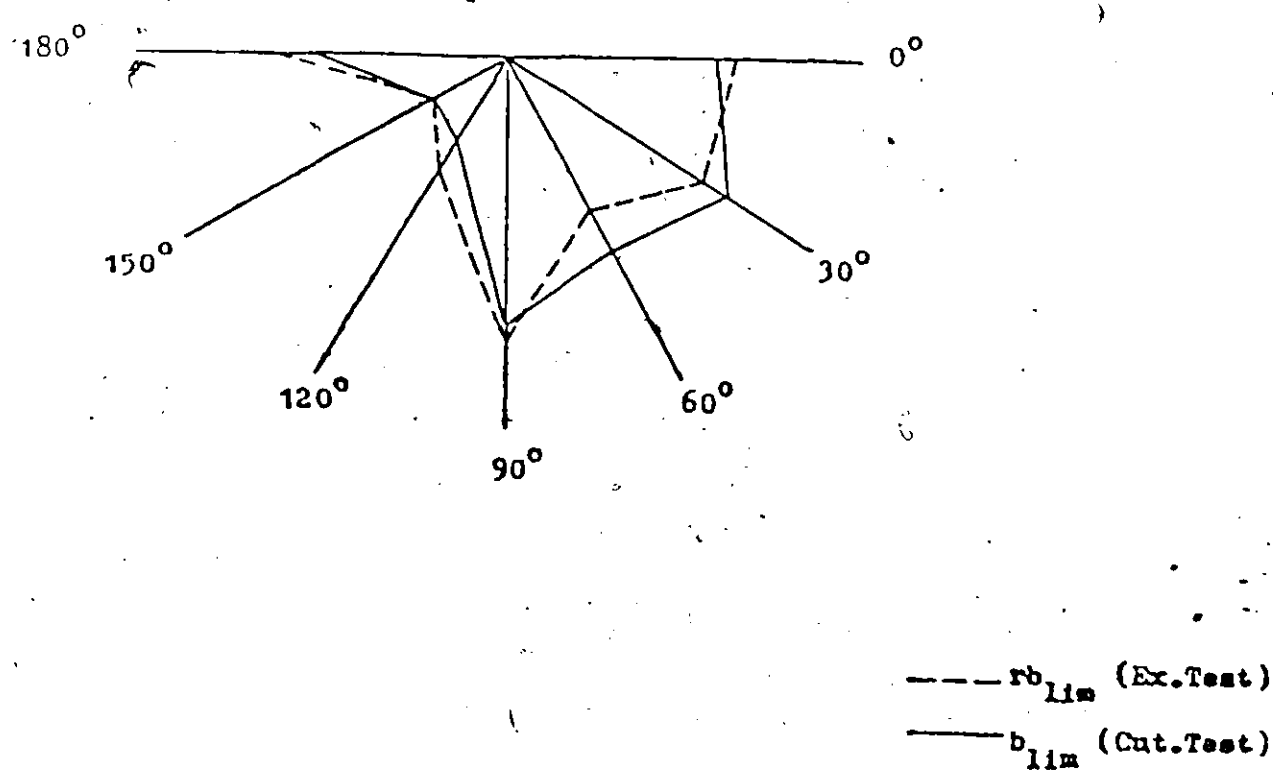

Tool loc.	Cutting test		Excitation Test		
	b_{lim} 10^{-3} in	f_{lim} Hz	$-G_{min}$ u in/lb	rb_{lim} 10^3 lb/in	f_{lim}
0°	110.	172.	14.67	34.1	195.
30°	130.	230.	15.16	33.0	216.
60°	110.	230.	18.74	26.7	216.
90°	145.	215.	12.02	41.5	216.
120°	45.	185.	26.10	19.2	196.
150°	40.	172.	39.34	12.7	196.
180°	130.	200.	14.63	34.1	195.

Fig. 2.4 (b) Cutting Test Data as Compared to Computed Results - Configuration B

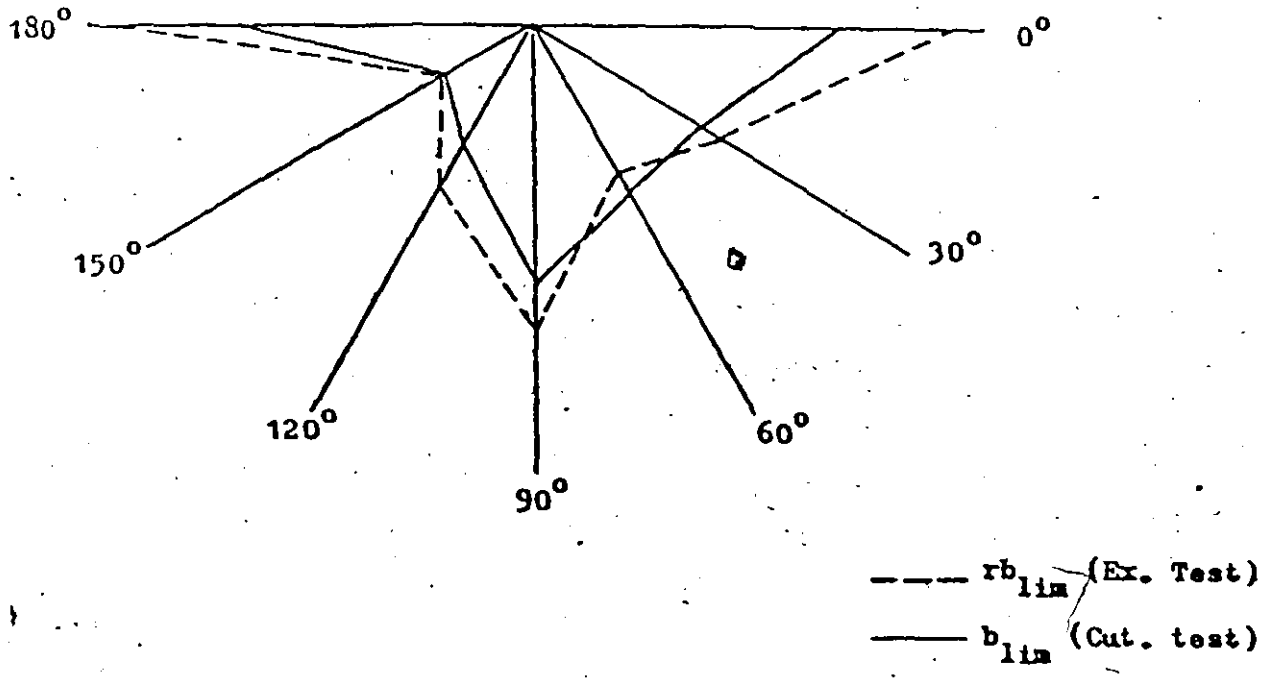

Tool loc.	Cutting Test		Excitation Test		
	b_{lim} 10^{-3} in	f_{lim} Hz	$-G_{min}$ u in/lb	rb_{lim} 10^3 lb/in	f_{lim} Hz
0°	310.	210.	3.95	126.5	245.
30°	200.	275.	7.66	65.0	292.
60°	195.	286.	9.68	51.3	292.
90°	250.	310.	5.89	89.5	292.
120°	140.	256.	9.08	55.0	247.
150°	110.	250.	14.94	33.4	248.
180°	285.	250.	3.96	126.5	245.

Fig. 2.4 (c) Cutting Test Data as Compared to Computed Results - Configuration C

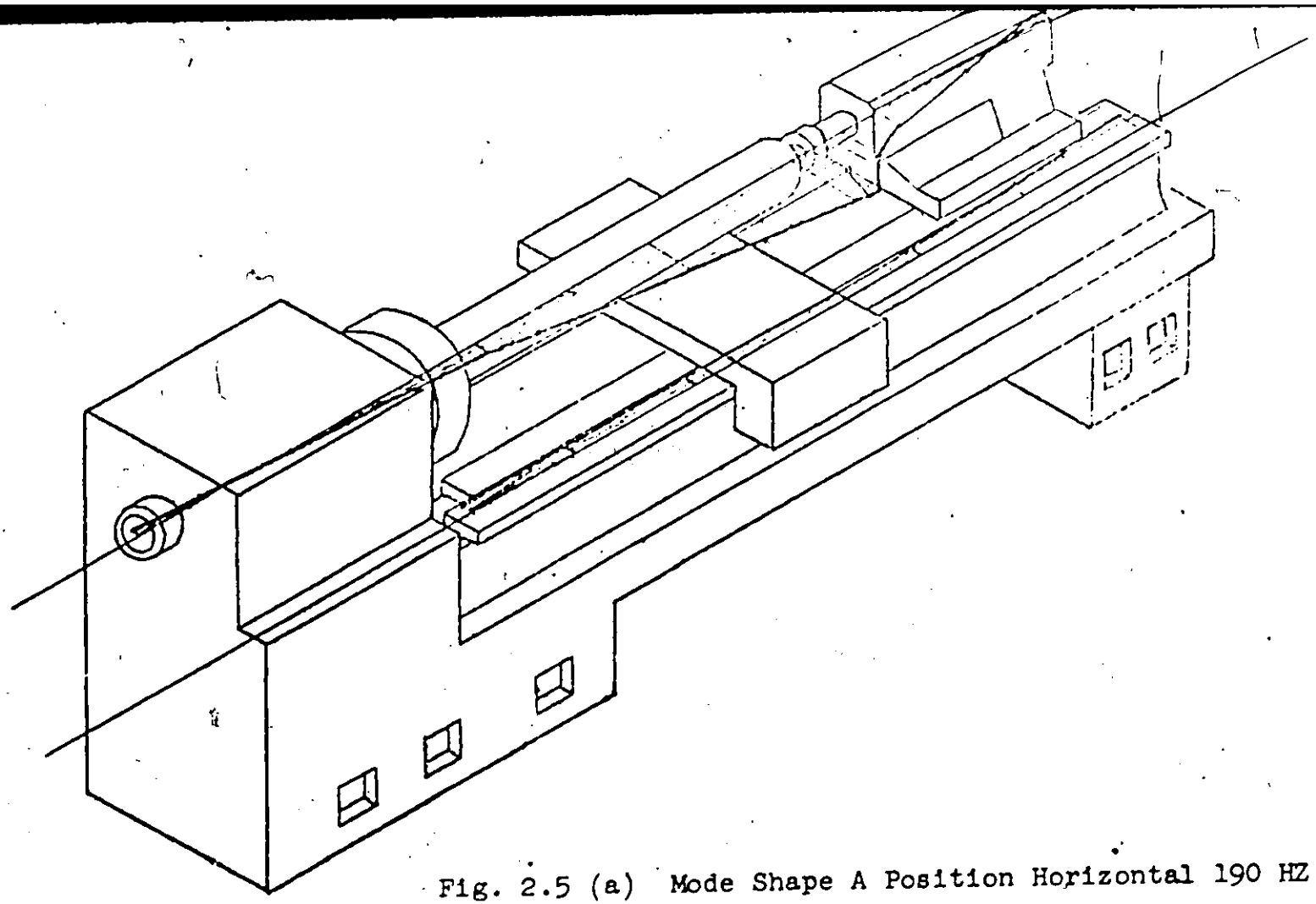

Fig. 2.5 (a) Mode Shape A Position Horizontal 190 HZ

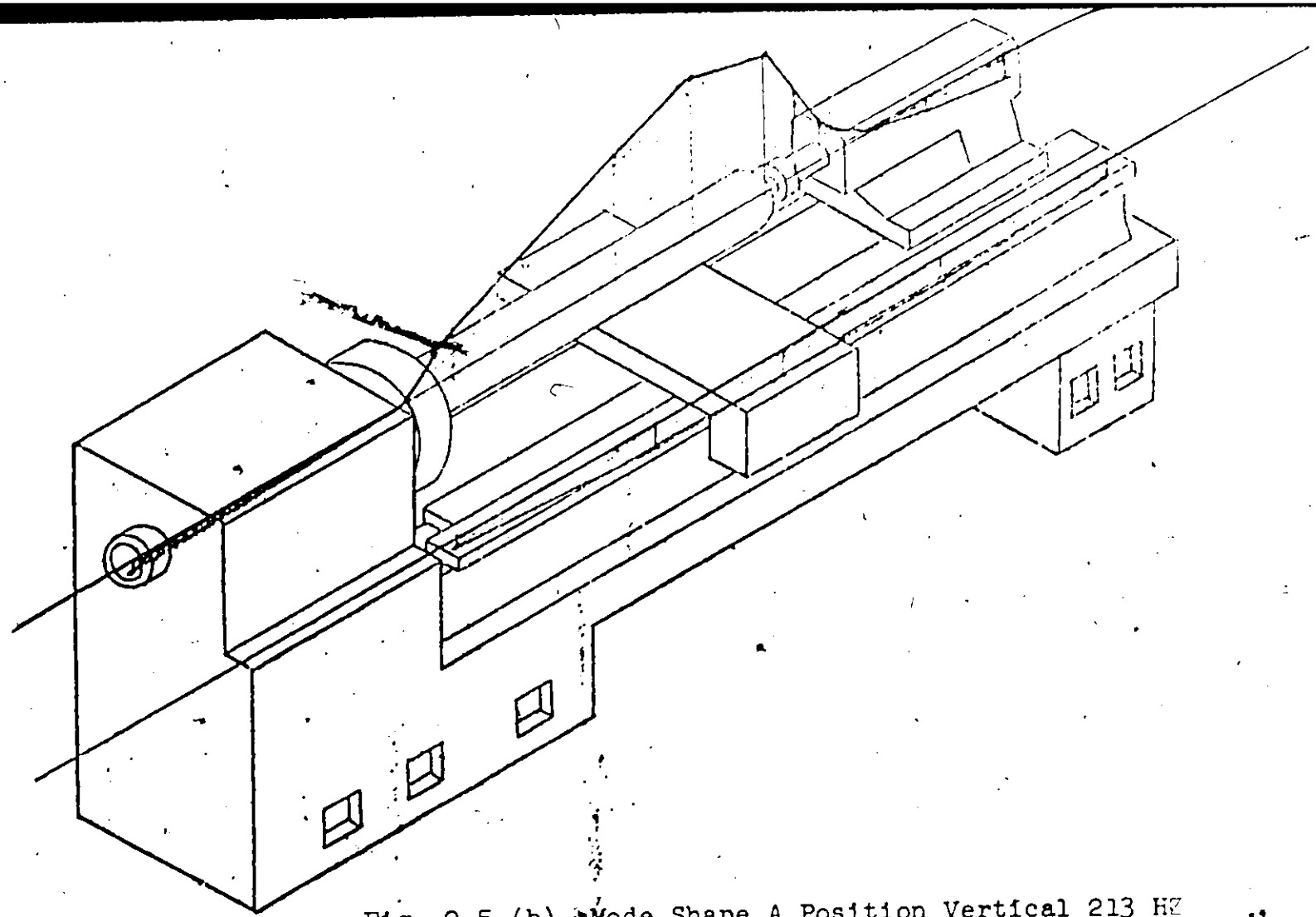

Fig. 2.5 (b) Mode Shape A Position Vertical 213 HZ

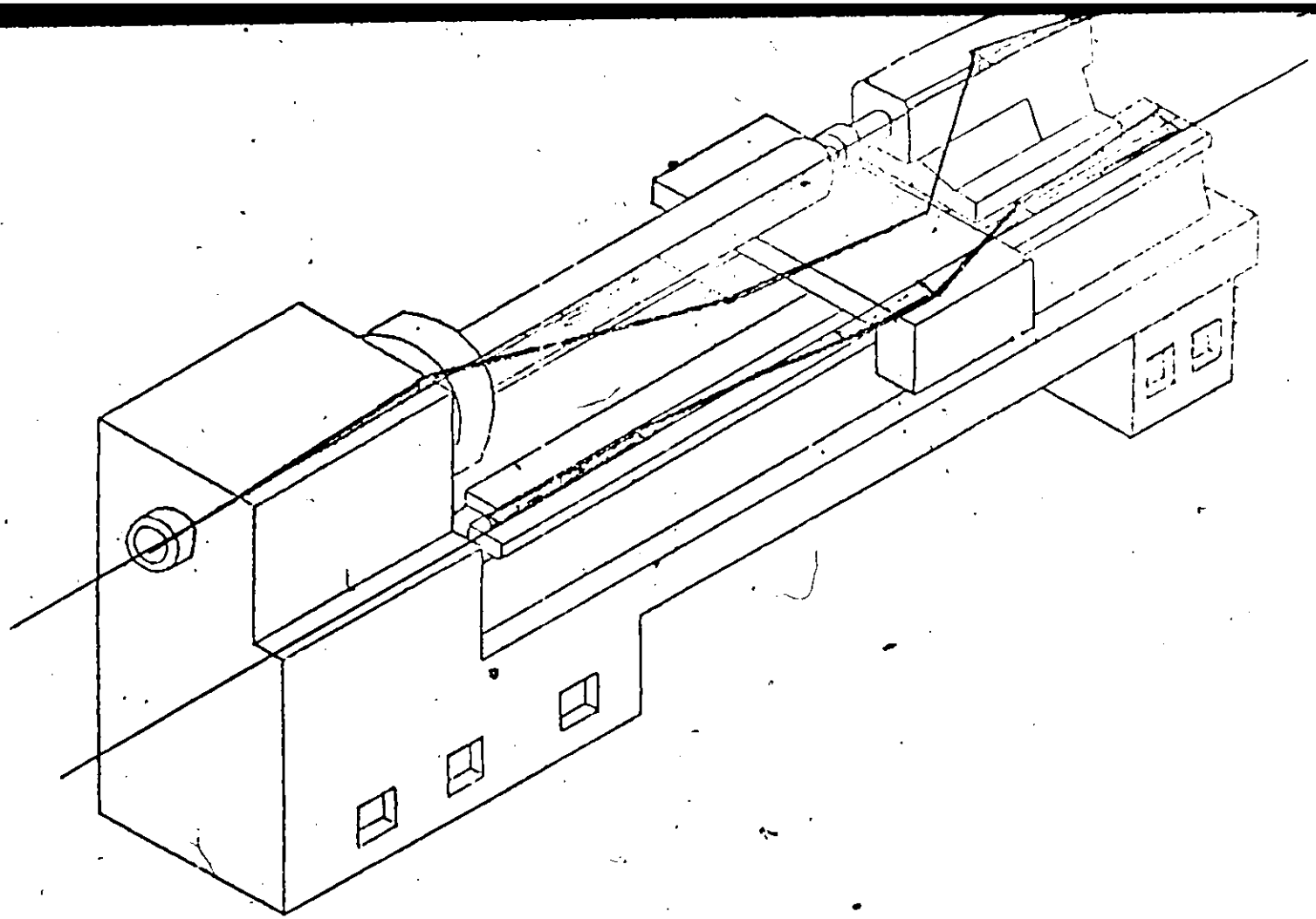

Fig. 2.5 (e) Mode Shape B Position Horizontal 190 HZ

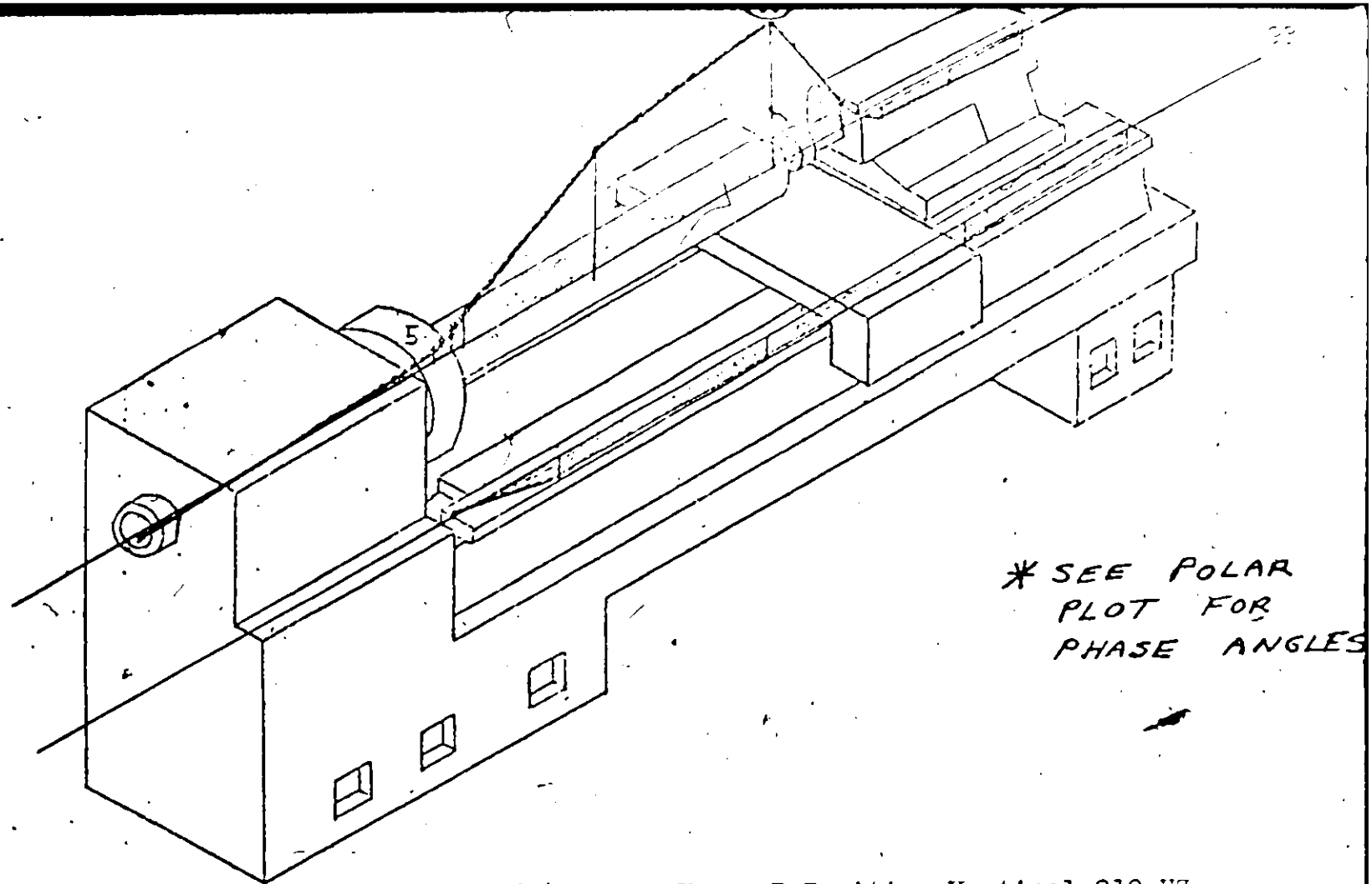

Fig. 2.5 (d) Mode Shape B Position Vertical 210 HZ

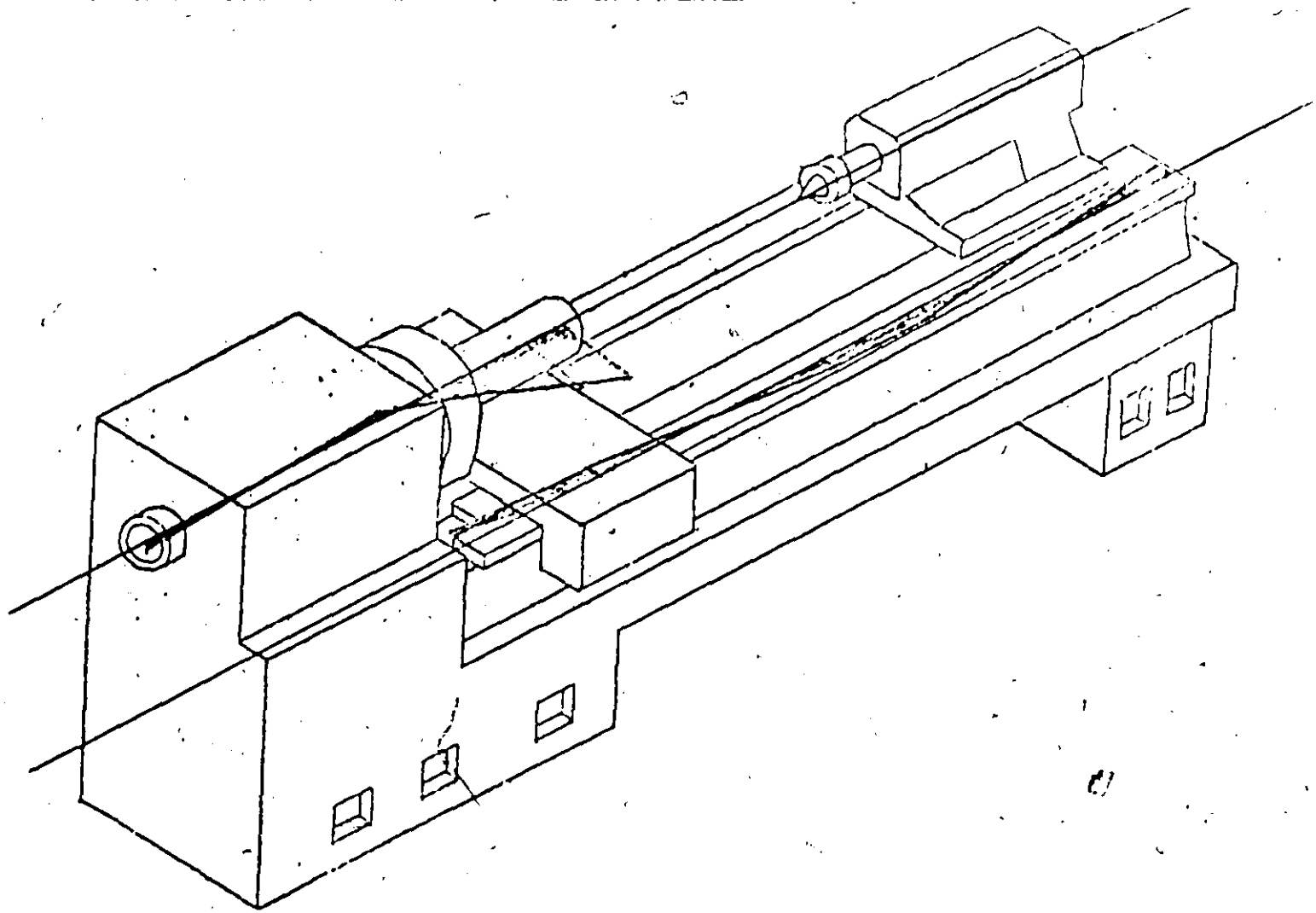

Fig. 2.5 (e) Mode Shape C Position Horizontal 230 HZ

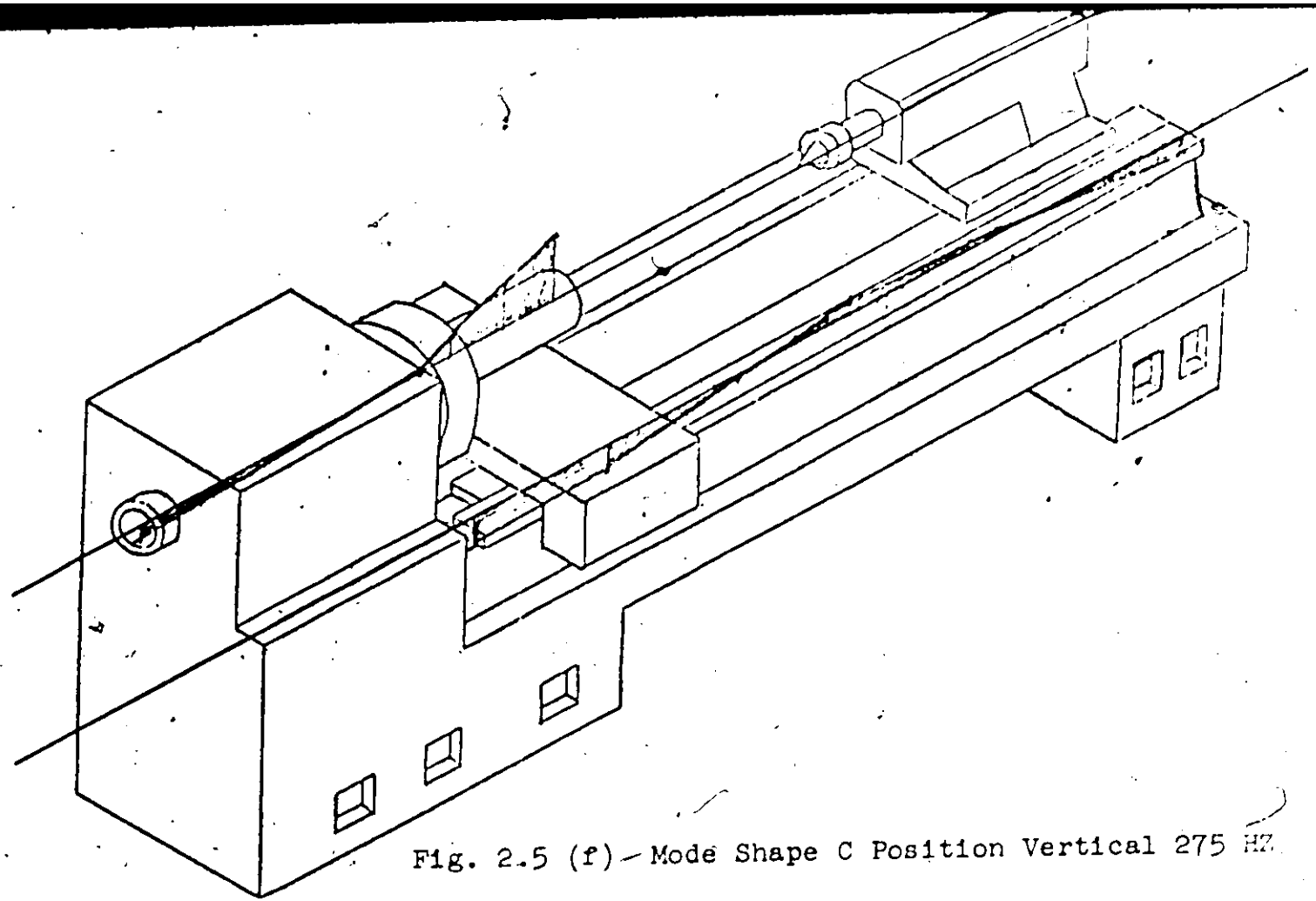

Fig. 2.5 (f) – Mode Shape C Position Vertical 275 HZ

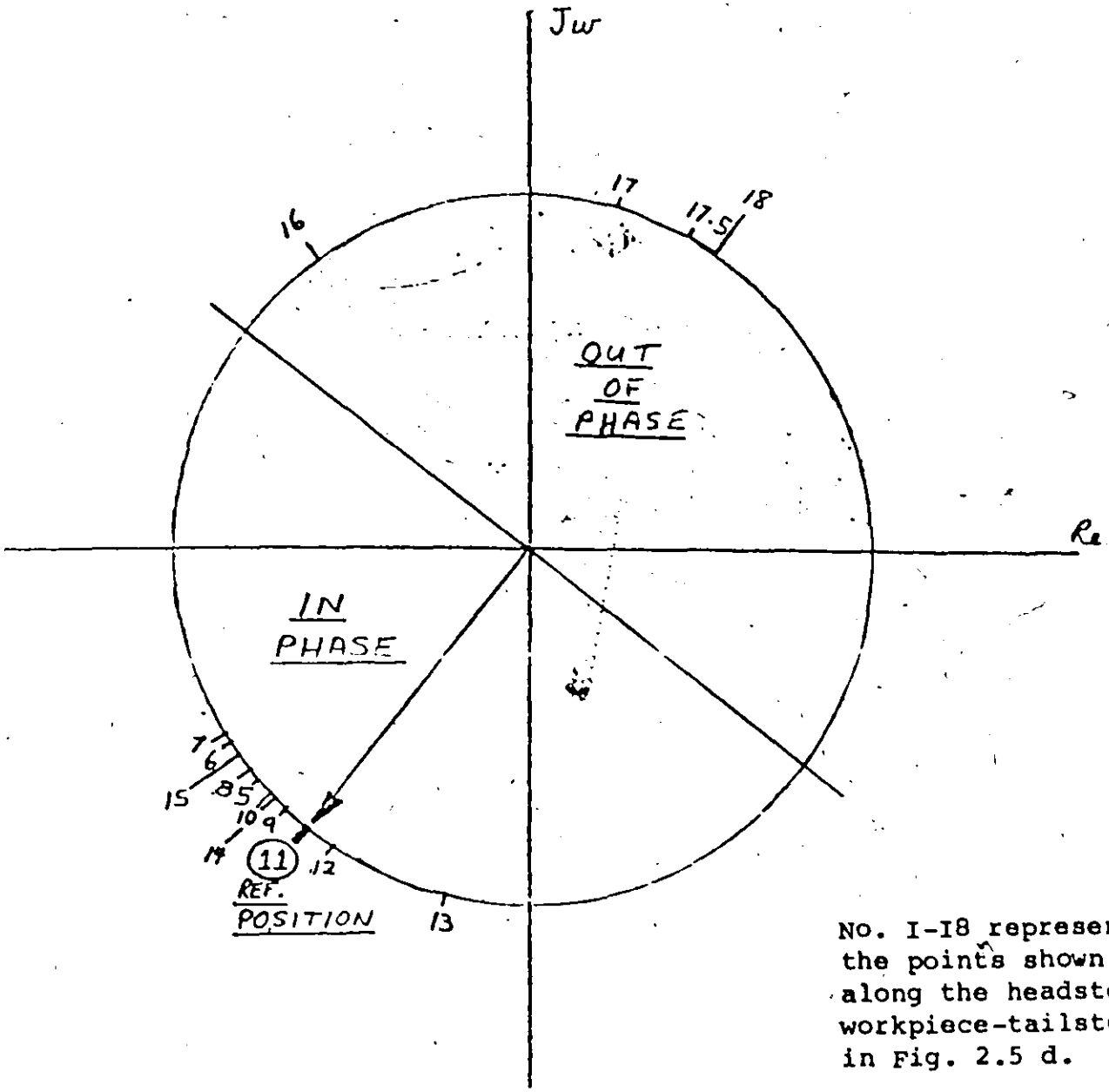

No. I-18 represent the points shown along the headstock-workpiece-tailstock in Fig. 2.5 d.

POLAR PLOT OF PHASE ANGLES FOR "B" POSITION VERTICAL (SPINDAL)

Fig. 2.6

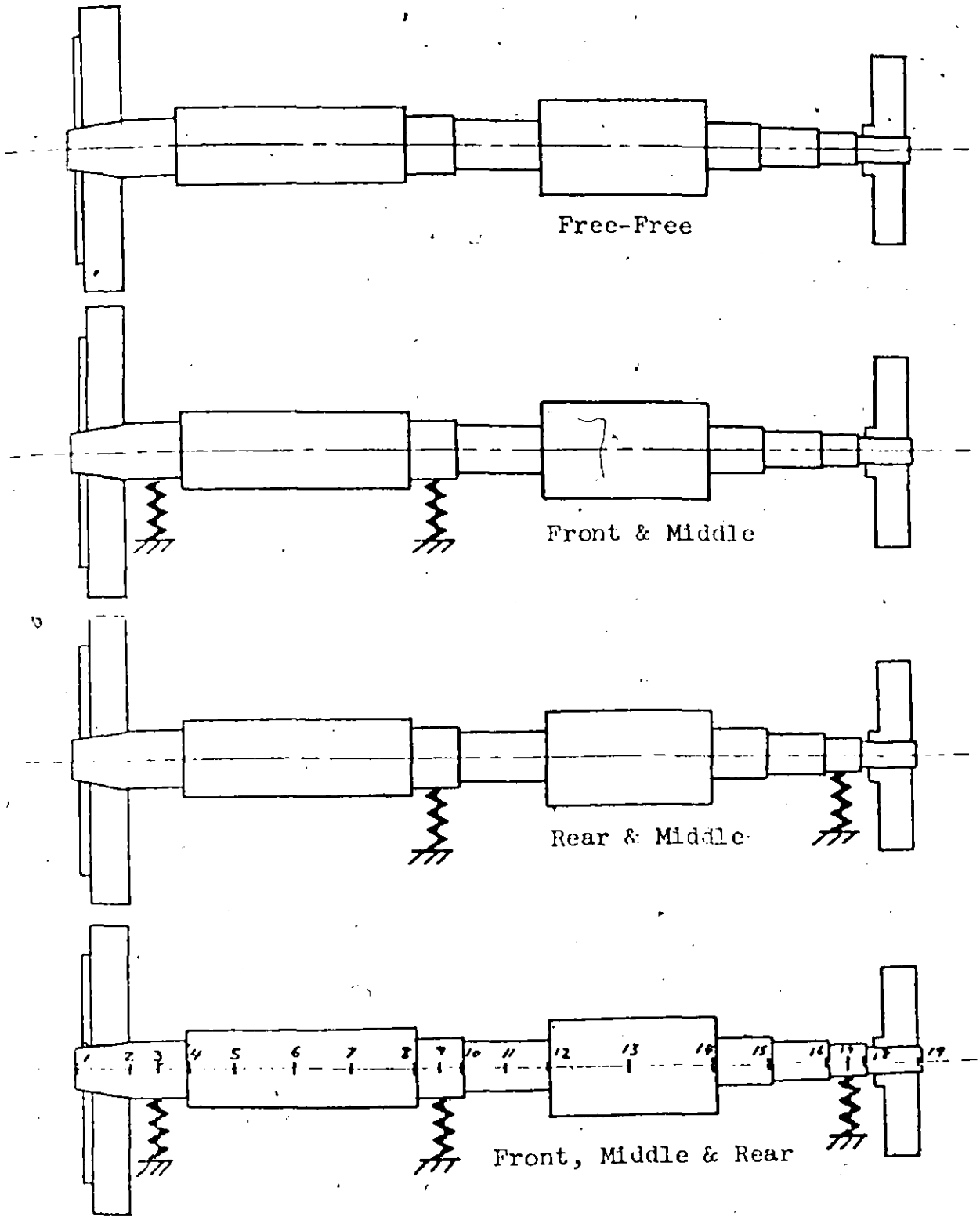

Fig. 3.1 Three Bearing Configurations and Free-Free State

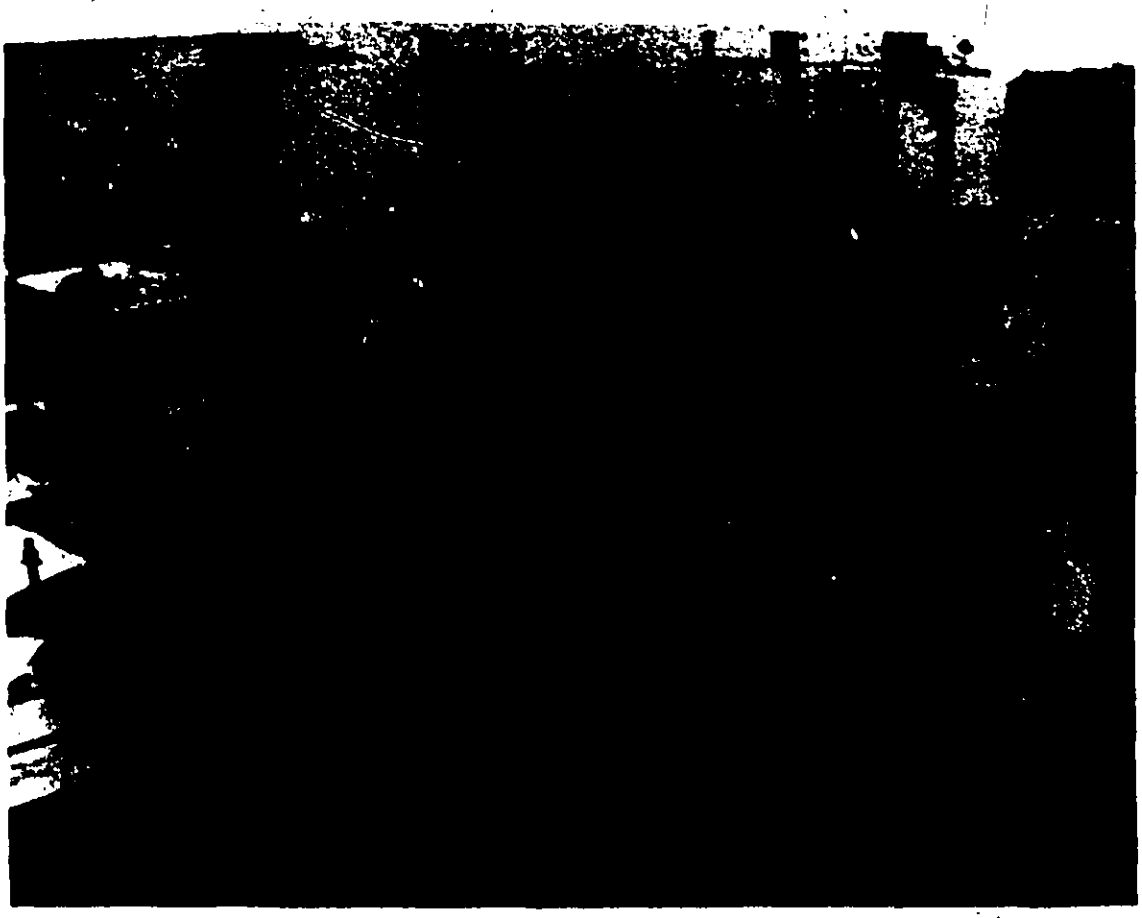

Fig. 3:2 Grinding Headstock Mounted on the Bed Plate

Fig. 3.3 Grinding Headstock With Capacitive Probe Mounted at Spindle Position #1

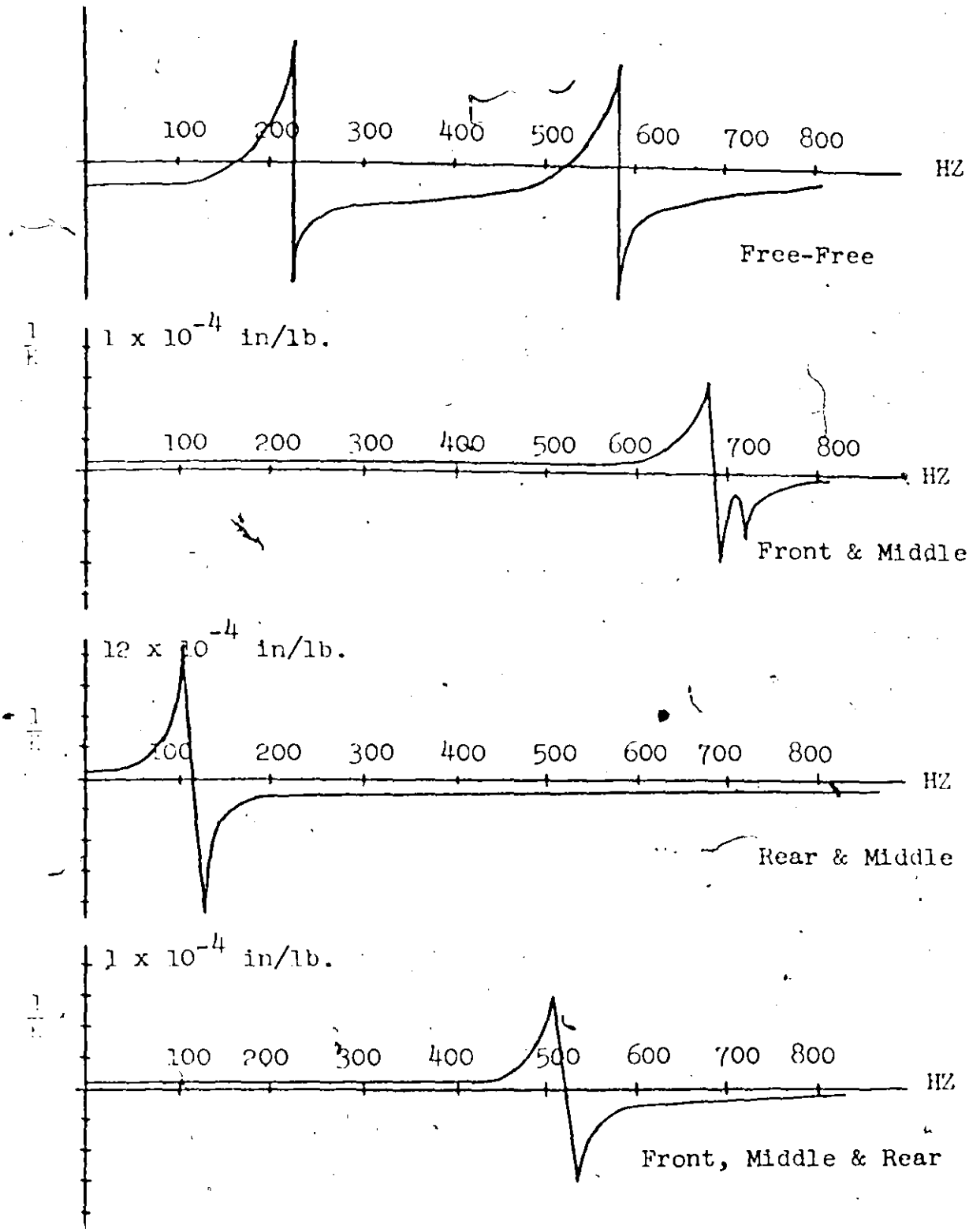

Fig. 3.4 Receptance Curves for the Three Bearing Configurations and Free-Free

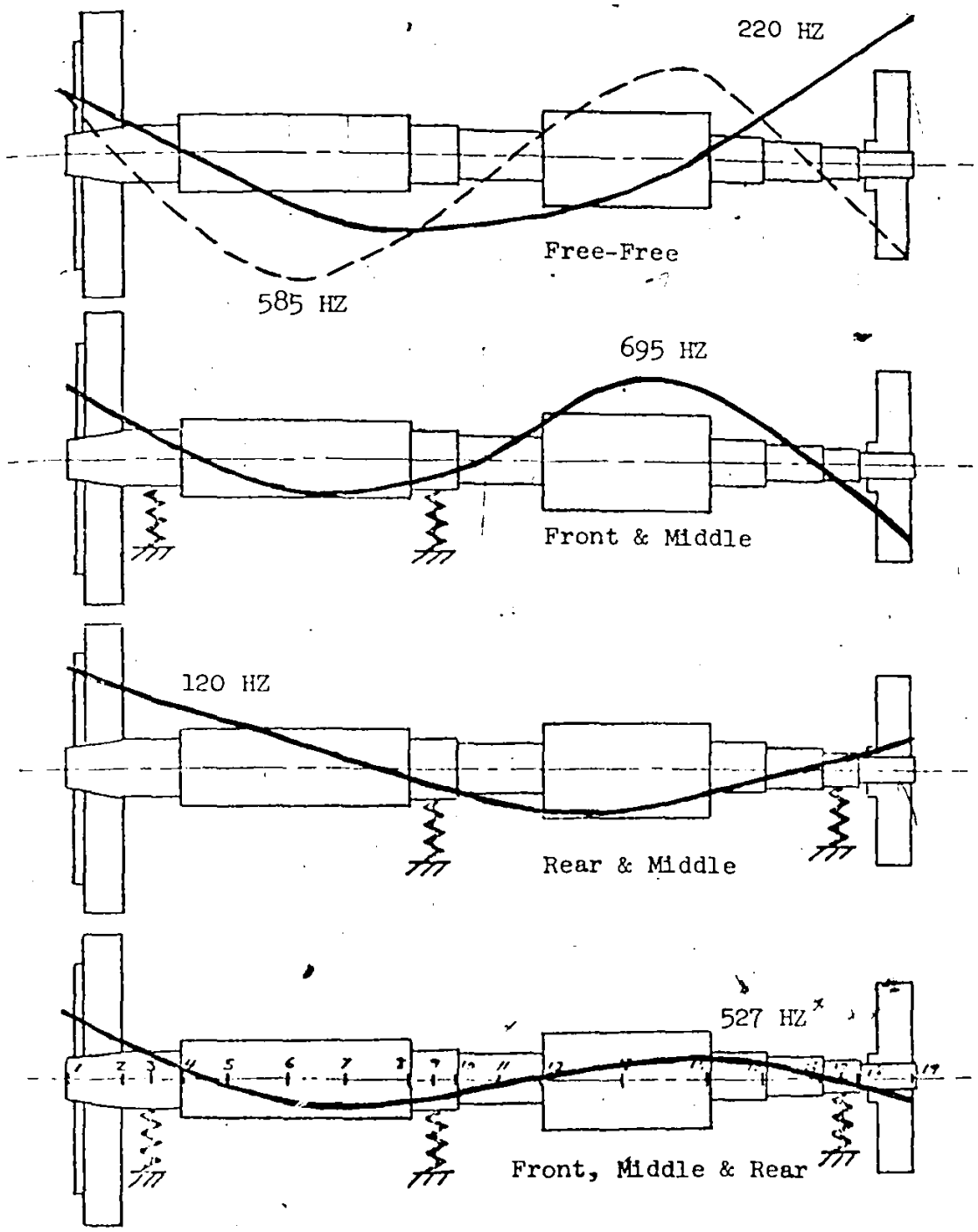

Fig. 3.5 Mode Shapes for the Three Bearing Configurations and the Free-Free Case

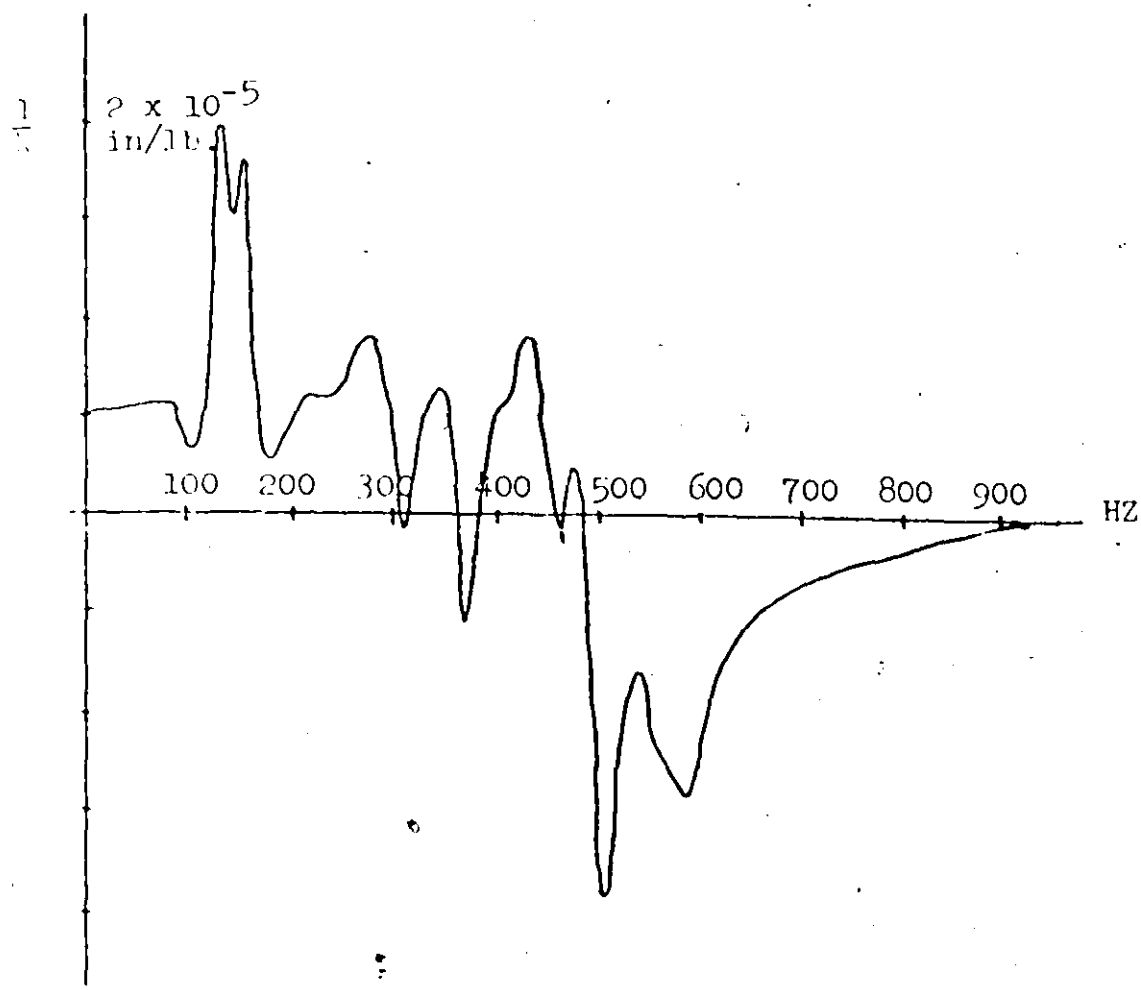

Fig. 3.6 Faulty Receptance Curve for the Front, Middle and Rear Bearing Configuration.

Fig. 3.7 Rigid Probe Holder for Relative Vibration Between Spindle and Case

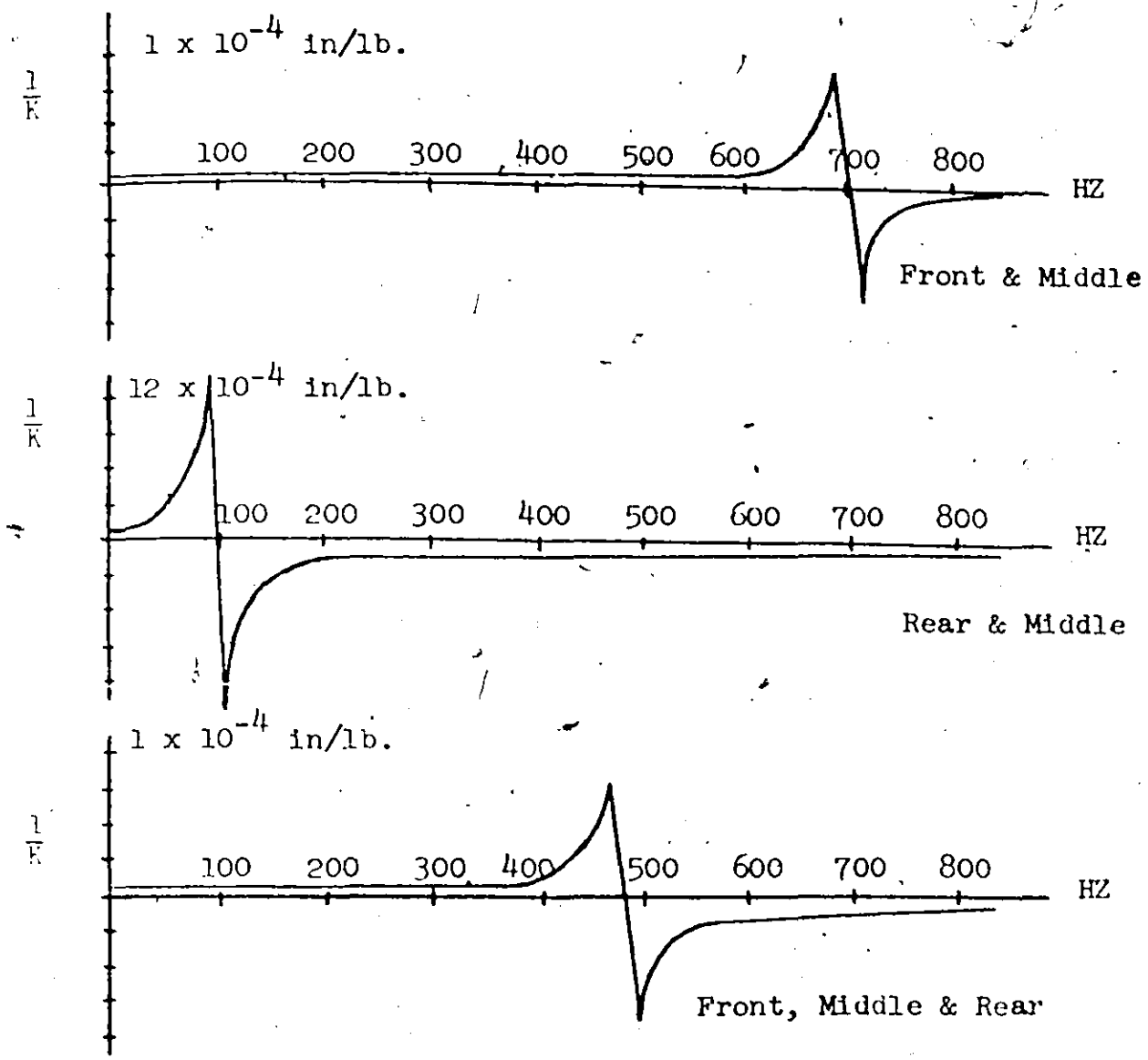

Fig. 3.8 Computed Receptance Curves for the Three Bearing Configurations

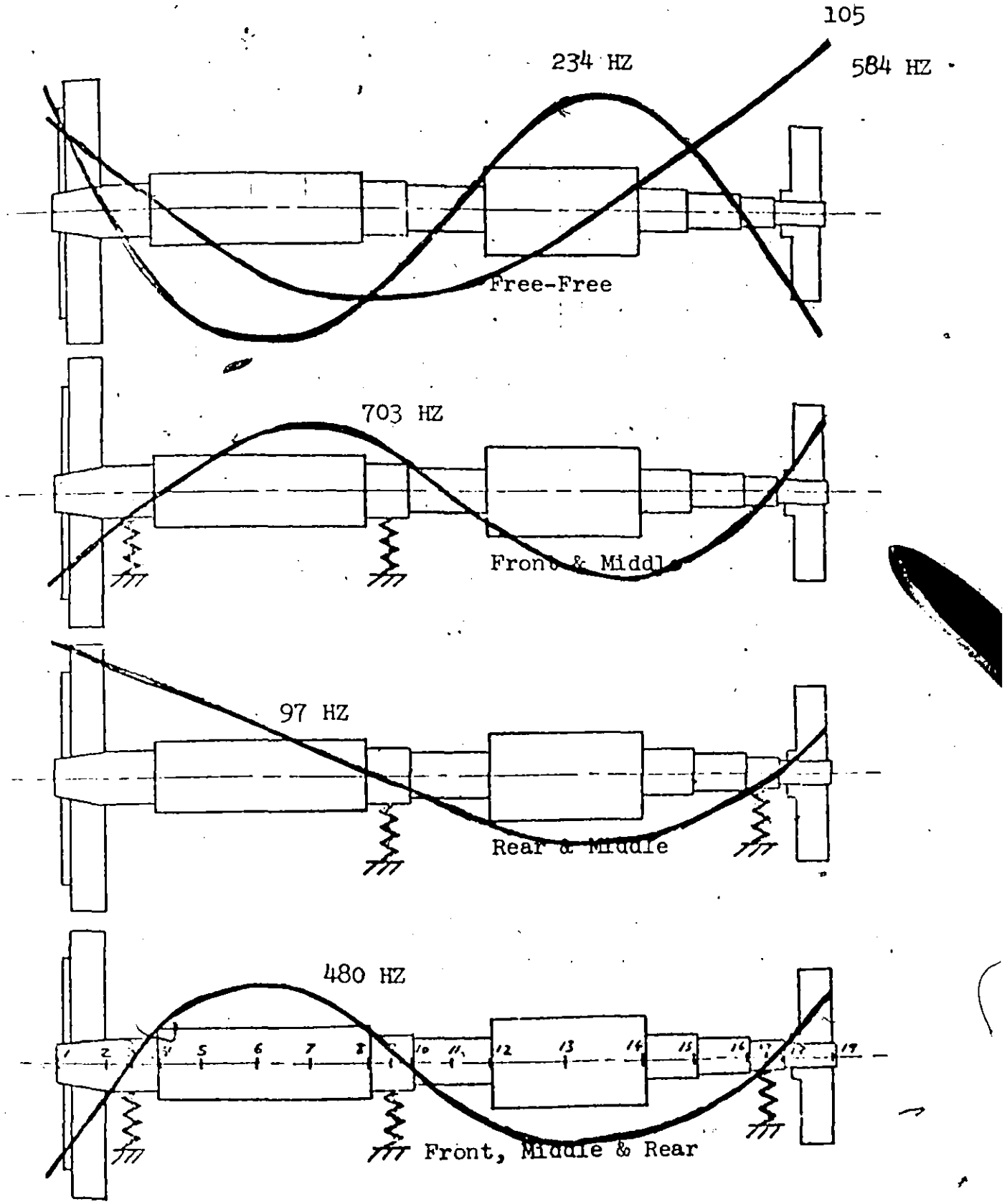

Fig. 3.9 Computed Mode Shapes for the Three Bearing Configurations and the Free-Free State

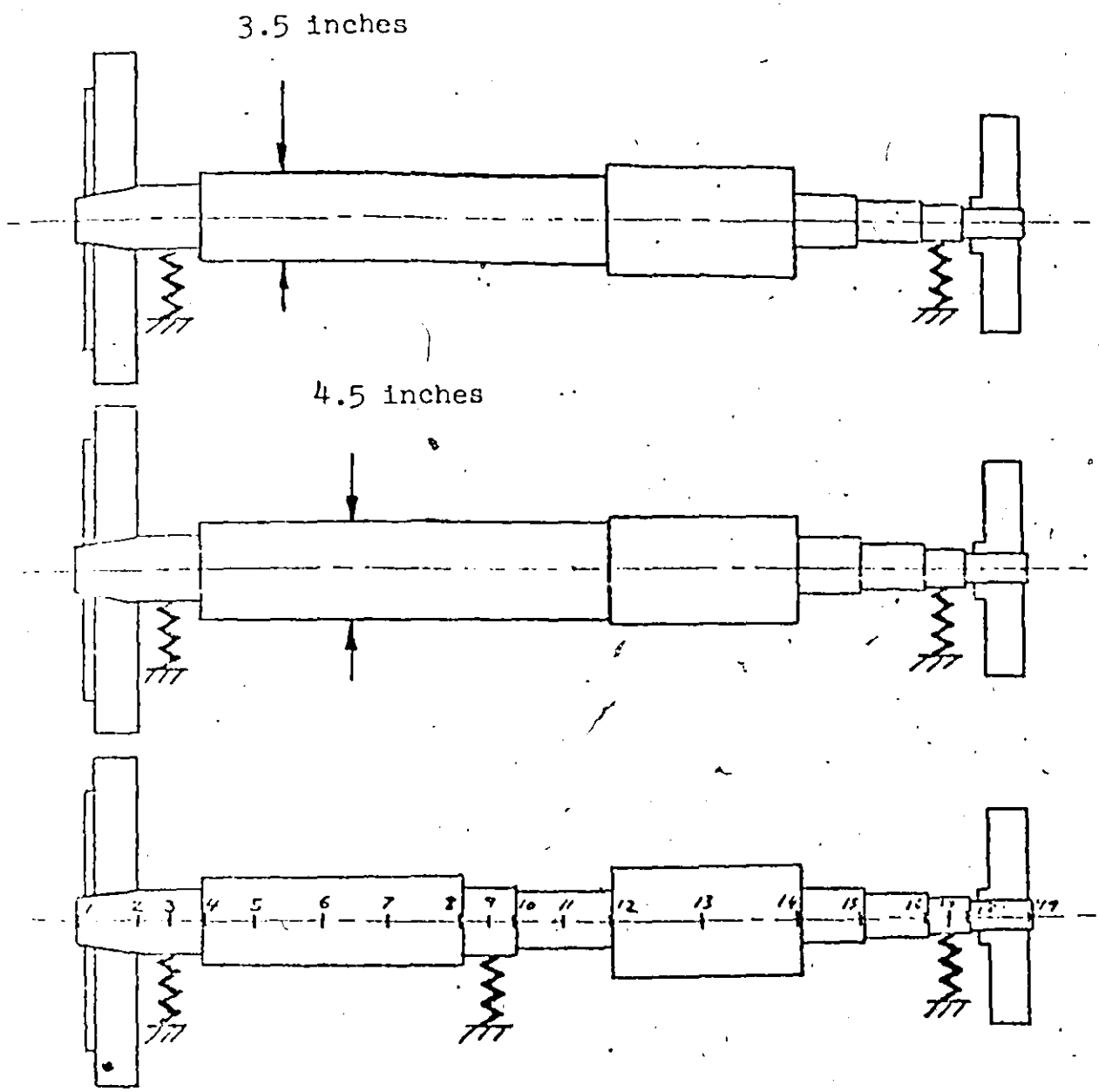

Fig. 3.10 Two Bearing Spindle Configurations and Original Three Bearing Spindle

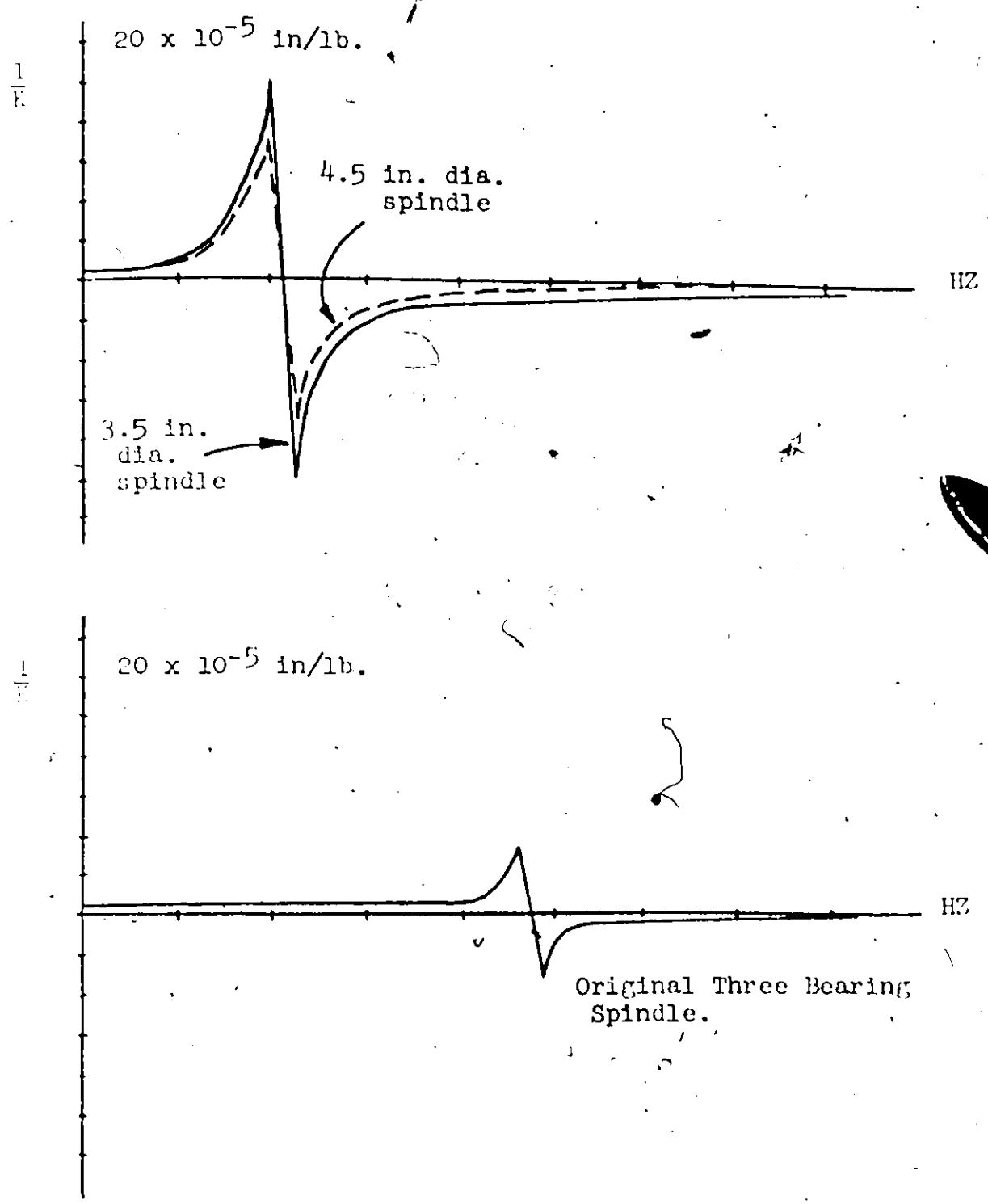

Fig. 3.11 Receptance Curves for the Two Bearing Spindle Designs as Compared to that of the Original Spindle

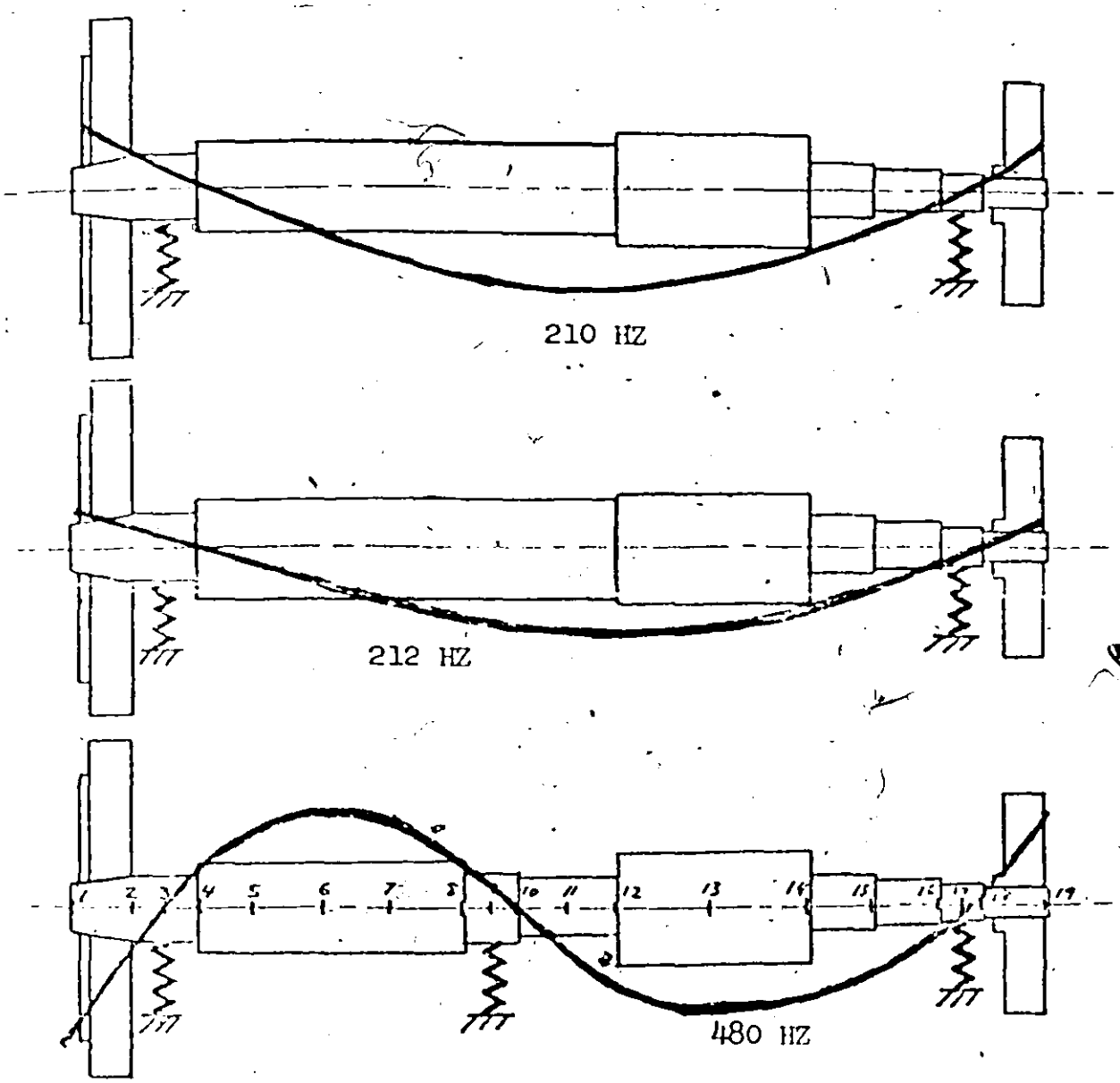

Fig. 3.12 Mode Shapes for the Two Bearing Spindle Designs as Compared to that of the Original Spindle

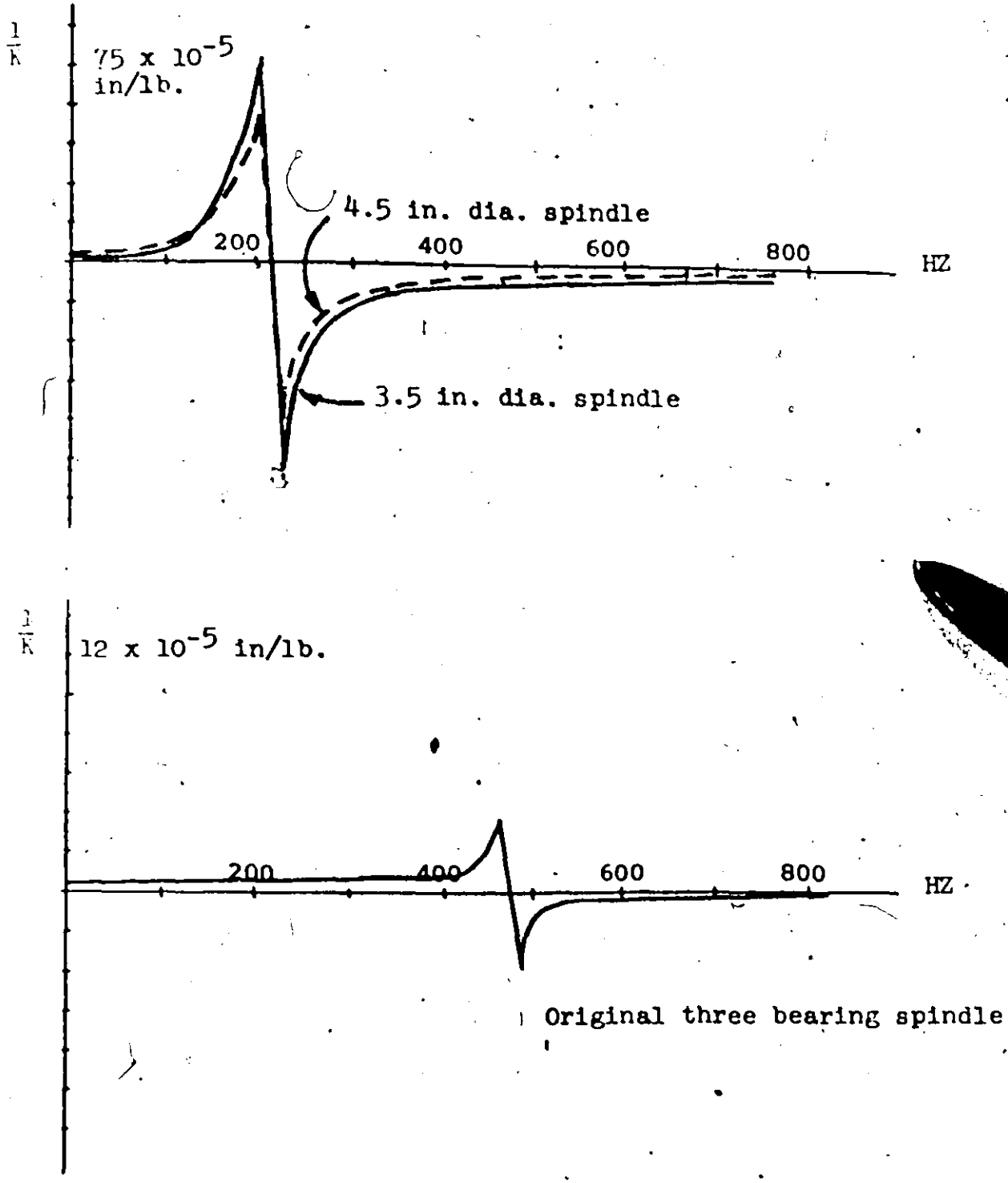

Fig. 3.13 Receptance Curves of the Two Bearing Spindles and of the Original Spindle (forced at the centre of the rotor)

Fig. 4.1 Steering Knuckle with Disk Brake Caliper Mounting Slot Machined

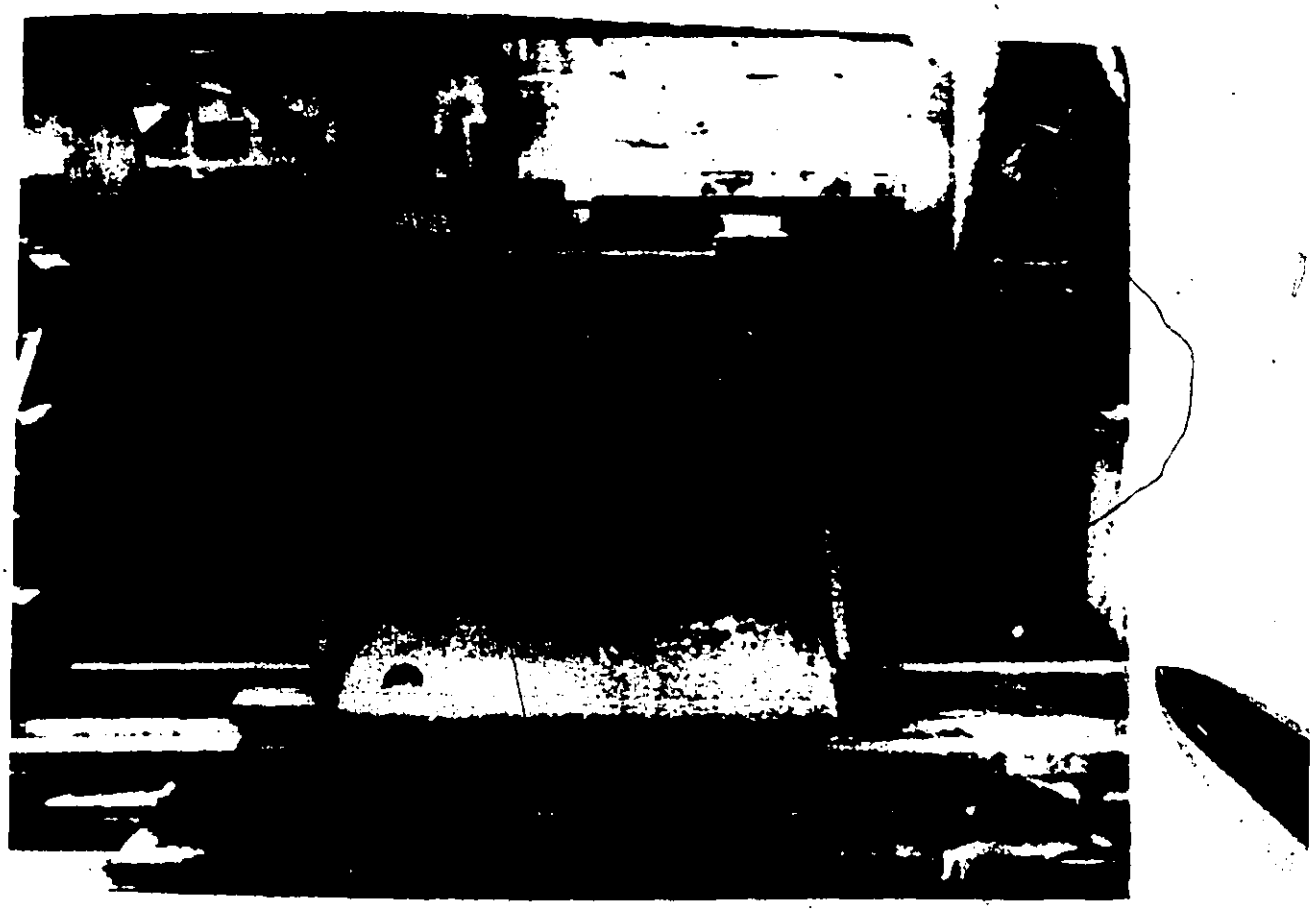

Fig. 4.2 Horizontal View of Steering Knuckle Clamped in Machining Pallet

Fig. 4.3 Vertical View of Steering Knuckle Clamped in Machining Pallet (Slots already machined)

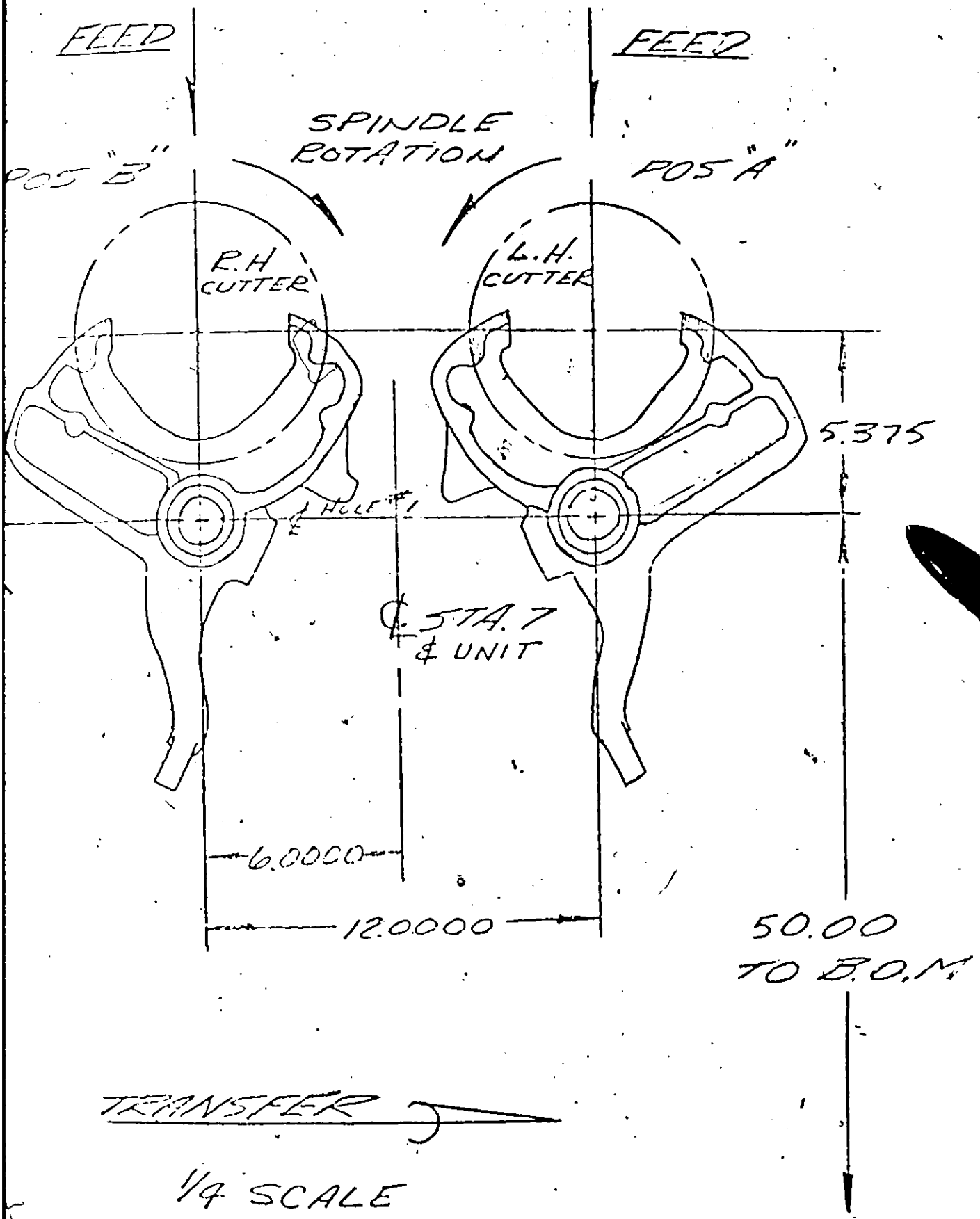

Fig. 4.4 Schematic of the Slot Milling of Steering Knuckles

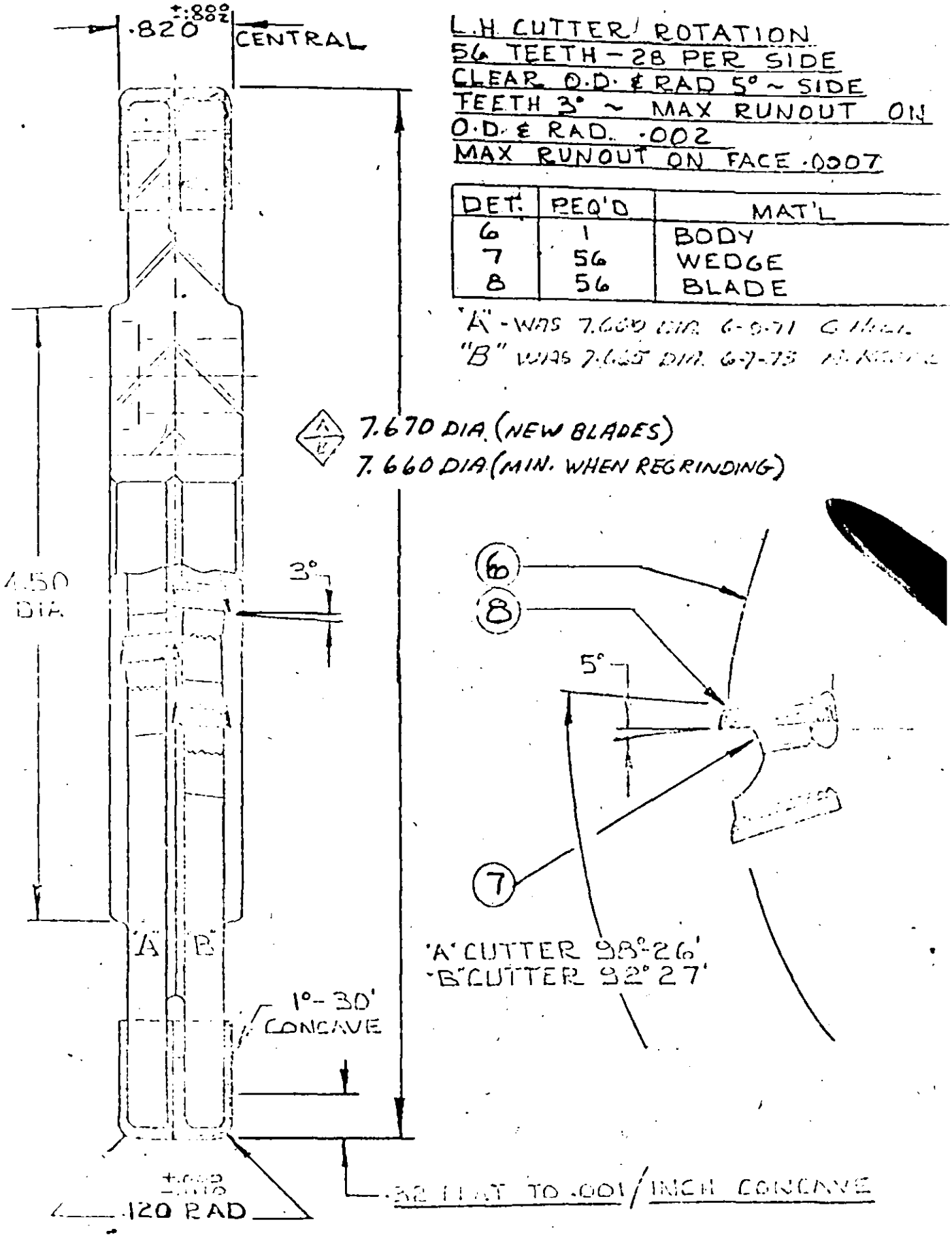

Fig. 4.5 Present Milling Cutter Design

Fig. 4.6 Phillips Vibration Pickup Being Used To Sense Vertical Vibration Of The Pallet During Machining

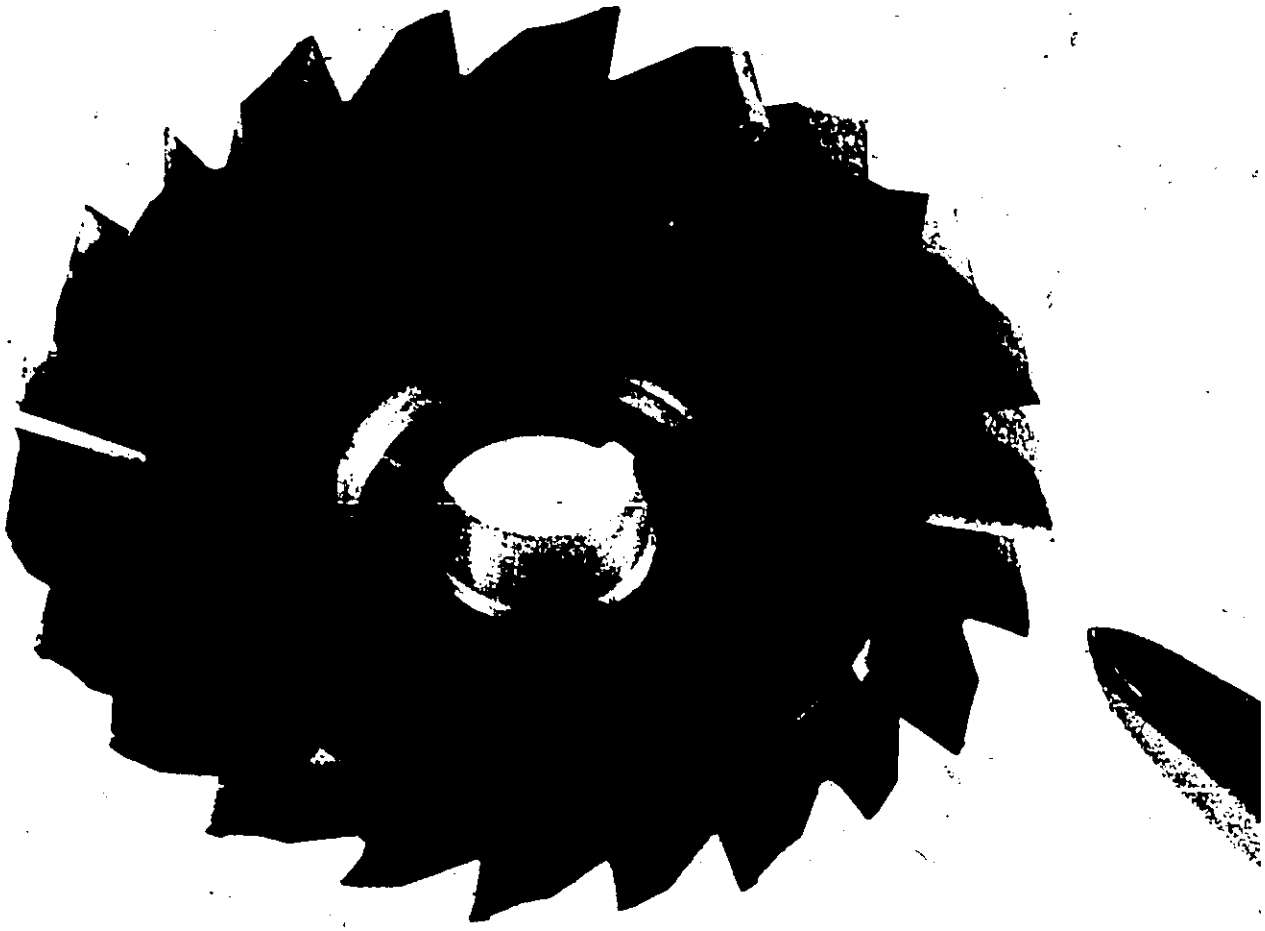

. 4.7 Milling Cutter With Alternate Helix Angles

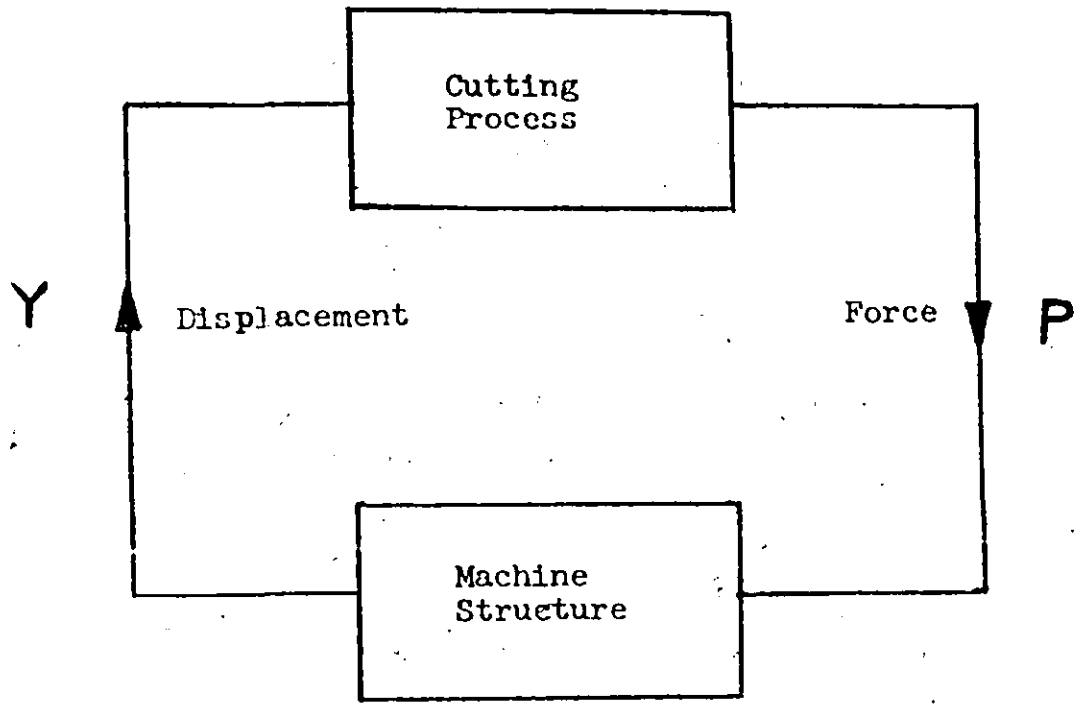

Fig. 4.8 Chatter Feedback Loop

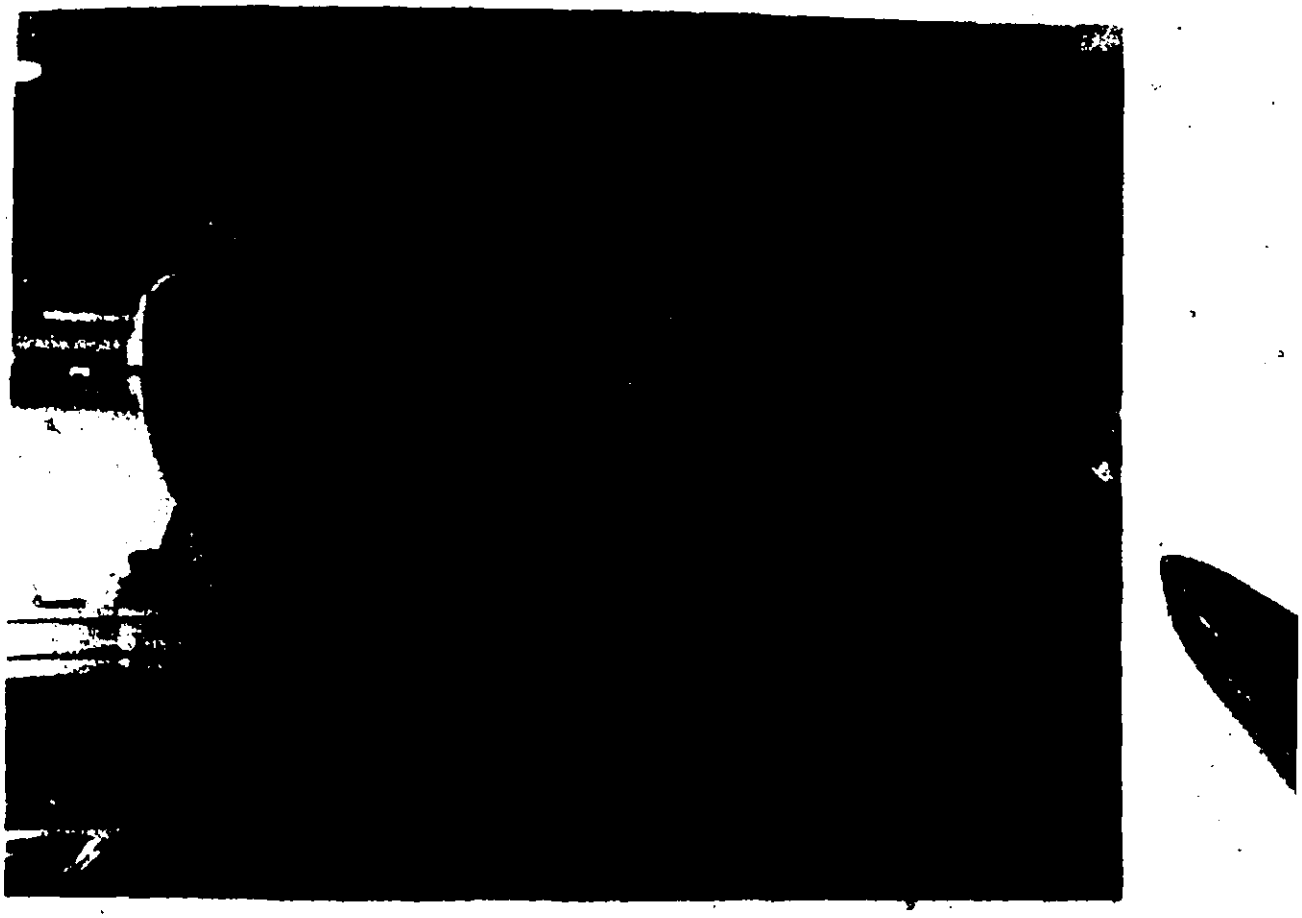

Fig. 4.9 Special Fixture For Two Tools Cutting Simultaneously.

Fig. 4.10 Special Fixture For Two Tools Cutting Simultaneously

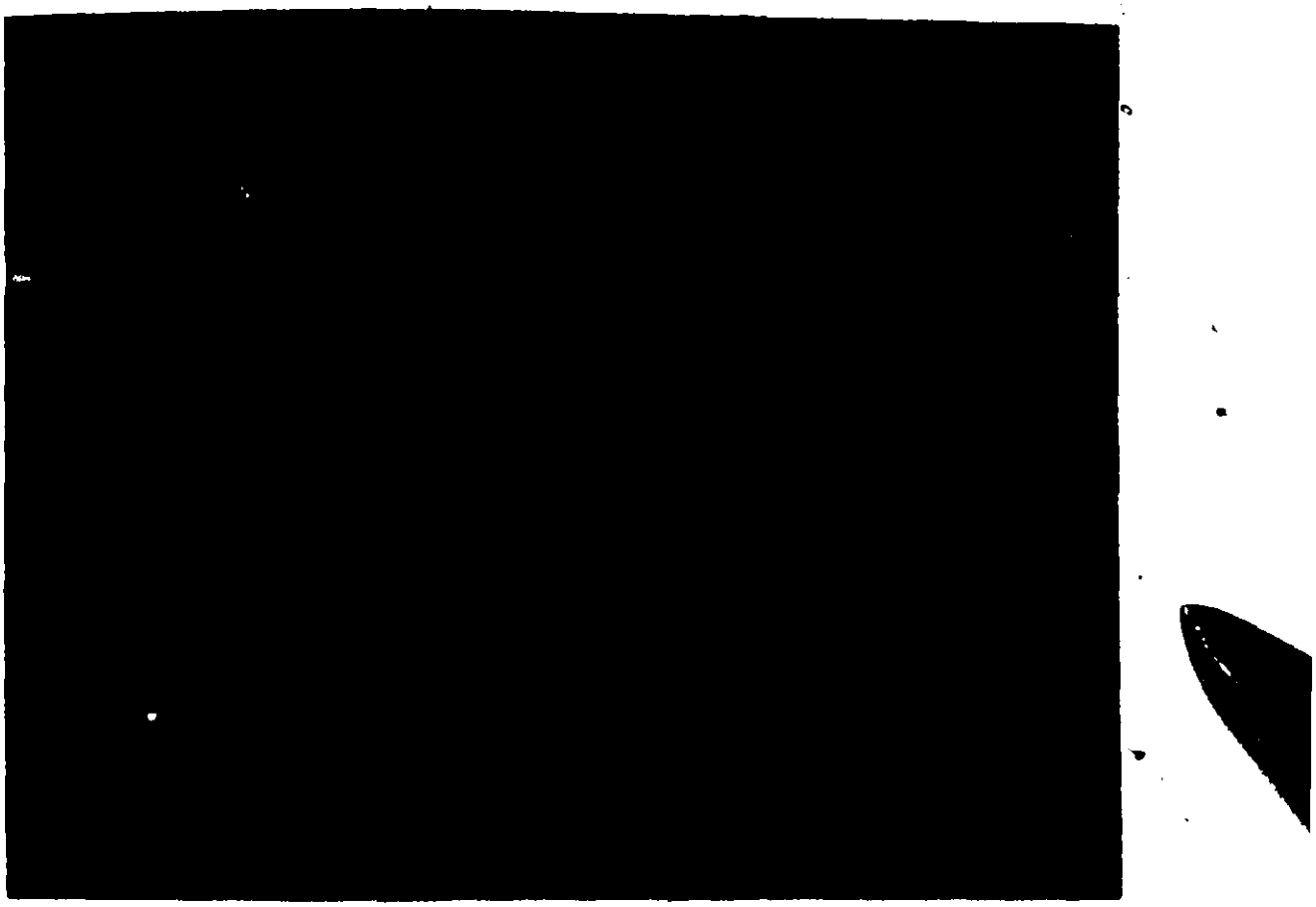

Fig. 4.11 Special Fixture For Two Tools Cutting Simultaneously

Fig. 4.12 Special Fixture For Two Tools Cutting Simultaneously

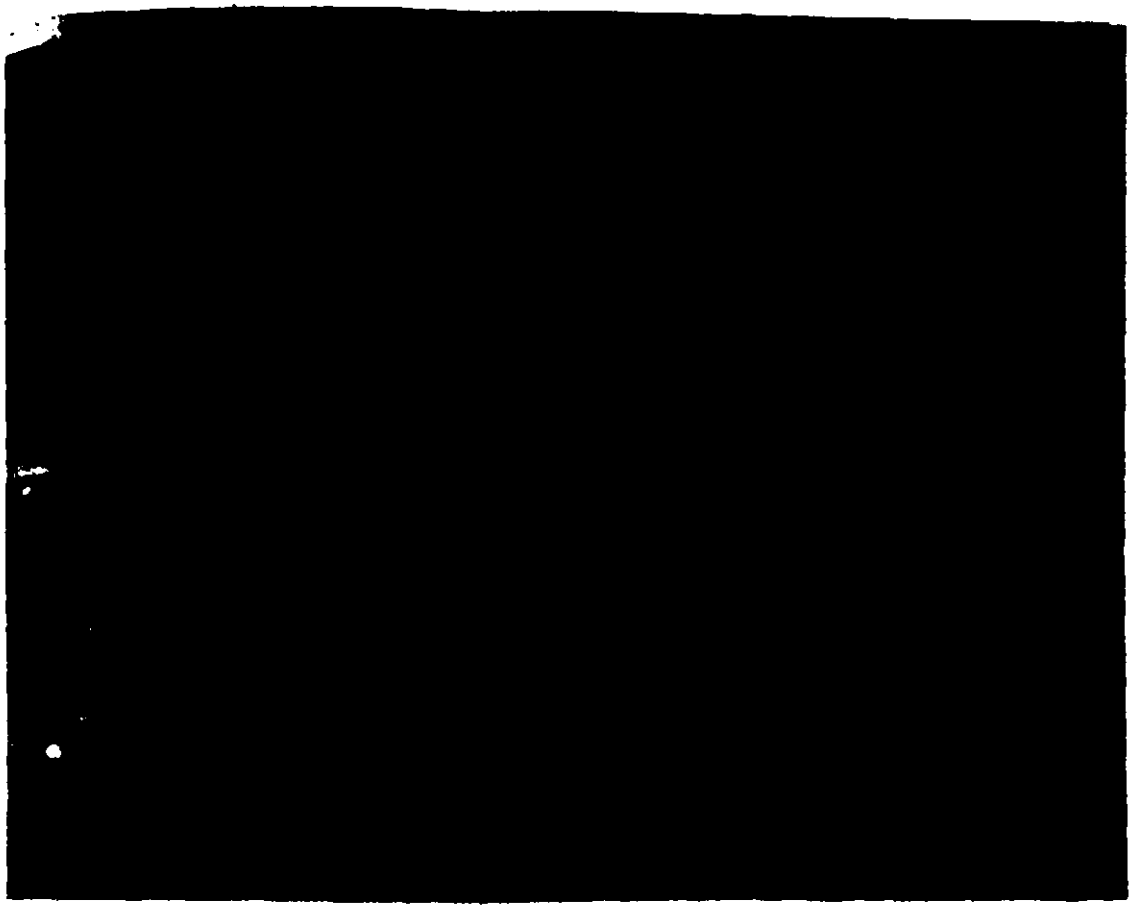

Fig. 4.13 Cutting with Two Tools Inclined to Eliminate Regenerative Chatter
(Note large depth of cut)

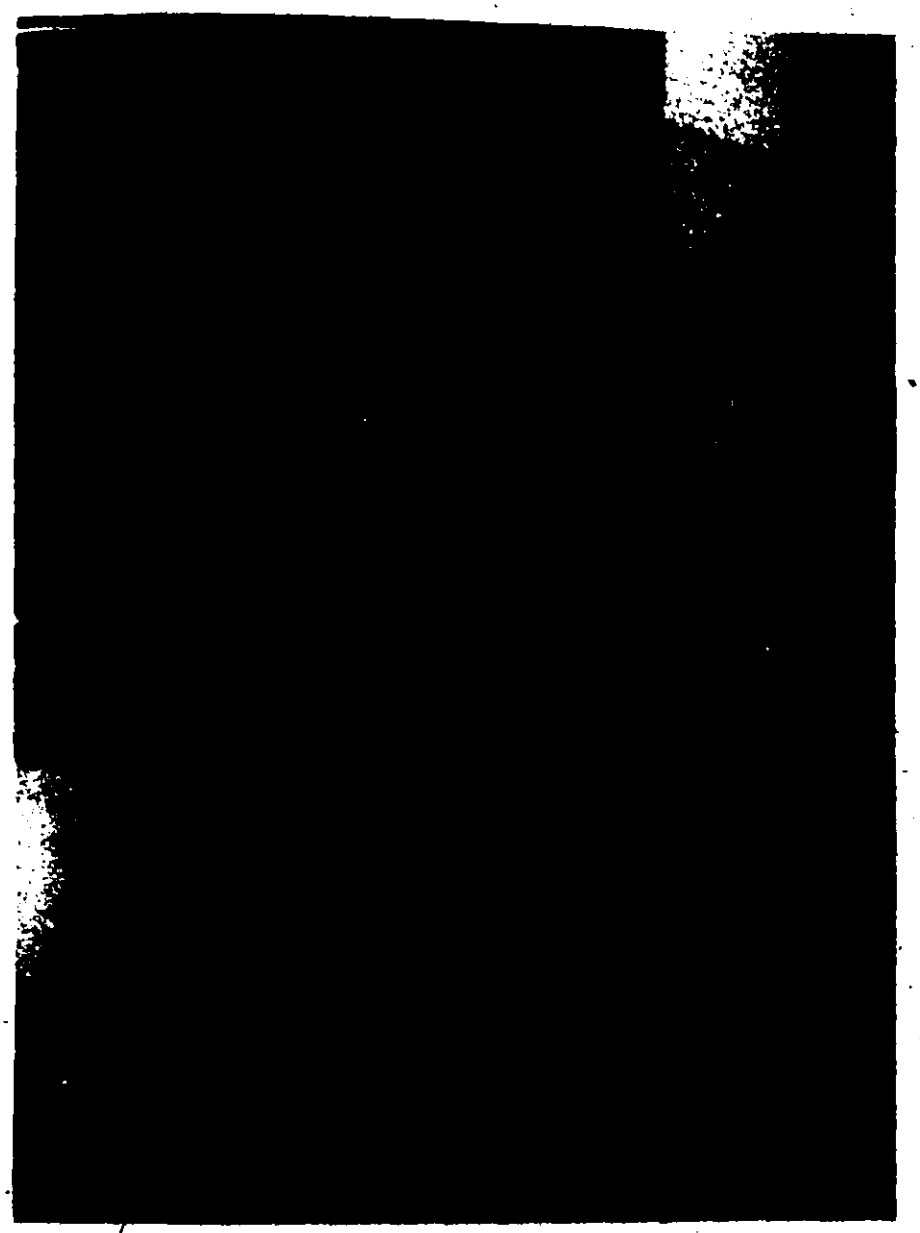

Fig. 4.14 Cutting with Two Tools Inclined to Eliminate Regenerative Chatter (Note large depth of cut)

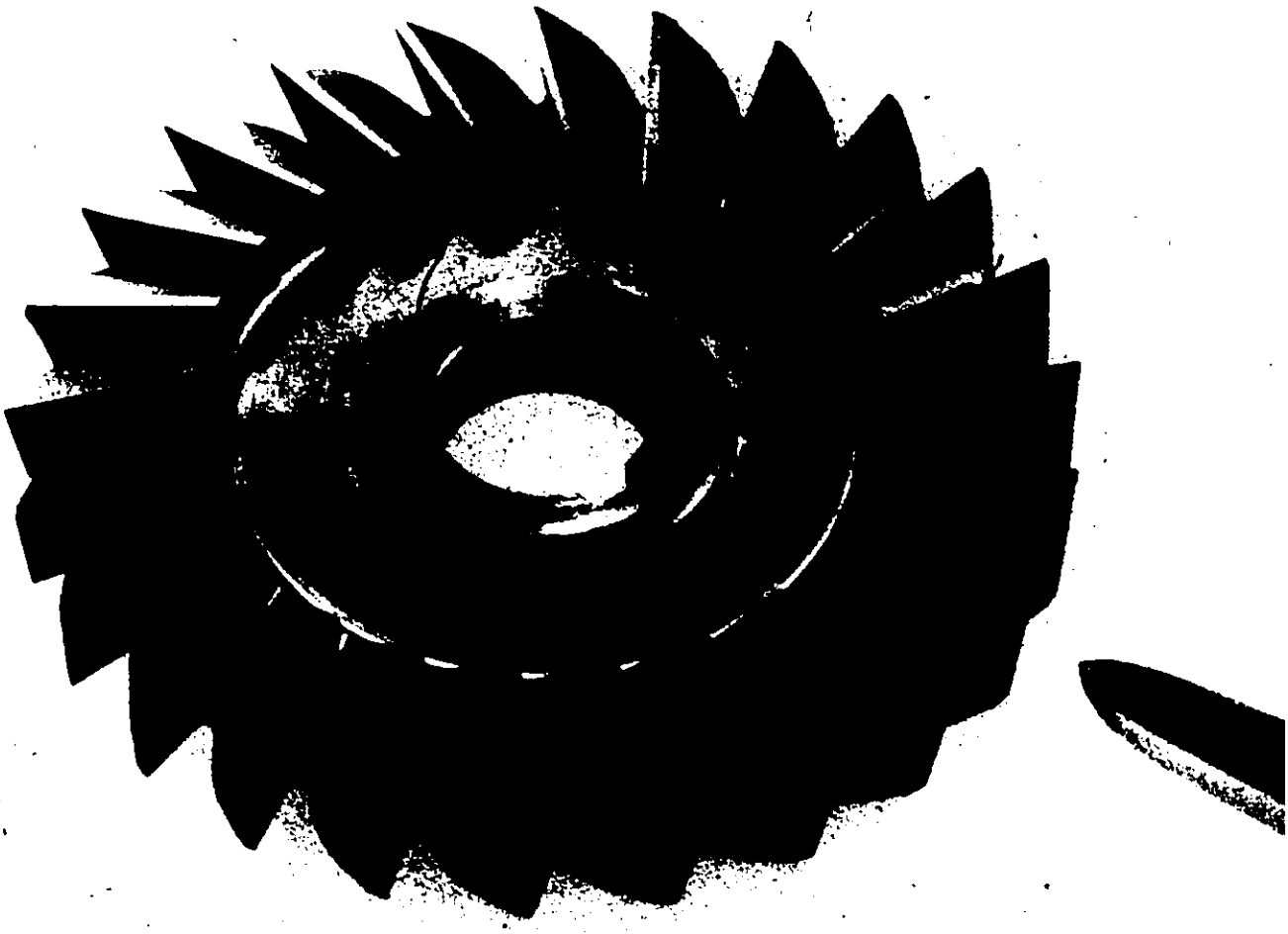

Fig. 4.15 Milling Cutter with Constant Helix Angle

Fig. 4.16 Chatter Obtained During the Milling of a Stepped Test Piece

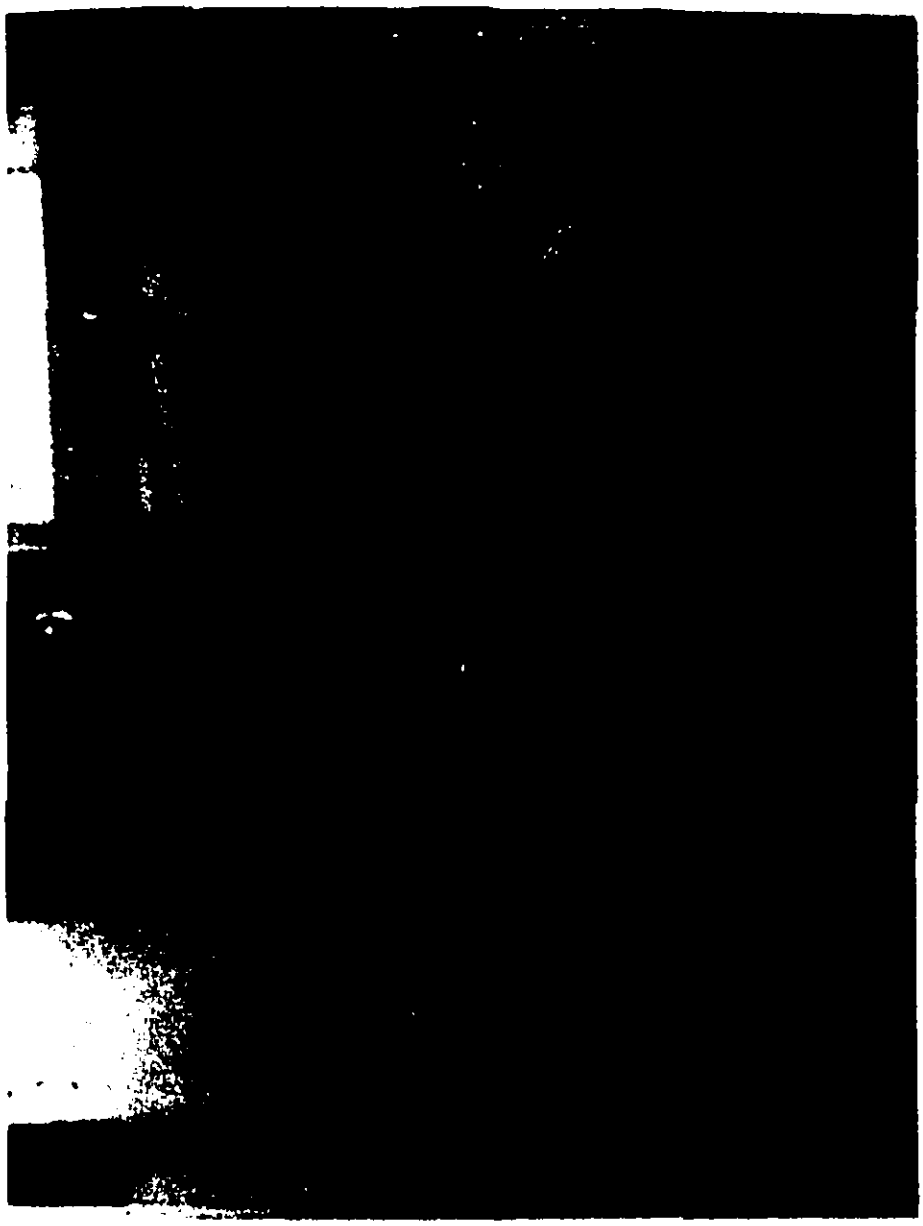

Fig. 4.17 Vibration Absorber Attached to the Milling Cutter to Increase Stability

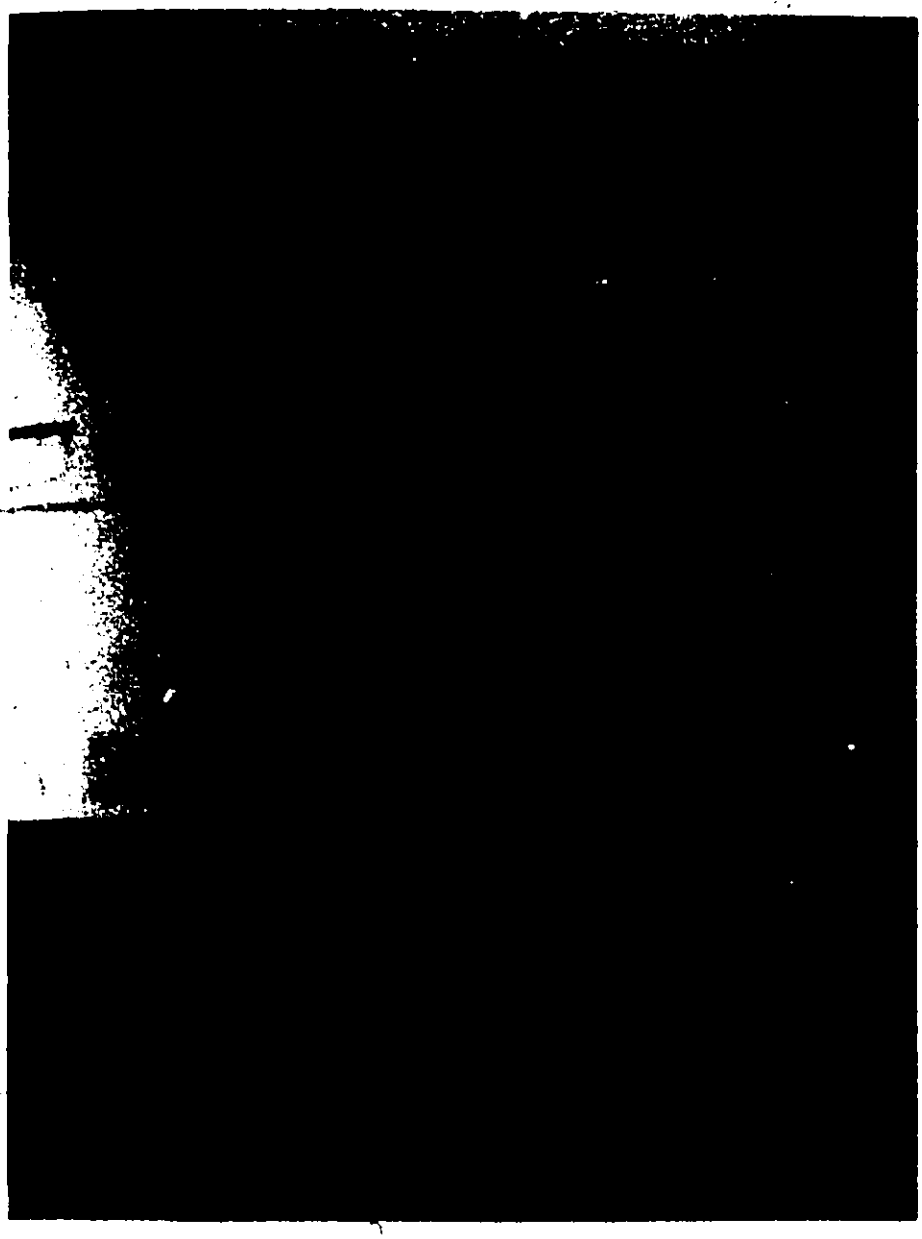

Fig. 4.18 Vibration Absorber Attached to the Milling Cutter to Increase Stability

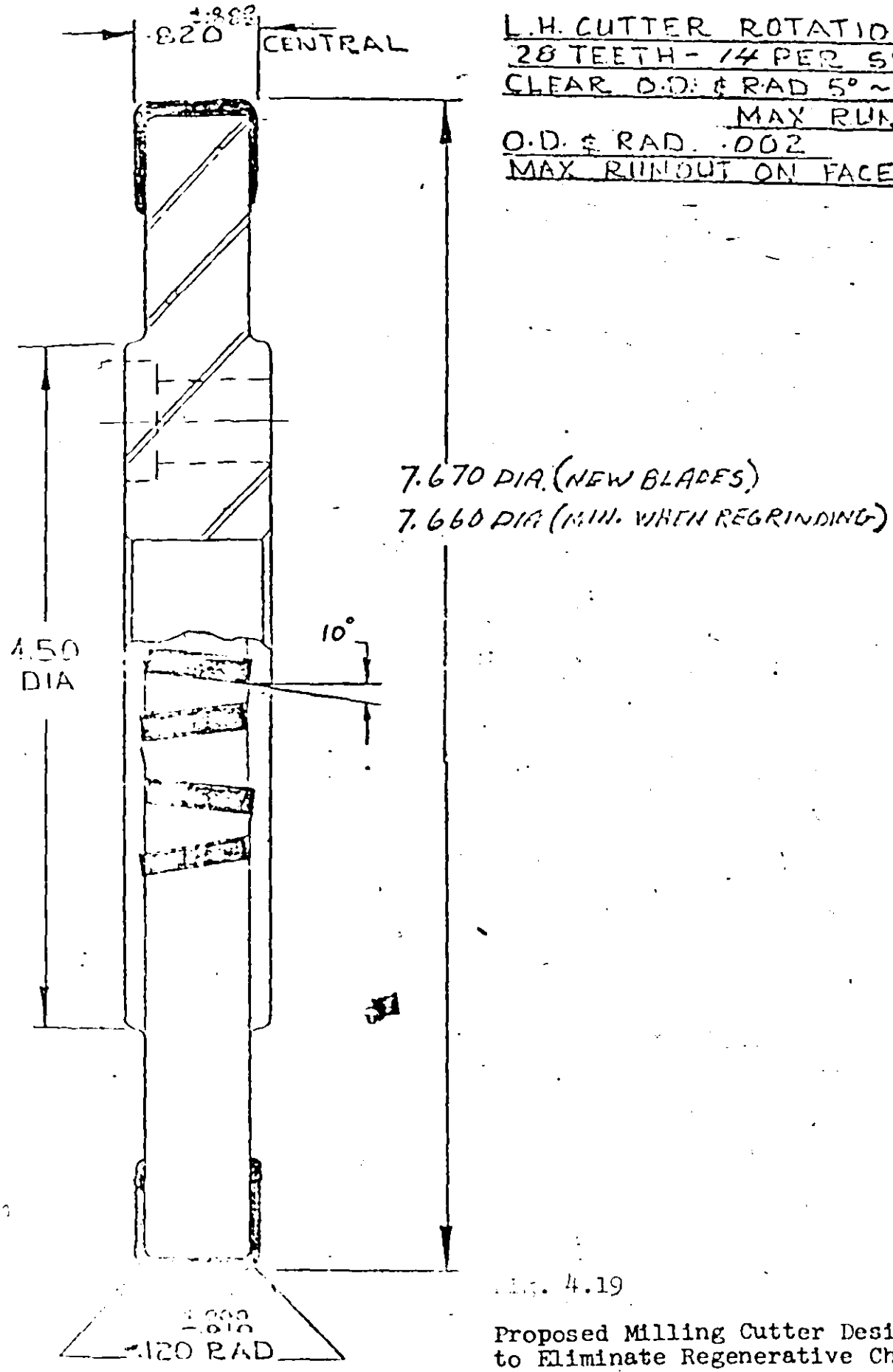

Fig. 4.19

Proposed Milling Cutter Design
to Eliminate Regenerative Chatter

Steering Knuckle Showing the Tapered Holes for the Ball Joint and the Tie Rod End

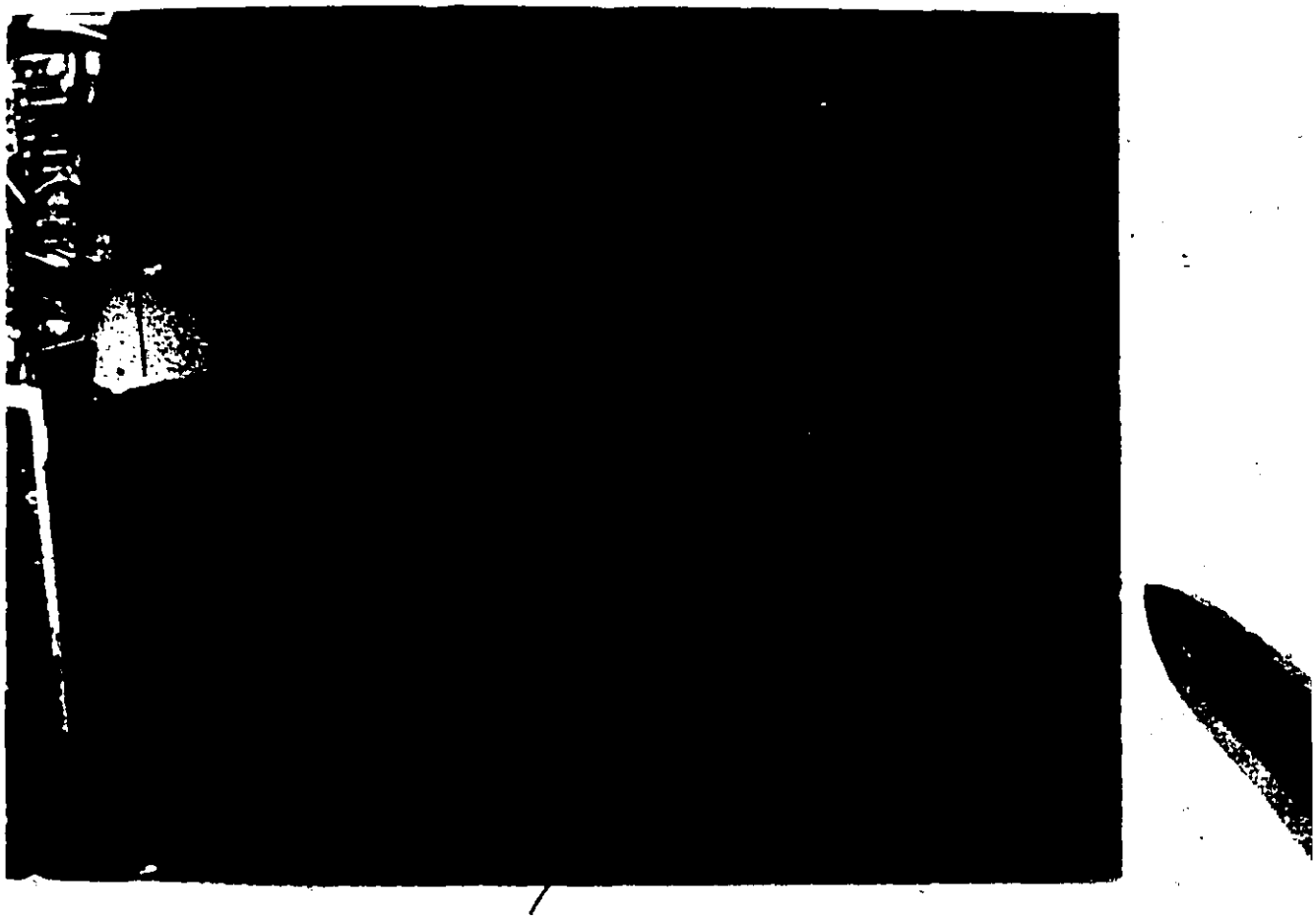

. 5.2 Machining of the Tie Rod End Hole

Fig. 5.3 Machining of the Tie Rod End Hole

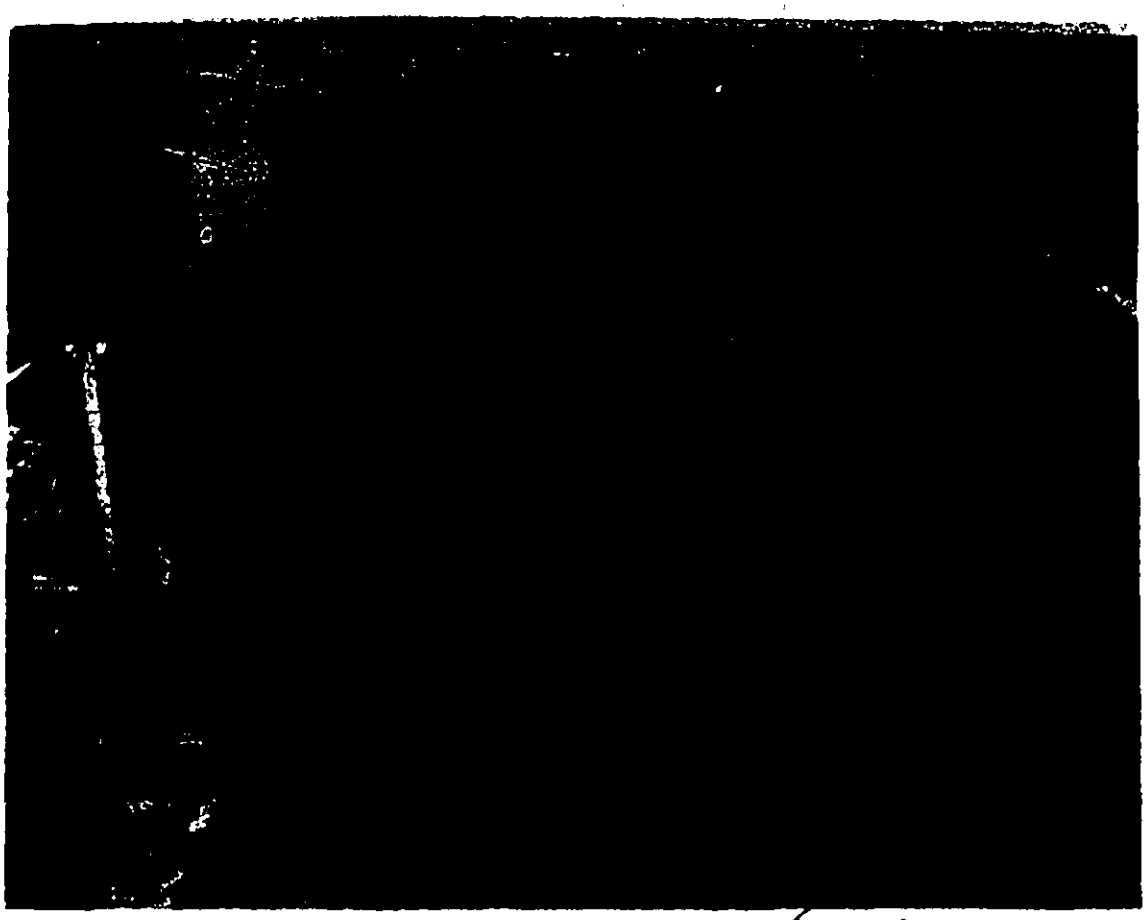

Fig. 5.4 Parts Clamped in a Machining Pallet

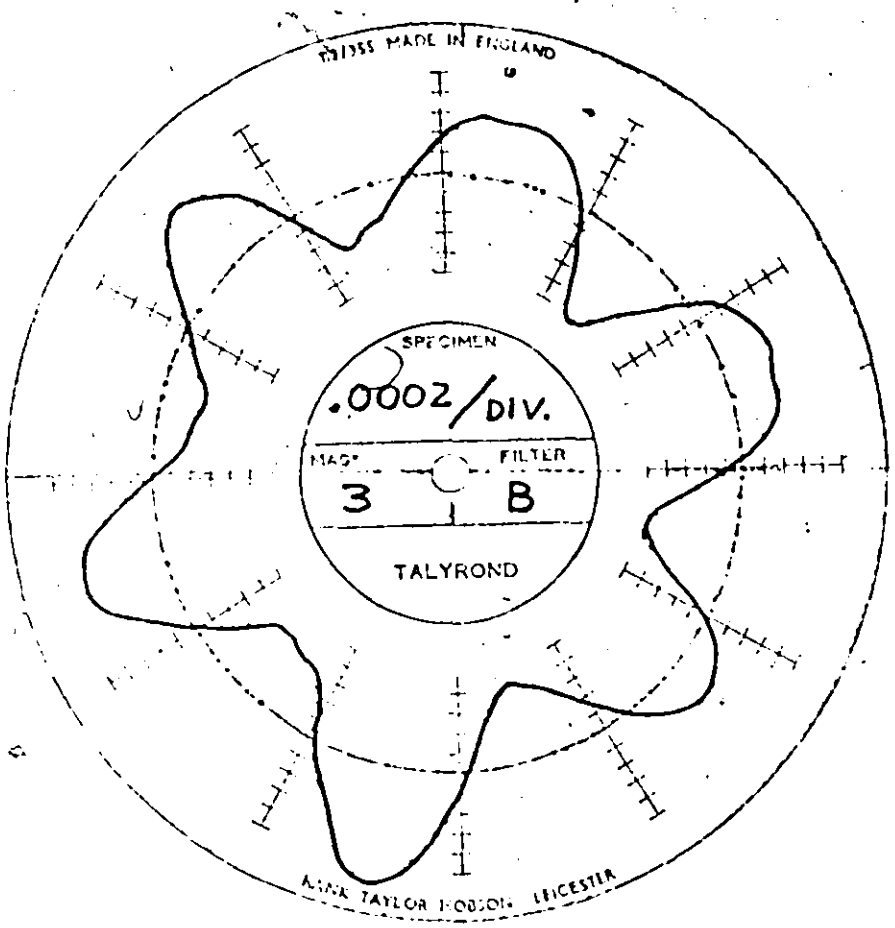

Fig. 5.5 Talyround Graph of Lobes (6) Produced By a Five-Flute Taper Reamer

Fig. 5.6 A Taper Reamer

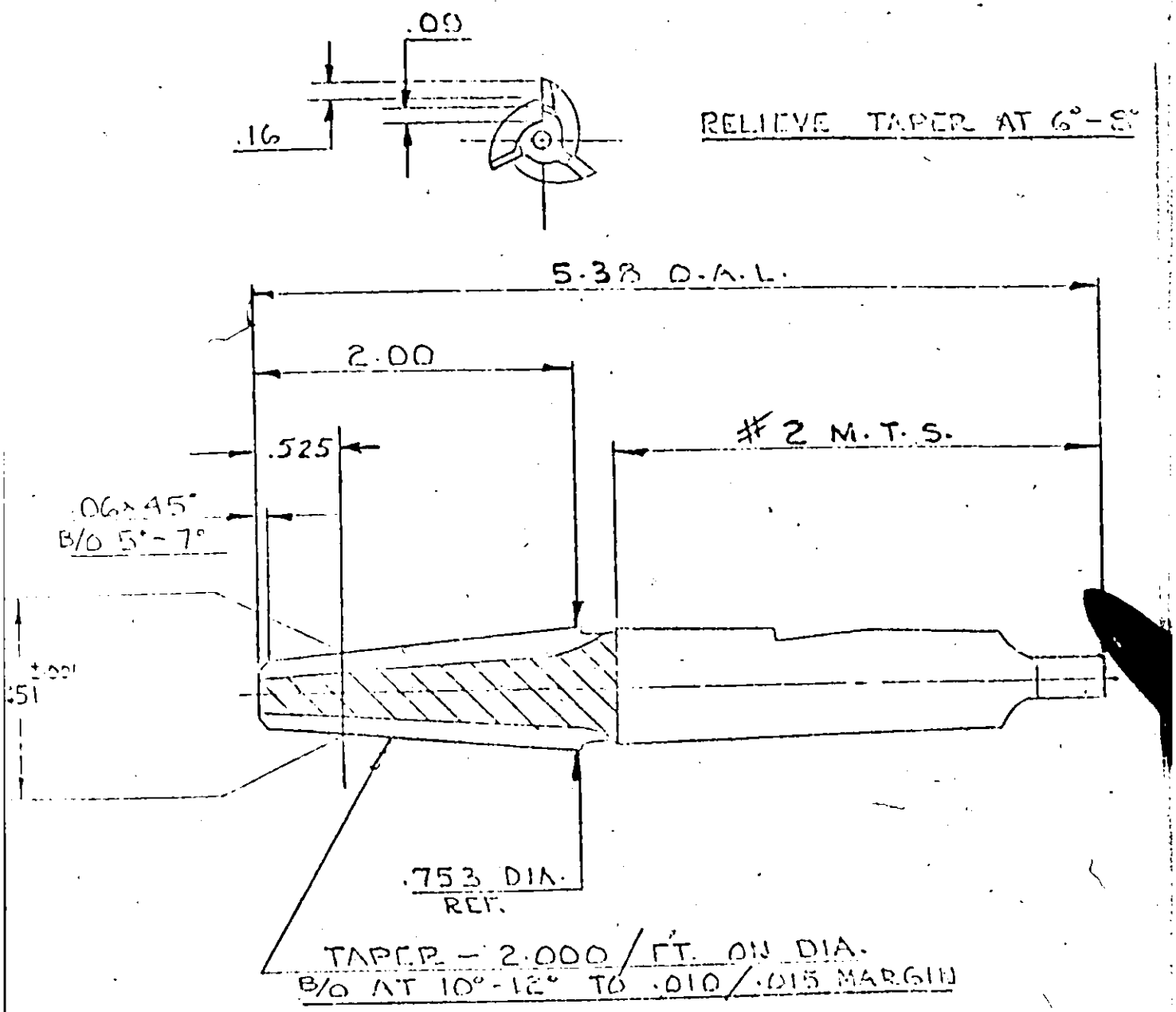

(61) RGH TAPER REAMER 'A' CAR
3 FLUTES

Fig. 5.7 Print of the Taper Reamer

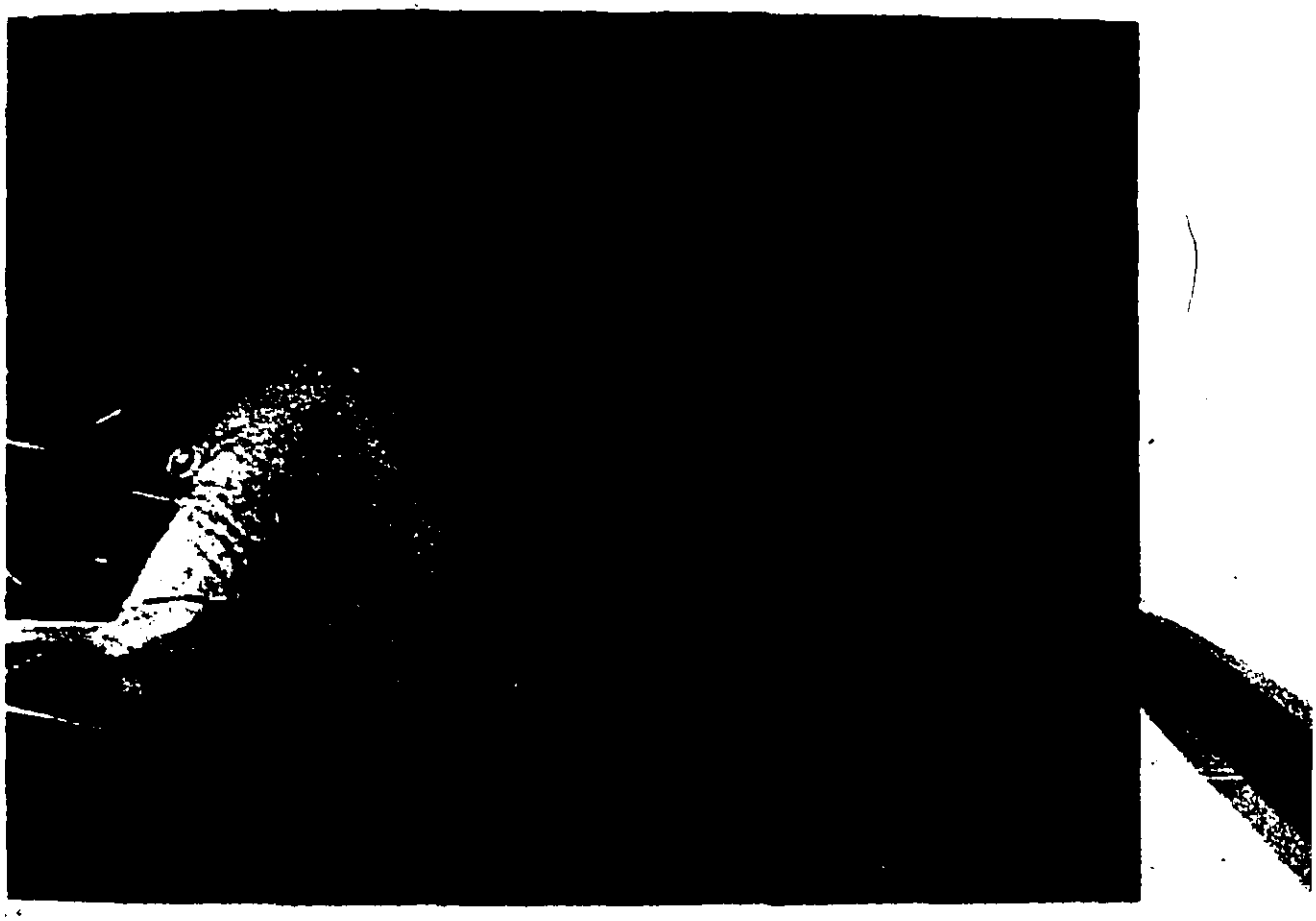

Fig. 5.8 Using a Velocity Pickup for the Purpose of Vibration Detection on the Grill of the Reaming Head

FIG. 5.9 Set-up to Detect Relative Movement Between the Tool and the Workpiece using Capacitive Probes and a U-V Recorder

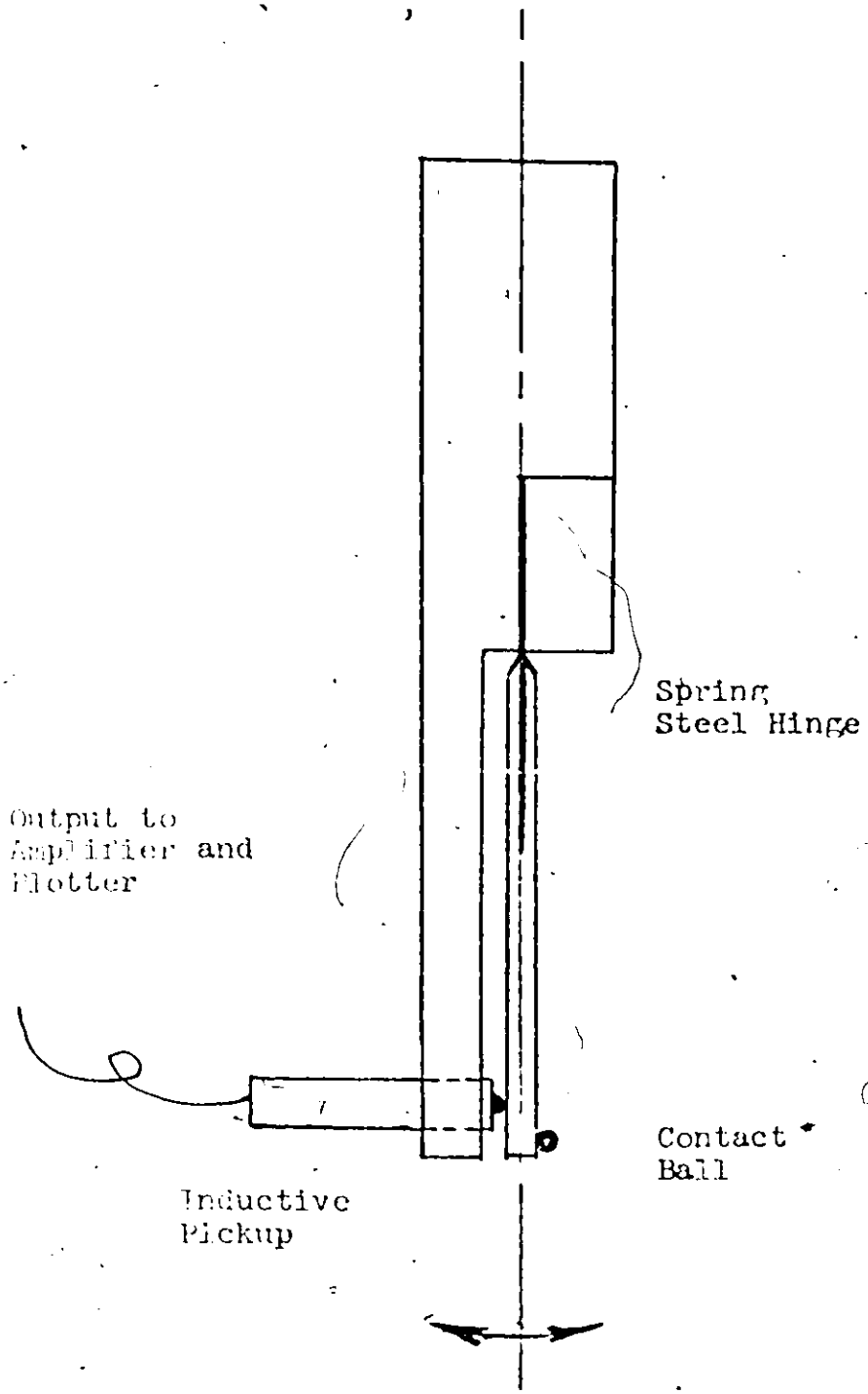

Fig. 5.10 Special Fixture for the Recording of the Profile of a hole (lobe detector)

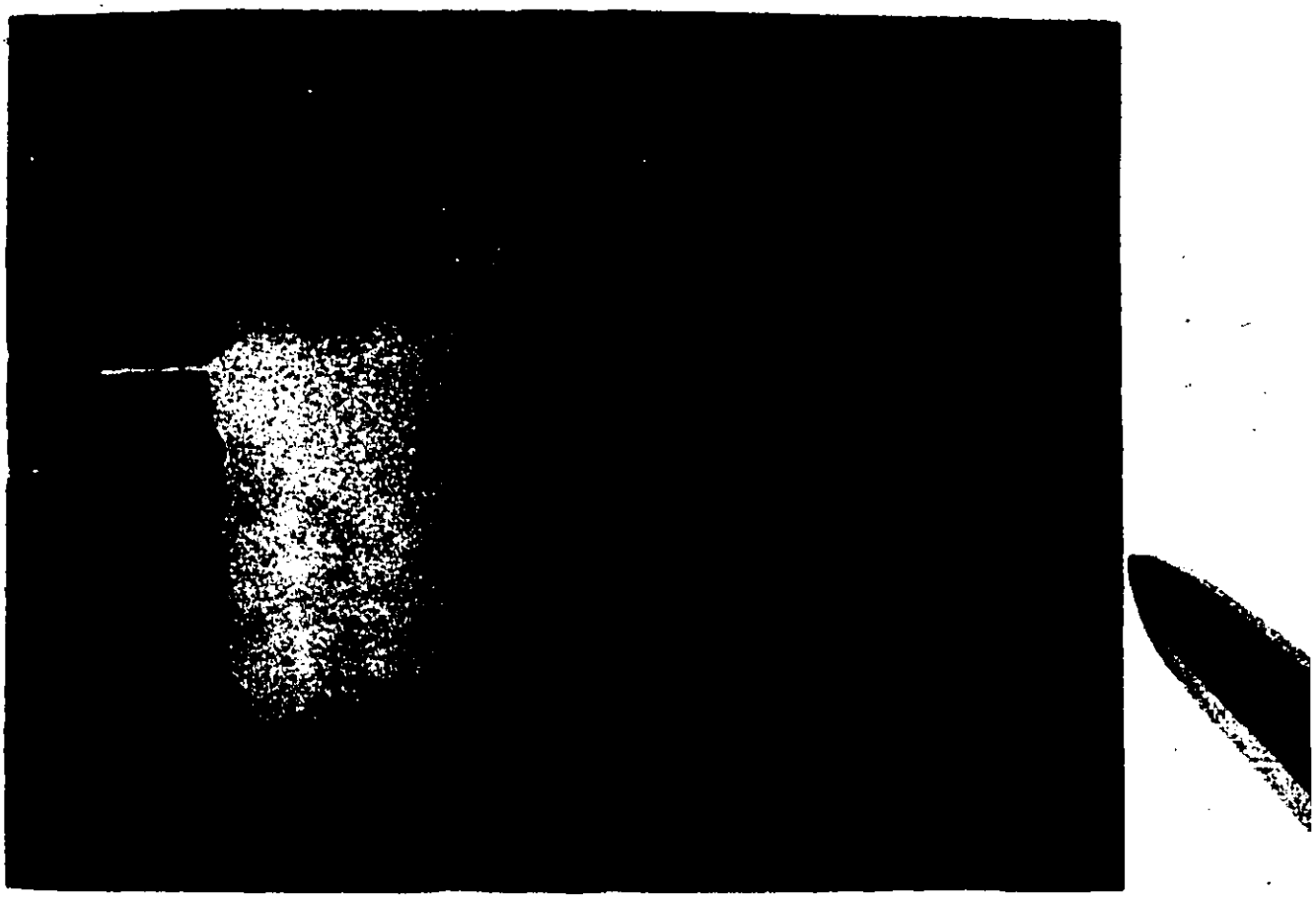

Fig. 5.11 Set-up for the Recording of the Profile of a hole

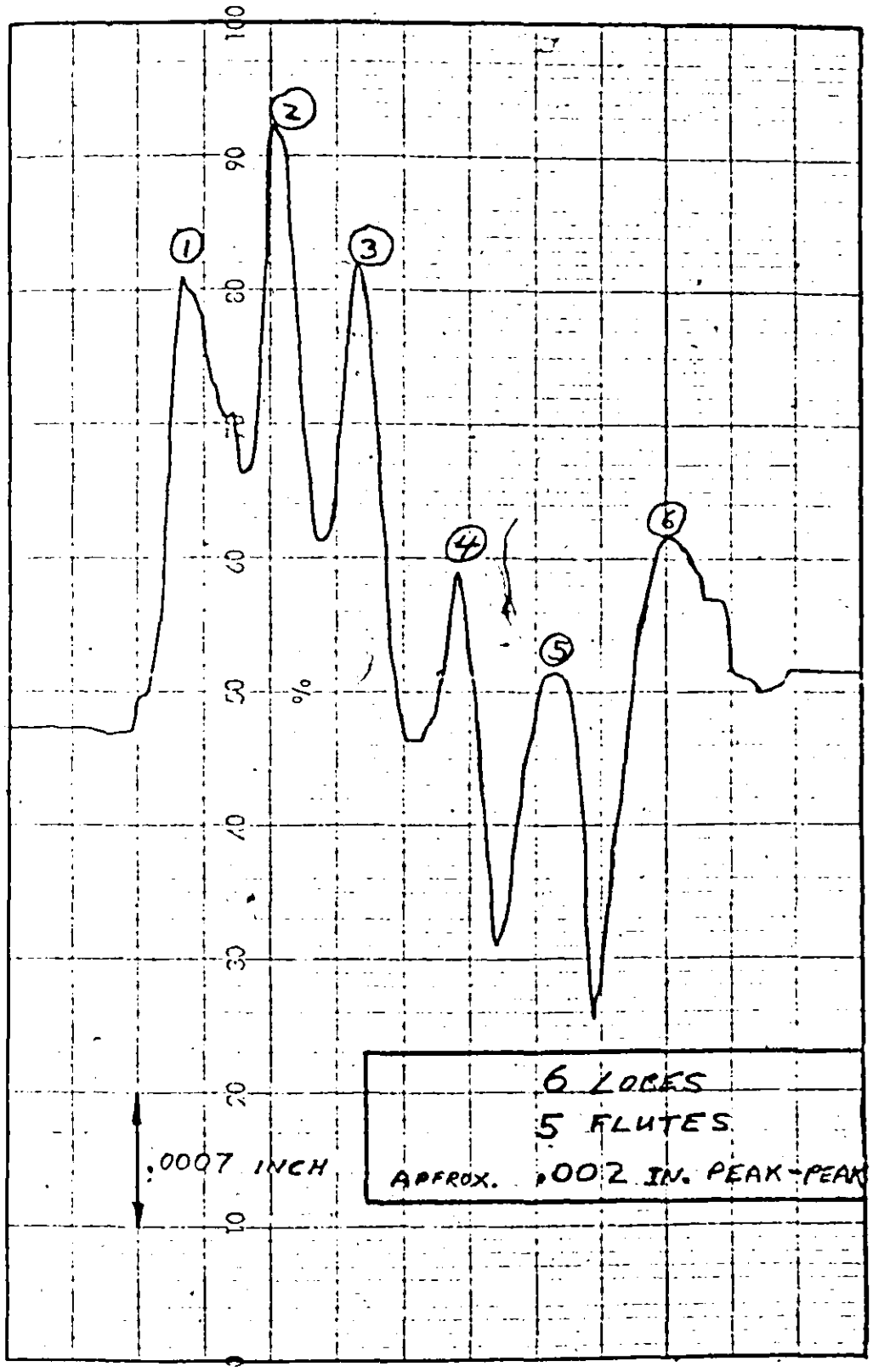

Fig. 5.12 Sample Record from the Lobe Detector

Fig. 5.13 Set-up for the Detection of Relative Motion Between Tool and Workpiece in Two Directions Simultaneously

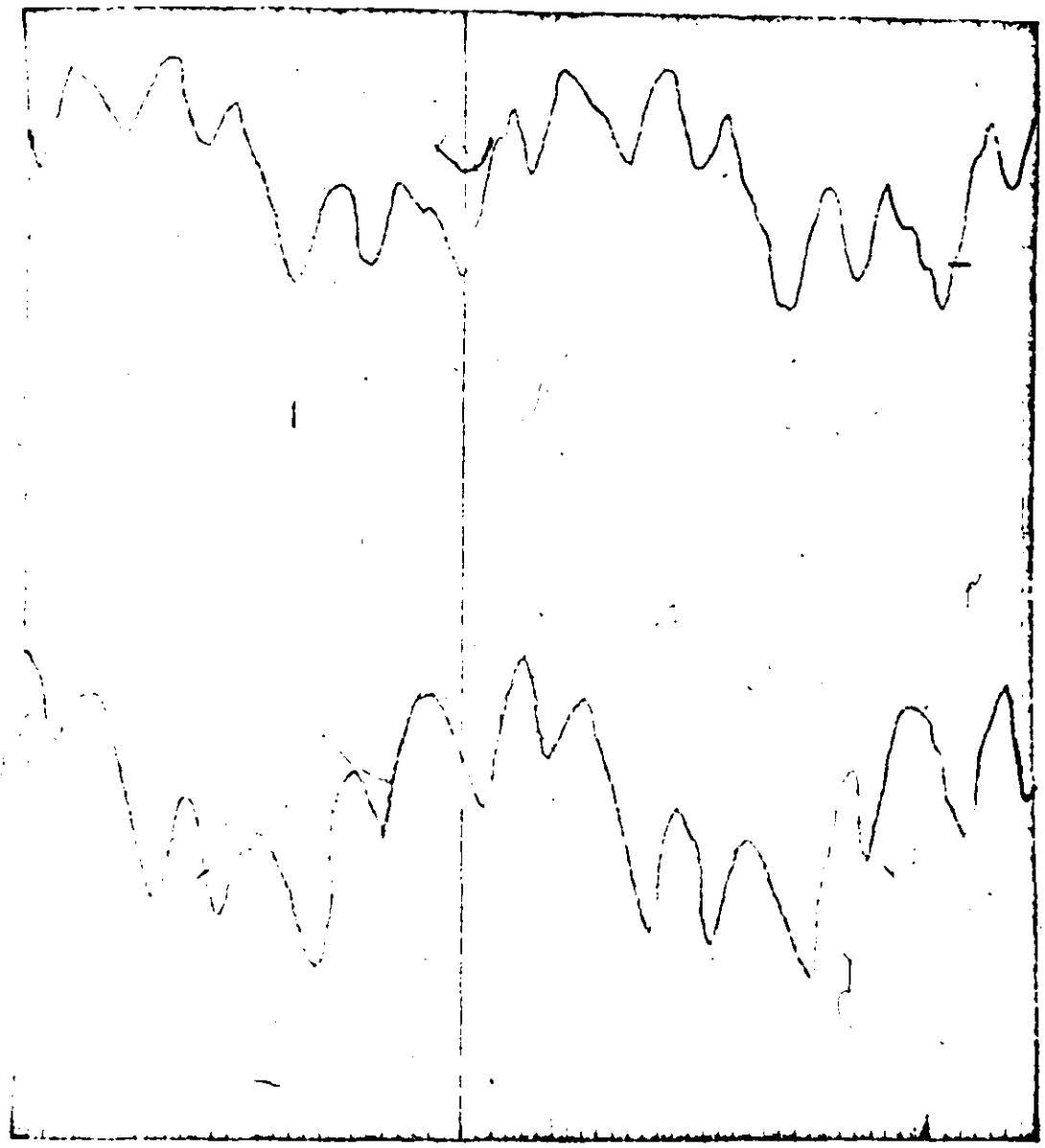

Fig. 5.14 A Typical Vibration Record from the Two Capacitive Probes (note phase shift between the two probes)

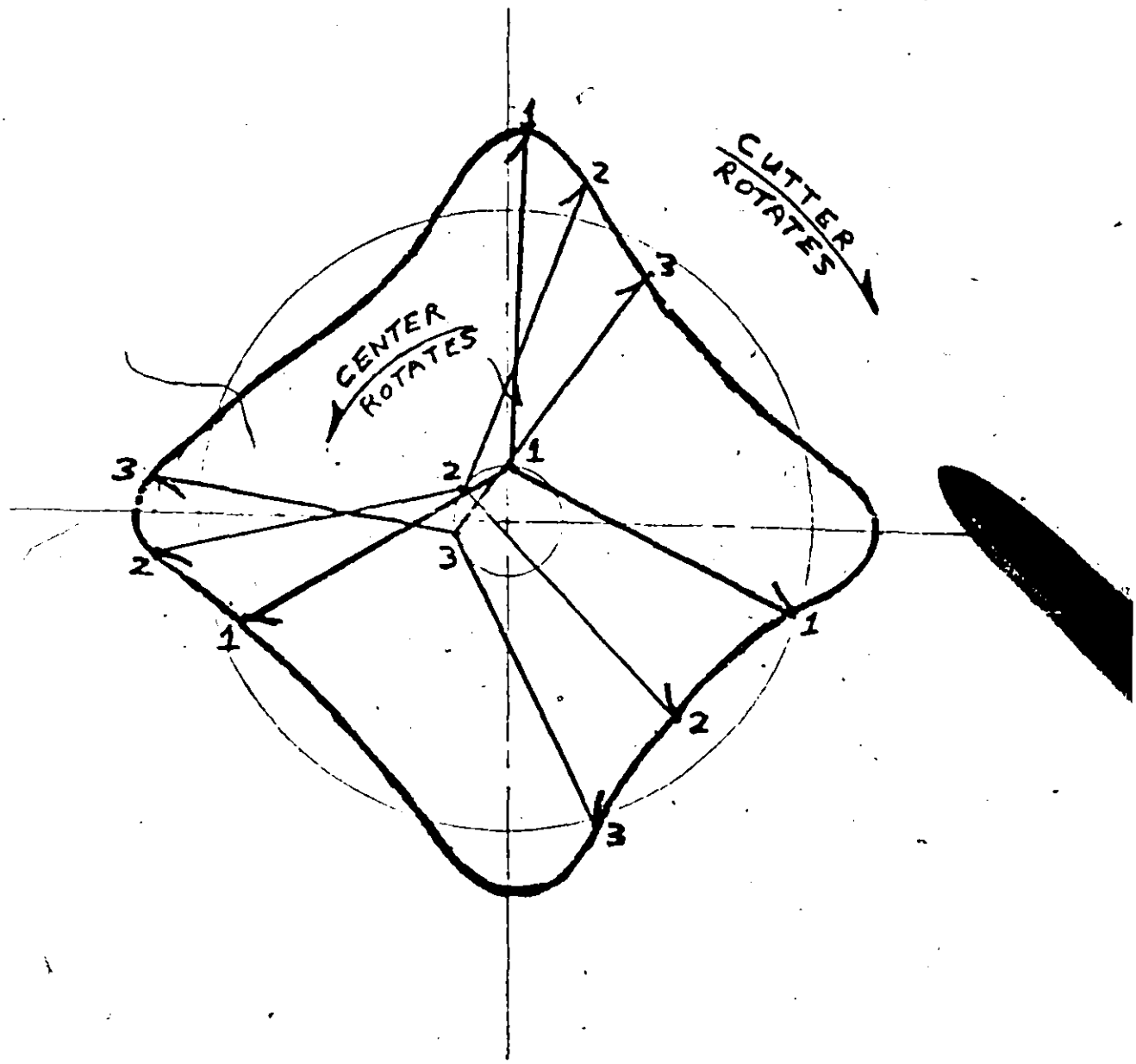

Fig. 5.15 Graphical development of lobing based on the Kinematic model

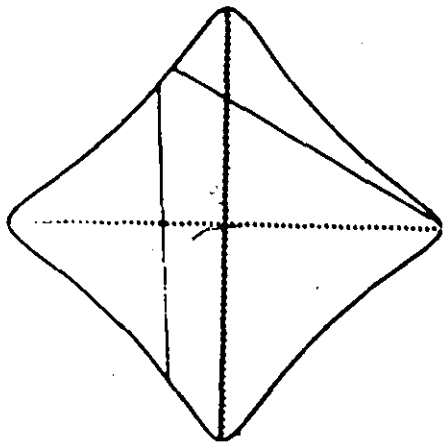

I = 1 (Lobing)

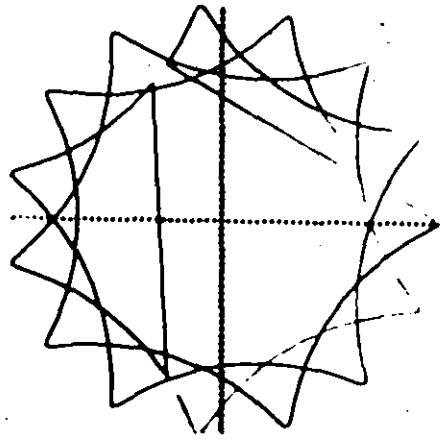

I = 2

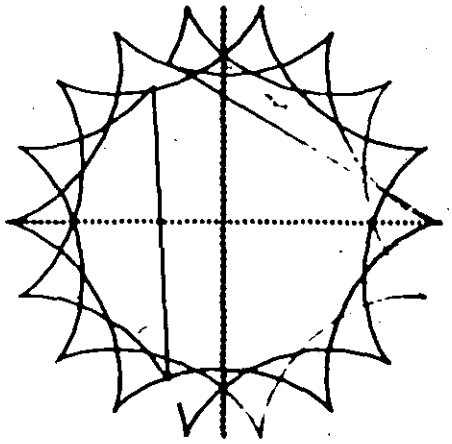

I = 3

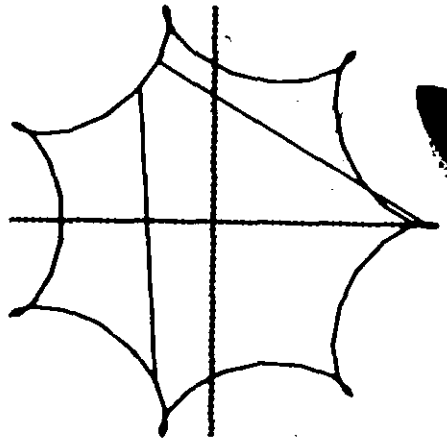

I = 4 (Lobing)

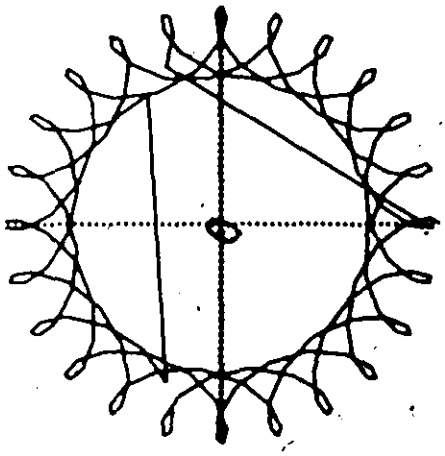

I = 5

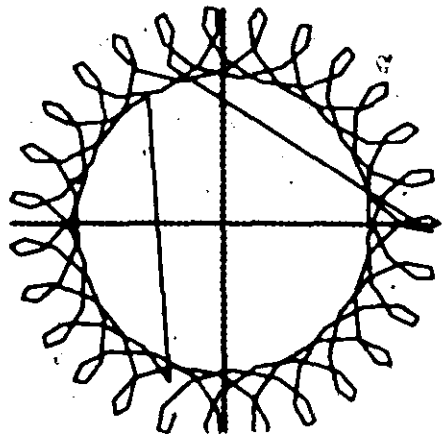

I = 6

Fig. 5.16 Computer Generated Profiles for the Kinematic Model of a 3 Flute Reamer (Lobes produced where indicated)

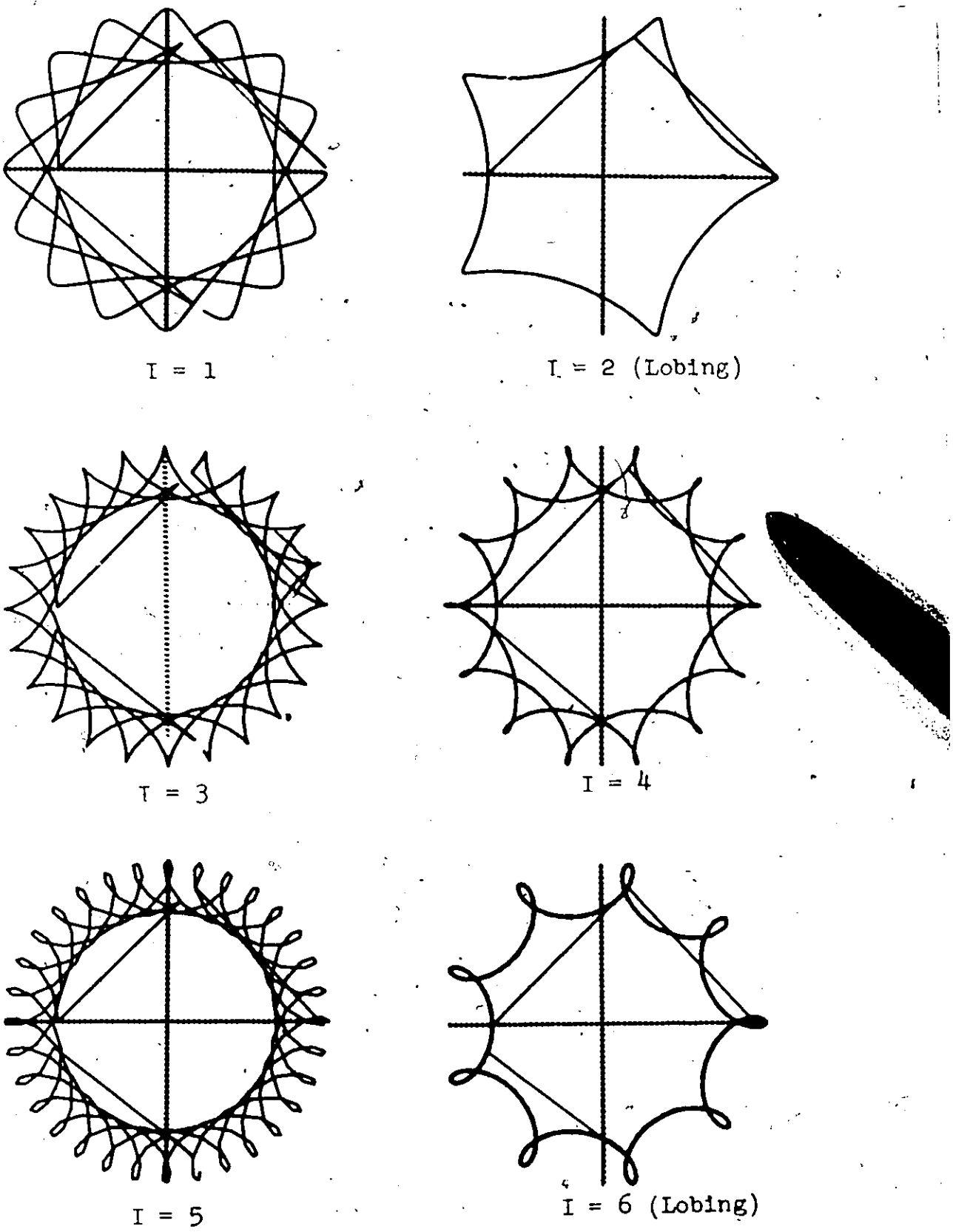

Fig. 5.17 Computer Generated Profiles for the Kinematic Model of a 4 Flute Reamer (Lobes produced where indicated)

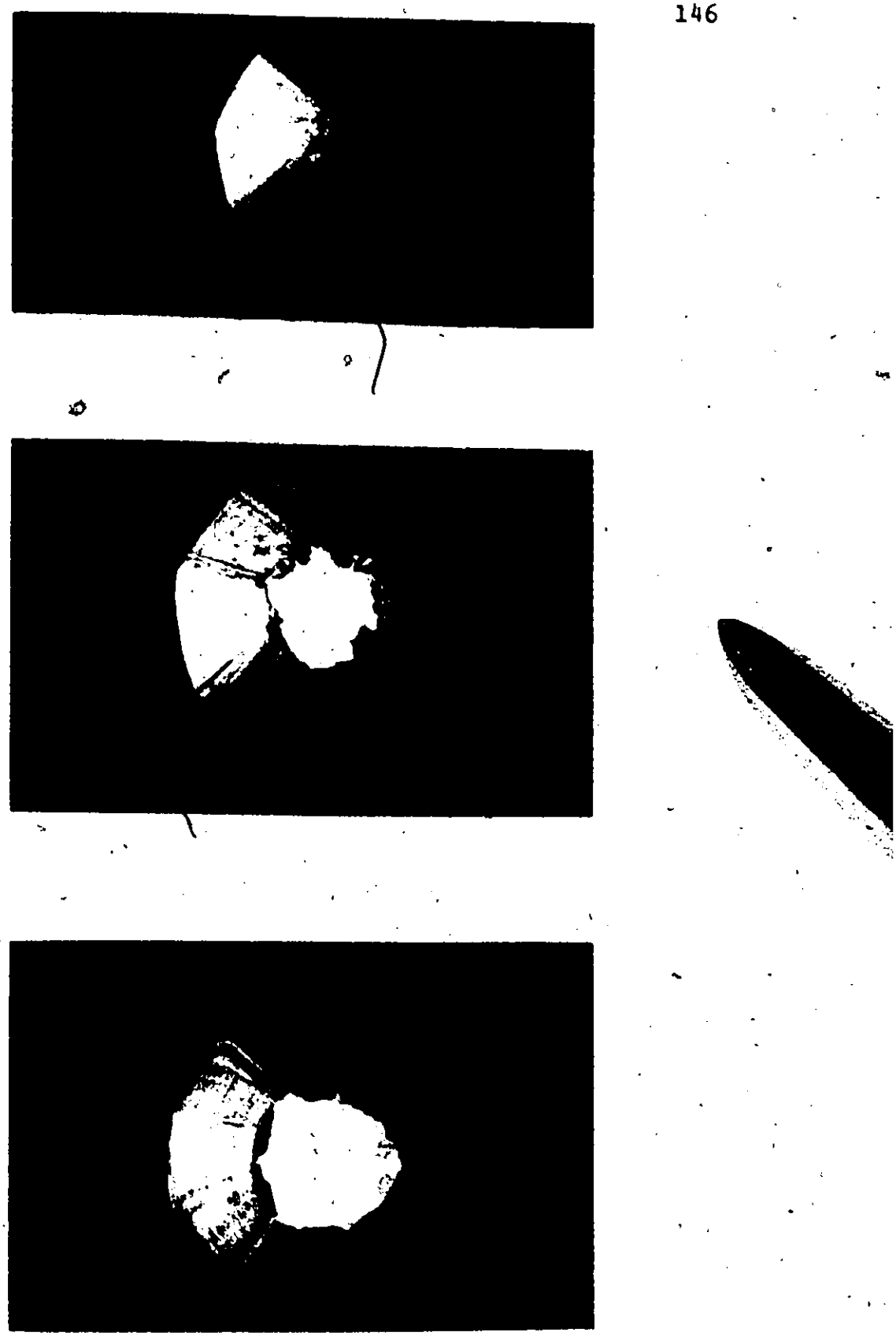

Fig. 5.18 Drilling Chatter

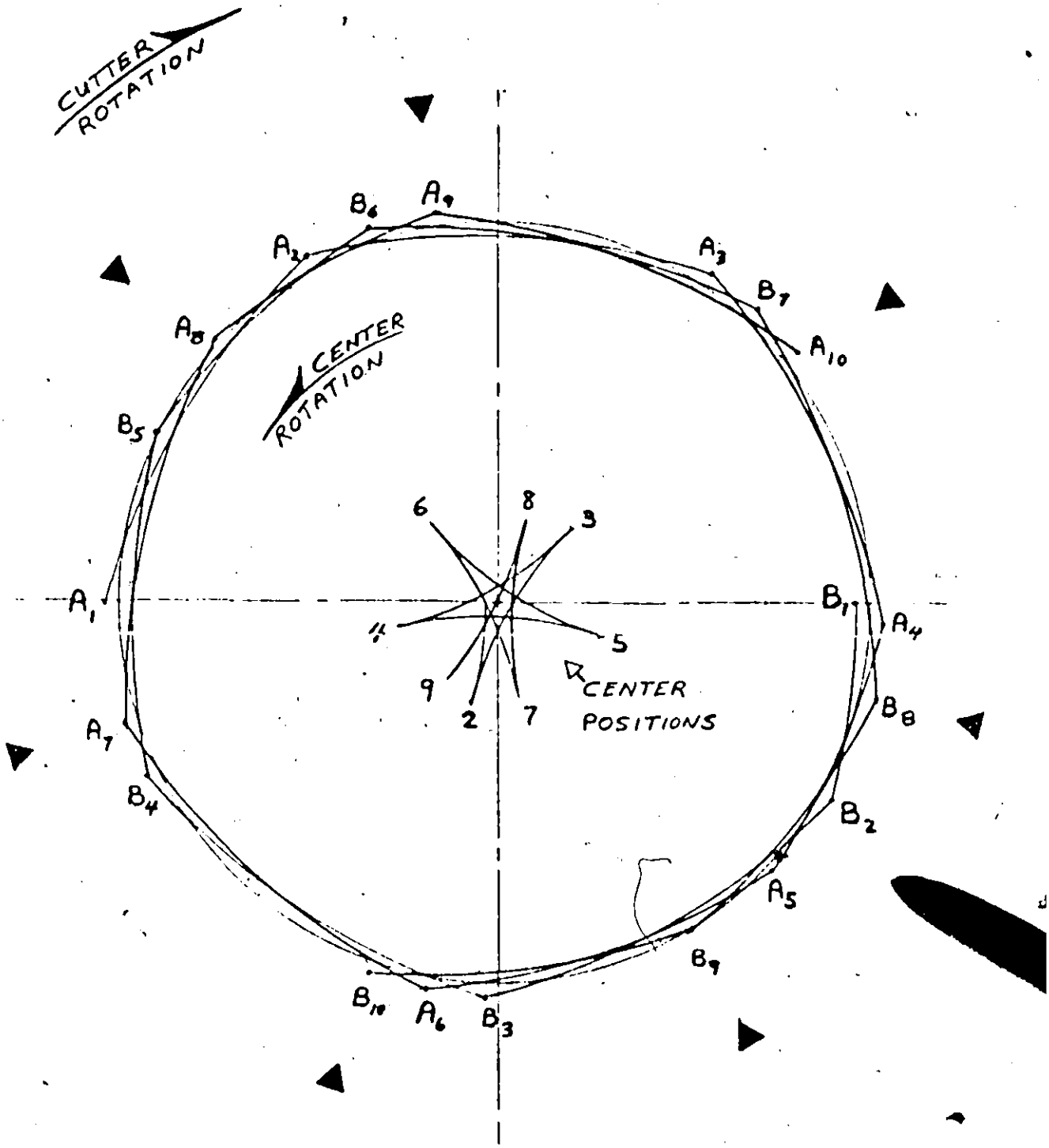

Fig. 5.19 Graphical Development of Drilling Chatter
Two Flutes Marked A & B
(Peaks produced during the last revolution are marked ▲)

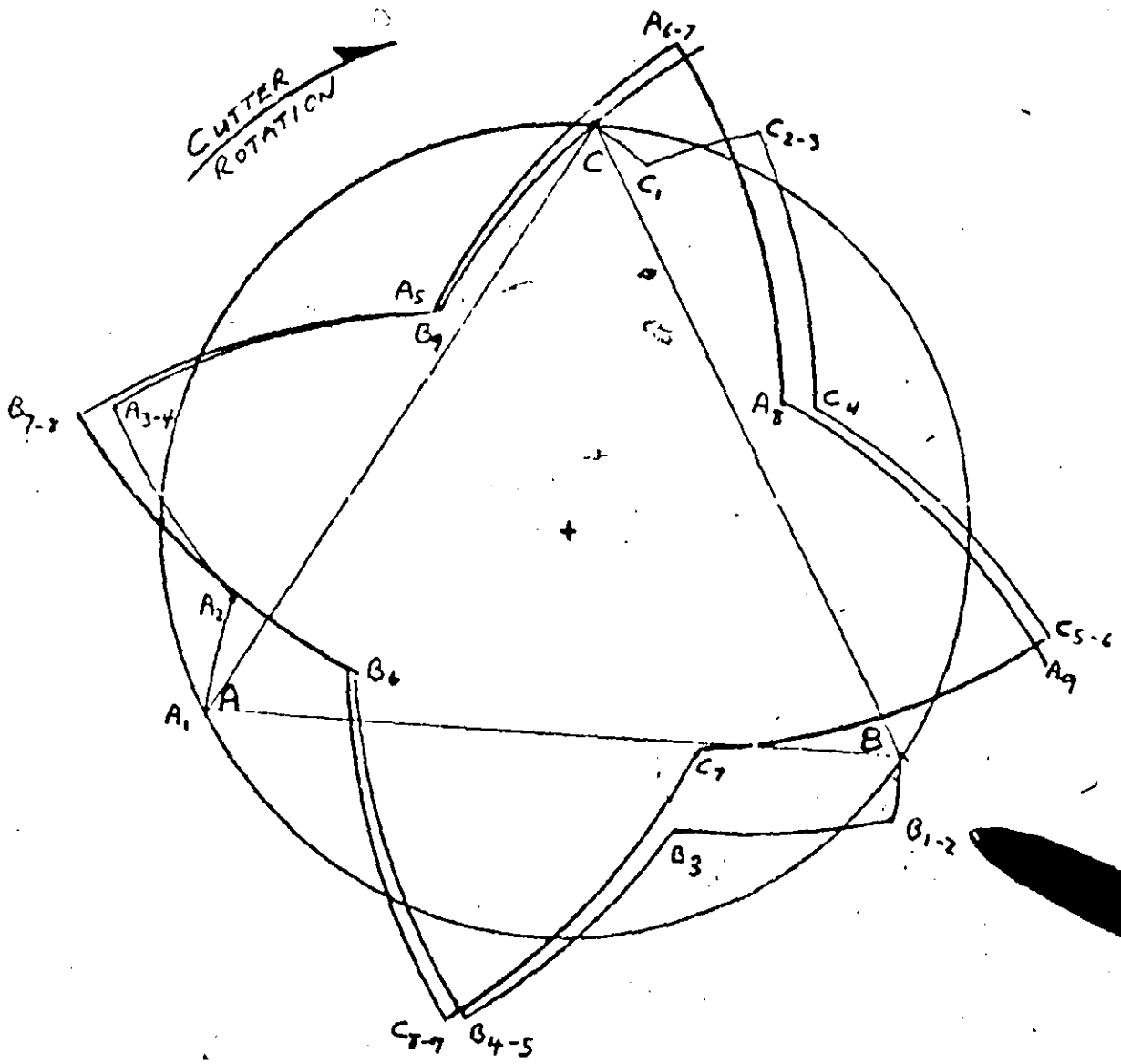

Fig. 5.19 Graphical Development of Reaming Chatter
(Stop-Start Model)

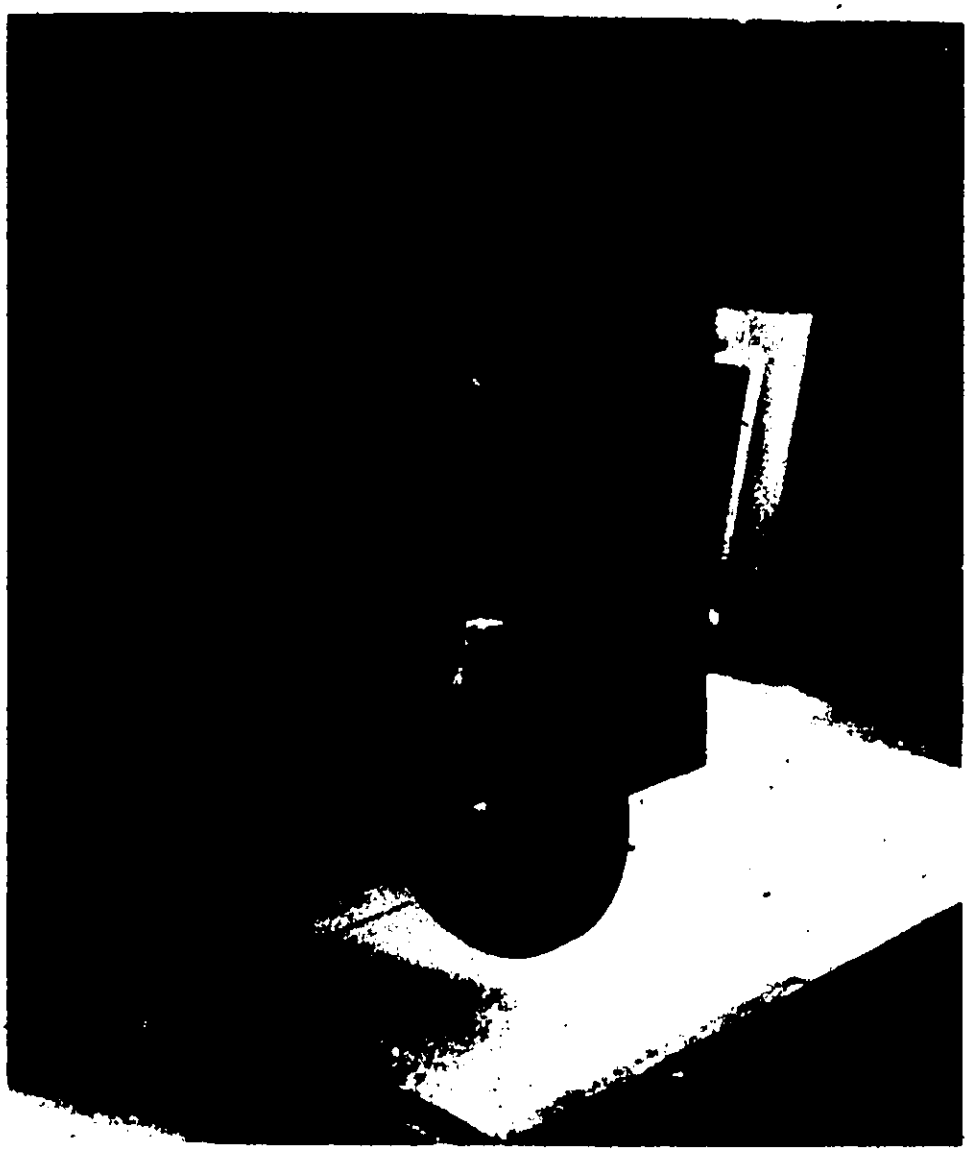

Fig. B1 Grinding Wheel Suspended to Determine its Mass Moment of Inertia (J)

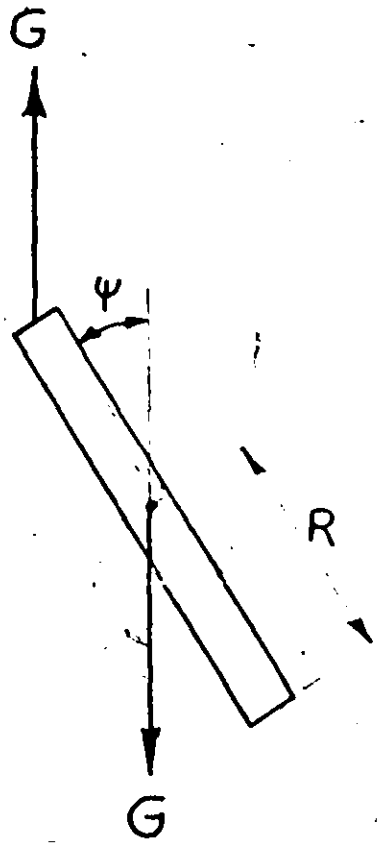

Fig. B 2 Free-body diagram of the grinding wheel hanging and oscillating